

**Isolation and characterization of novel anti-infective
specialized metabolites from *Actinobacteria***

Dissertation

zur Erlangung des
Doktorgrades der Naturwissenschaften (Dr. rer. nat.)

der

Naturwissenschaftlichen Fakultät I – Biowissenschaften –

der Martin-Luther-Universität
Halle-Wittenberg,

vorgelegt

von Herrn Dominik Wichner

geb. am 24.11.1990 in Traunstein

Gedruckt mit Genehmigung der Naturwissenschaftlichen Fakultät I der Martin-Luther-Universität Halle-Wittenberg.

Tag der mündlichen Qualifikation:

09.04.2021

Dekan:

Prof. Dr. Dietrich Nies

1. Berichterstatter*in

Prof. Dr. Timo H. J. Niedermeyer

2. Berichtserstatter*in

Prof. Dr. Jörg Degenhardt

3. Berichterstatter*in

Prof. Dr. Yvonne Mast

Erklärung

Ich erkläre, dass ich mich an keiner anderen Hochschule einem Promotionsverfahren unterzogen bzw. eine Promotion begonnen habe.

Ort, Datum

Unterschrift des Antragstellers

Erklärung

Ich erkläre, dass ich die vorliegende Dissertationsschrift selbstständig ohne unzulässige Hilfe Dritter verfasst habe und ausschließlich die angegebenen Hilfsmittel und Quellen verwendet wurden. Die wörtlich und inhaltlich entnommenen Stellen wurden als solche kenntlich gemacht.

Ort, Datum

Unterschrift des Antragstellers

Table of contents

A. Zusammenfassung	1
B. Summary.....	3
1. Introduction.....	5
1.1. The dilemma of antibiotic resistance	5
1.1.1. Gram-positive pathogenic <i>Bacteria</i>	5
1.1.2. Gram-negative pathogenic <i>Bacteria</i>	7
1.1.3. The advance of antibiotic resistance	10
1.2. <i>Actinobacteria</i> as specialized metabolites producers	13
1.3. Natural products in infectious disease therapy	19
1.4. Aim of this thesis	21
2. Materials and methods	22
2.1. Applied bacterial strains	22
2.2. Analysis	27
2.3. Isolation of endophytic <i>Bacteria</i> from macroalgae	29
2.4. Bacteria cultivation and extraction	31
2.5. Additional extraction of medium extracts	34
2.6. Antibacterial bioactivity assay.....	36
2.6.1. Reporter-based bioassay.....	37
2.6.2. Test for synergistic antimicrobial activity.....	39
2.6.3. Test for inhibitory bioactivity against MDR strains.....	40
2.7. Cytotoxicity assay	41
2.8. Molecular biology.....	43
2.9. Determination of the absolute configuration using Marfey's reagent	45
3. Results and discussion.....	47

3.1.	Tübingen actinomycetes strain collection	47
3.1.1.	Concept verification by rediscovering pactamycin from Tü 6448	48
3.1.2.	<i>Streptomyces fradiae</i> Tü 27	50
3.1.3.	Isolation and structure elucidation	56
3.1.3.1.	Dereplication of daidzeine	59
3.1.3.2.	Hydrazone derivatives of amino acids	59
3.1.3.3.	Test for cytotoxic and inhibitory bioactivity of leucine hydrazone	64
3.2.	MiMo_ALe project	72
3.2.1.	Macroscopic and microscopic characterization	72
3.2.2.	Isolated endophytes – primary screening	78
3.2.3.	Secondary screening	84
3.2.4.	Verification of globomycin production	89
3.3.	Determination of the absolute configuration of a siderophore	92
4.	Conclusion and Outlook	96
5.	References	97
6.	Abbreviations	112
7.	Curriculum Vitae	118
8.	Appendix	121

List of tables

Table 1: Applied strains from the actinomycetes strain collection of the Eberhard Karls University in Tübingen and the biological activity they were selected for. This information was obtained by the project partners in Tübingen before the start of this thesis.	22
Table 2: Applied bacterial endophytes isolated from macroalgae from Moroccan ecosystems and their host organism.	24
Table 3: 16 bacterial endophytes isolated from Moroccan aromatic plants including sampling side and (part of the) plant they were isolated from. The strain code is composed as follows: VW-XYZ and a number. VW are the initials of the host plant, X is the first letter of the sampling side, Y is the first letter of the part of the plant that was used for the isolation (R = root, L = leaf, S = stem), and z is an additional information on the isolation medium (y = YECD medium, w = WYEA medium). These strains have been isolated by the Moroccan project partners before.	25
Table 4: Frequently used HPLC methods for screenings, micro-fractionation, and HPLC-HRMS analyses.	28
Table 5: Template for the checkerboard assay including the used concentrations of leucine hydrazone, and hygromycin B.	42
Table 6: Results of the bioassays of the withdrawn culture samples obtained from the OSMAC approach for Tü 27 against <i>B. subtilis</i> ATCC6051. (-) indicates no observed inhibitory bioactivity. The numbers represent the diameter of the inhibition zone in cm.	50
Table 7: Results of the reporter-based bioassay performed by the project partners in Tübingen targeting RNA biosynthesis of the withdrawn culture samples that showed inhibitory bioactivity against <i>B. subtilis</i> ATCC6051. The intensity of inhibition/induction is illustrated by “+” and “++”. “++” means there was a stronger inhibition/induction observed than when “+” is used. “±” means no relevant inhibition/induction and “n.d.” means “not determined”.	51
Table 8: Optimized HPLC method for compound isolation from the basic fraction obtained from the ethyl acetate medium extract of Tü 27.	57
Table 9: Isolated compounds and estimated sum formulae.	58
Table 10: ¹ H (600 MHz) and ¹³ C (125 MHz) NMR spectroscopic data of leucine hydrazone in DMSO-d ₆	59
Table 11: Bacterial endophytes from Moroccan aromatic plants that were selected to further work due to their antibacterial activity against MDR bacteria. The index “static” means there was only a	

static inhibition. The composition of the strain-code can be found in chapter 2.1, Table 3. This screening was performed by the author of this thesis together with the Moroccan project partners in their laboratories.	79
Table 12: Results of the bioactivity screening of medium extracts (ME) obtained from liquid fermentation in ISP2 medium of bacterial endophytes from Moroccan aromatic plants. The screening of the medium extracts was performed by the Moroccan project partners. The screening for the initial bioactivity was performed by the author of this thesis together with the Moroccan project partners in their laboratories.	80
Table 13: Results of the primary bioactivity screening against non-MDR Gram-positive and Gram-negative bacteria performed by the Moroccan project partners. Results are given as diameter of inhibition zone in [cm]. <i>S. aureus</i> (Sa), <i>B. cereus</i> (Bc), <i>M. luteus</i> (Ml), <i>E. coli</i> (Ec), <i>P. aeruginosa</i> (Pa), <i>K. pneumoniae</i> (Kp). (-) means that no inhibitory bioactivity was observed. This screening was performed by the Moroccan project partners.	82
Table 14: Results of the primary bioactivity screening of the isolated endophytes against fungi performed by the Moroccan project partners. <i>C. albicans</i> (L4), <i>C. glabrata</i> (L7), <i>C. krusei</i> (10), and <i>C. parapsilopsis</i> (L18). "+" means that there was inhibitory bioactivity but the inhibition zone was too small to be reasonably measured. "-" means no inhibitory activity was observed. This screening was performed by the Moroccan project partners.	83
Table 15: Bioactivity assay against MDR strains using 7 different antibiotics (10 μ L of antibiotic dissolved in water with a mass concentration of 5 mg/mL followed by sterile filtration) to find an appropriate positive control for all 5 strains. (+) states inhibitory bioactivity, (-) states no inhibitory bioactivity. Static inhibition is not included in the table. The bioassay was performed in duplicate.	84
Table 16: Experimentally observed retention times of globomycins in positive ion mode of HRMS analysis.	90
Table 17: Assignment of different globomycins to the micro-fractions of the ethyl acetate medium extract of MiMo_ALe#7 after cultivation in NL333 medium for 4 days.	91
Table 18: Integration report for Marfey's derivative of the hydrolysate of compound 1	94

List of figures

Figure 1: Schematic illustration of the cell envelope of Gram-positive and Gram-negative bacteria. CAP = covalently attached protein; IMP = integral membrane protein; LP = lipoprotein; LPS = lipopolysaccharide; LTA = lipoteichoic acid; OMP = outer membrane protein; WTA = wall teichoic acid. ³⁴	7
Figure 2: Chemical structures of isoniazid (1), ⁶¹ ethambutol (2) ⁶² and dapson (3). ⁶³	9
Figure 3: Antimicrobial agents approved by the Food and Drug Administration from 1983-2012. ⁶⁹	10
Figure 4: Classical bioactivity-guided workflow for NP isolation from Bacteria. ^{115,116}	14
Figure 5: Chemical structures of netilmicin (4) ¹²⁷ and pikromycin (5). ¹²⁸	15
Figure 6: Chemical structures of huanglongmycin A (6) and chaxalactin B (7). ¹²⁹	16
Figure 7: Chemical structures of lentzeoside C (8), D (9) and E (10). ¹³⁴	16
Figure 8: Sampling place for the macroalgae at the west coast of Morocco (32°03'02.0"N 9°20'27.6"W). The pictures show (from left to right) the sampling location on a map of Morocco, the sampling location itself and a water basin containing the macroalgae.....	23
Figure 9: Different macroalgae used for the isolation of endophytic bacteria: (a) <i>Codium elongatum</i> , (b) <i>Cystoseira ericoide</i> , (c) <i>Cystoseira tamariscifolia</i> , (d) <i>Calliblepharis jubata</i> , (e) <i>Bryopsis balbisia</i> , and (f) <i>Halopteris scoparia</i> . Classification was done by the Moroccan project partners.	24
Figure 10: YECD agar plates with surface-sterilized macroalgae fragments for the macroalgae <i>Laurentia pinnatifida</i> , <i>Cystoseira tamariscifolia</i> , and <i>Ulva lactuca</i> (from left to right).....	29
Figure 11: Setup for the extraction of larger scale fermentation culture broths.....	33
Figure 12: Workflow of the additional extraction procedure of medium extracts.	34
Figure 13: Illustration of the blue induction in the reporter-based assay (here caused by the positive control (rifampicin) from a screening of micro-fractions of Tü 27 for RNA biosynthesis interfering properties).....	38
Figure 14: An MH agar plate with drilled holes to test supernatants of bacterial cultures for inhibitory bioactivity against ceftazidime-resistant <i>P. aeruginosa</i> . The lower left corner represents the positive control (10 µL of an apramycin solution with a mass concentration of 5 mg/mL in water).....	40
Figure 15: Chemical structure of FDAA (11). ¹⁸⁵	45

Figure 16: (A) Extracted ion chromatogram of the ethyl acetate medium extract of Tü 6448. The signal at 3.42 min belongs to pactamycin. (B) The mass spectrum showing the signal at m/z 559.2771 caused by pactamycin obtained in positive ion mode.....	48
Figure 17: Reporter-based bioassay for the medium extracts of Tü 6448 and Tü 6457 generated after 72 and 168 h. For this agar plate, <i>B. subtilis</i> 1S34 modified with an <i>yhel</i> promoter was employed to screen for protein biosynthesis interfering compounds.....	49
Figure 18: Chemical structure of pactamycin (12) with the sum formula C ₂₈ H ₃₈ N ₄ O ₈ . ^{187,188}	49
Figure 19: HPLC-UV chromatograms of ethyl acetate medium extracts obtained from (A) the 1 L culture and (B) the 12 L culture of Tü 27 after fermentation in NL 19 for 14 d. The detection was done at 210 nm (blue), 254 nm (magenta), 280 nm (brown), 430 nm (green), and with the ELSD (black).....	53
Figure 20: HPLC-UV chromatograms of the fractions containing (A) crude bases, (B) neutral compounds, and (C) crude acids after the additional extraction. Detection was carried out at 210 nm (blue), 254 nm (magenta), 280 nm (brown), 430 nm (green), and with the ELSD (black).....	55
Figure 21: HPLC-UV chromatogram of the optimized isolation method for fraction 1, basic compounds. The signals corresponding to the isolated compounds are highlighted in blue. The detection was done at 210 nm (black), 254 nm (blue), 280 nm (magenta), and 430 nm (brown). .	57
Figure 22: Chemical structure of leucine hydrazone and HMBC (arrows) and ¹ H- ¹ H COSY (bold bars) correlations.	60
Figure 23: Illustration of possible hydrogen bonding (dashed line) between a hydrogen atom of the NH ₂ group and the oxygen of the carbonyl moiety in leucine hydrazone causing magnetic inequivalence of the two NH ₂ hydrogens in the ¹ H-NMR spectrum.....	60
Figure 24: Chemical structures of katorazone (14) ²⁰⁰ , yoropyrazone (15) ²⁰¹ and negamycin (16). ²⁰⁴	61
Figure 25: Chemical structures of valanimycin (17), ¹⁹⁹ azaserine (18) ¹⁹⁸ and thrazarine (19). ¹⁹⁸	62
Figure 26: Results of the cytotoxicity assay of leucine hydrazone using HeLa cells (normalized data).	64
Figure 27: Chemical structures of hygromycin B (20), ²¹⁸ G418 (21), ²¹⁹ and actinomycin D (22). ²²⁰ .	65
Figure 28: Results of the cytotoxicity assay of leucine hydrazone using HeLa cells as well as the test for synergistic effects with hygromycin B (normalized data).....	66
Figure 29: Results of the cytotoxicity assay of leucine hydrazone using HeLa cells as well as the test for synergistic effects with G418 (normalized data).....	68

Figure 30: Results of the cytotoxicity assay of leucine hydrazone, and actinomycin D using HeLa cells as well as the test for synergistic effects with actinomycin D (normalized data).	69
Figure 31: Results of the checkerboard assay of the combination of leucine hydrazone and hygromycin B including the legend of the checkerboard assay indicating the cell viability from 0-100 % and the corresponding color code.....	70
Figure 32: A : Macroscopic picture of a well-separated colony MiMo_ALe#1. B (measure bar 50 μ m), and C (measure bar 20 μ m): microscopic pictures of this strain.....	73
Figure 33: A : Macroscopic picture of a well-separated colony MiMo_ALe#3. B (measure bar 50 μ m), and C (measure bar 20 μ m): microscopic pictures of this strain.....	74
Figure 34: A : Macroscopic picture of a well-separated colony MiMo_ALe#5. B (measure bar 50 μ m), and C (measure bar 20 μ m): microscopic pictures of this strain.....	75
Figure 35: A : Macroscopic picture of a well-separated colony MiMo_ALe#7. B (measure bar 100 μ m), and C (measure bar 20 μ m): microscopic pictures of this strain.....	76
Figure 36: A : Macroscopic picture of a well-separated colony MiMo_ALe#10. B (measure bar 50 μ m), and C (measure bar 20 μ m): microscopic pictures of this strain.....	77
Figure 37: Chemical structure and formulae of globomycin and its derivatives. ²³²	86
Figure 38: Base peak chromatogram of the ethyl acetate medium extract of MiMo_ALe#2 after cultivation in NL300 medium for 3 days. The signals can be assigned to the globomycins as follows: SF1902A ₂ (t_R = 5.25 min), SF1902A ₃ (t_R = 5.59 min), SF1902A ₁ (t_R = 5.84 min), and SF1902A _{4b} (t_R = 6.15 min).	87
Figure 39: Extracted ion chromatograms of the ethyl acetate medium extract of MiMo_ALe#2 after cultivation in NL300 for 3 days. (A) SF1902A ₂ , (B) SF1902A ₃ , (C) SF1902A ₁ , and (D) SF1902A _{4b}	88
Figure 40: HPLC-UV chromatogram obtained for the ethyl acetate medium extract of MiMo_ALe#1 using a Phenomenex® Kinetex (2.6 μ m) C-18, 100x3.0 mm ID column at 50 °C. Detection was done at 210 nm (blue), 254 nm (magenta), 280 nm (brown), 430 nm (green), and with the ELSD (black).	89
Figure 41: Chemical structures of compound 1 (23) and compound 2 (24) that were used for determination of the absolute configuration using Marfey's reagent.	92
Figure 42: HPLC-UV chromatograms of Marfey's derivatives of the hydrolysate of compound 1 and the authentic D- and L-Orn and D- and L-Ser. Detection was done at 340 nm.....	93
Figure 43: Integration report for Marfey's derivative of the hydrolysate of compound 1.....	94
Figure 44: HPLC-UV chromatograms of Marfey's derivatives of the hydrolysate of compound 2 and the authentic D- and L-Orn and D- and L-Ser. Detection was done at 340 nm.....	95

A. Zusammenfassung

Im Zuge dieser Dissertation wurden Bakterien des Phylums *Actinobacteria* für die Isolierung und die Charakterisierung von spezialisierten Metaboliten verwendet. Seit Jahrzehnten sind *Actinobacteria* mit ihren 6 Klassen und 53 Familien eine wertvolle Quelle für biologisch aktive spezialisierte Metaboliten. Bezüglich der Produktion von biologisch aktiven spezialisierten Metaboliten stellt *Streptomyces* das wohl wichtigste Genus der *Actinobacteria* dar.

Für diese Dissertation wurden insgesamt 138 Bakterienstämme mit Hilfe einer bioaktivitätsgeleiteten Herangehensweise bearbeitet. Diese 138 Stämme setzen sich wie folgt zusammen: 13 Stämme der Actinomyceten Stammsammlung der Eberhard Karls Universität in Tübingen, 115 bakterielle Endophyten, welche von den marokkanischen Projektpartnern der Cadi Ayyad Universität in Marrakesch, Marokko, aus marokkanischen Heilpflanzen isoliert wurden sowie 10 bakterielle Endophyten, welche im Zuge dieser Arbeit aus Makroalgen aus Marokko isoliert wurden.

Die Isolierung sowie Charakterisierung neuer spezialisierter Metaboliten wurde mittels analytischer und semipräparativer Hochleistungsflüssigchromatographie (*High-Performance Liquid Chromatography*; HPLC), hochauflösender Massenspektrometrie in Kombination mit HPLC sowie ein- und zweidimensionaler Kernspinresonanzspektroskopie (*Nuclear Magnetic Resonance Spectroscopy*; NMR) durchgeführt.

Für die Stämme der Tübinger Actinomyceten Stammsammlung beinhaltete die bioaktivitätsgeleitete Herangehensweise einen reporter-basierten Assay, welcher von den Projektpartnern der Eberhard Karls Universität in Tübingen durchgeführt wurde und welcher Informationen über den Wirkmechanismus einer bioaktiven Substanz gibt. Die Stämme marokkanischen Ursprungs hingegen, wurden auf ihre das Wachstum hemmende Bioaktivität gegenüber 5 multiresistenten, humanpathogenen Bakterien getestet, welche im Krankenhaus in Marrakesch isoliert wurden.

Auf diese Weise konnte für die 10 bakteriellen Endophyten, welche aus den Makroalgen isoliert wurden, nachgewiesen werden, dass alle diese Stämme Globomycine produzieren. Da die Makroalgen in einem Gebiet gesammelt wurden, welches nur einige 100 m² umfasste, deutet dies auf eine nahe Verwandtschaft der Stämme hin. Des Weiteren konnte ein Hydrazonderivat der

Aminosäure Leucin isoliert werden, welches vom Stamm *Streptomyces fradiae* Tü 27 produziert wird.

Dieses Hydrazonderivat wurde auf Bioaktivität im reporter-basierten Assay getestet sowie auf einen möglichen Synergismus mit verschiedenen Antibiotika (Actinomycin D, Hygromycin B und Geneticin). Dabei zeigte das Hydrazonderivat keine das Wachstum hemmende Bioaktivität gegen *Bacillus Subtilis* oder *Pseudomonas fluorescens*. Zudem deutet der IC₅₀ Wert auf keine relevante Zytotoxizität hin. Kombination mit Actinomycin D oder Tetrazyklin führte zu keiner verstärkten antimikrobiellen Aktivität dieser Antibiotika. Eine erhöhte Zytotoxizität in Kombination mit Actinomycin D war ebenfalls nicht zu beobachten. Jedoch war eine Zunahme der Zytotoxizität zu beobachten, wenn die Substanz mit Hygromycin B oder Geneticin kombiniert wurde. Die Bestimmung des FIC (*Fractional Inhibitory Concentration*) Index für die Kombination des Hydrazonderivats mit Hygromycin B ergab einen FICI von 1.0 und zeigte somit, dass es sich dabei um eine additive Wirkung handelt.

B. Summary

In the course of this PhD thesis, bacterial strains of the phylum *Actinobacteria* have been used for the isolation and characterization of novel specialized metabolites. *Actinobacteria*, which contain 6 classes and 53 families, have represented a major source for novel biologically active specialized metabolites for decades. The most important genus of *Actinobacteria* in regard of biologically active specialized metabolites is the genus *Streptomyces*.

In total 138 actinobacterial strains were applied using bioactivity-guided approaches. The number of 138 strains is composed of 13 strains of the actinomycetes strain collection of the Eberhard Karls University in Tübingen, 115 endophytic strains isolated from Moroccan aromatic plants by the project partners of the Cadi Ayyad University in Marrakesh, Morocco, and 10 endophytic bacterial strains that were isolated from different macroalgae as part of this thesis.

The isolation and characterization of novel specialized metabolites were performed using analytical and semi-preparative High-Performance Liquid Chromatography (HPLC), high-resolution mass spectrometry connected to an HPLC system, and 1 and 2 dimensional Nuclear Magnetic Resonance Spectroscopy (NMR) experiments.

The bioactivity-guided approach included a reporter-based bioactivity assay, which was performed by the project partners at the Eberhard Karls University in Tübingen that indicates different modes of action for the strains of the Tübingen actinomycetes strain collection as well as tests for inhibitory bioactivity against five multidrug-resistant bacterial human pathogens isolated in the hospital in Marrakesh, Morocco. Further, assays for synergism regarding inhibitory bioactivity and cytotoxicity were employed for the novel specialized metabolite, which was isolated from *Streptomyces fradiae* Tü 27.

Using these approaches, the production of globomycins for the 10 endophytic strains that were isolated from macroalgae was shown. This circumstance in combination with the fact that the macroalgae were collected within a rather narrow sampling place indicated a close relatedness of the 10 strains. Furthermore, the novel hydrazone-derivative of the amino acid leucine was isolated from a medium extract of *S. fradiae* Tü 27.

This hydrazone-derivative was tested for its bioactivity in the reporter-based bioassay and for synergistic activity in combination with different antibiotics (actinomycin D, hygromycin B, and

geneticin). The compound itself did not show inhibitory bioactivity against *Bacillus subtilis* or *Pseudomonas fluorescens* or significant cytotoxicity. Even though there was no observed increase in antimicrobial activity of neither actinomycin D nor tetracycline against *B. subtilis* when these antibiotics were combined with the compound, we observed an increased cytotoxicity of hygromycin B, and geneticin in combination with the hydrazone. The combination of the compound with actinomycin D did not cause an increase in cytotoxicity. For the combination of the compound with hygromycin B, the FICI (Fractional Inhibitory Concentration Index) was determined. An FICI of 1.0 revealed the additive effect of this combination.

1. Introduction

1.1. The dilemma of antibiotic resistance

1.1.1. Gram-positive pathogenic *Bacteria*

In the last decades, the raise of antibiotic resistance in human pathogens has become a global threat.¹ Infections that used to be nosocomial (hospital-acquired) became community-acquired in the last years. The most prominent example for such an infectious pathogen is methicillin-resistant *Staphylococcus aureus* (MRSA).²⁻⁴ Pathogens exhibiting resistance to antibiotics that were originally used to treat the infections caused by these pathogens are called multidrug-resistant (MDR) as the resistance to a certain antibiotic usually means resistance to a group or even a whole category of antibiotics. In the case of MRSA, the resistance to methicillin is based on the capability of β -lactamase production, which causes the resistance to several β -lactam antibiotics like methicillin, its derivatives, and the cephalosporins.⁵ Besides multidrug-resistant, also extensively (also called extremely) drug-resistant (XDR) and totally drug-resistant (TDR) pathogens have already occurred. These categories are defined by the antimicrobial agents the pathogens are non-susceptible for. MDR strains show non-susceptibility to at least one agent in three or more antimicrobial categories, XDR strains to at least one agent in all but two or less antimicrobial categories and TDR strains show non-susceptibility to all agents in all categories.⁶

For prominent examples like the Gram-positive MRSA or vancomycin-resistant *Enterococci* (VRE) but also for the Gram-negative human pathogen *Acinetobacter baumannii*, the occurrence and propagation of resistance mechanisms can be well understood.

MRSA and VRE

The first appearance of MRSA was documented in 1961, and thus only two years after the introduction of methicillin to the market.⁷ Within the same decade, MRSA became endemic in hospitals.⁸ The development of antibiotic resistance has been observed for *S. aureus* before regarding another β -lactam antibiotic, penicillin. In a period of ten years, the treatment of patients with *S. aureus* infections with penicillin became almost completely ineffective.⁹ The fact that the development of resistance to methicillin occurred within only two years compared to the ten years for penicillin indicated the rather troublesome trend of antibiotic resistance in the case of *S. aureus* already 60 years ago. By now, MRSA belongs to the leading causes of infections and deaths in regard

to infections caused by a single agent.⁸⁻¹⁰ Community-acquired outbreaks of MRSA affecting risk groups in the US started in the 1980s but happened to include patients that do not belong to any risk group worldwide in the 1990s as well.^{4,8,11}

The development of methicillin-resistance in MRSA is caused by two factors. One factor is the production and excessive secretion of β -lactamases. This yields a reduced effect of β -lactam antibiotics, as secreted β -lactamases hydrolyze the β -lactam ring, which results in a deactivation of the drug.^{12,13} Besides the production of β -lactamases, MRSA can show alterations of the penicillin binding protein (PBP), which represents the target of β -lactam antibiotics. PBPs are responsible for transglycosylation and transpeptidation reactions during peptidoglycan synthesis that is essential in bacterial cell wall biosynthesis.¹³⁻¹⁵ During these reactions, PBPs bind to the D-alanyl-D-alanine terminus of their natural substrate, the mucopeptides.¹⁵ β -lactam antibiotics represent structural analogs to this D-alanyl-D-alanine terminus and are bound by PBPs in a nonreversible reaction instead. This way, PBPs are not available for their natural substrates anymore, which results in the breakdown of the cell wall biosynthesis.¹⁵ The alteration of PBPs results in a lowered affinity to β -lactams. The combination of both factors consequently results in a very poor effectiveness of β -lactam antibiotics against pathogens like MRSA.^{13,16}

After the spread of methicillin-resistance, the glycopeptide vancomycin became the agent of choice to treat MRSA infections.¹⁷⁻¹⁹ Vancomycin interferes with bacterial peptidoglycan metabolism by binding to the D-alanyl-D-alanine moiety of the precursor peptide, causing the termination of bacterial cell wall biosynthesis.^{15,20,21} Thus, the structural alteration of the precursor peptides, especially from D-alanyl-D-alanine to D-alanyl-D-lactate, can cause vancomycin-resistance, even though the production and secretion of β -lactamases do not represent a problem for vancomycin.¹⁷

Nevertheless, the principle “use causes resistance” became true for vancomycin, too. The widespread application of vancomycin to treat MRSA is one of the possible reasons for the development and spread of vancomycin-resistant *S. aureus* (VRSA) and vancomycin-resistant *Enterococci* (VRE). Within approximately 10 years after their first appearance, by the year 2000, community-acquired VRE started to appear in Europe and the US.^{4,22,23}

1.1.2. Gram-negative pathogenic *Bacteria*

Acinetobacter baumannii and *Pseudomonas aeruginosa*

Besides the multidrug-resistant Gram-positive pathogens MRSA, VRSA or VRE, Gram-negative bacterial pathogens like *A. baumannii* and *P. aeruginosa* developed resistance to several antibiotics.^{24,25} The occurrence of antibiotic resistance in Gram-negative pathogens represents a special threat, as the number of effective antibiotics for the treatment of infections caused by Gram-negative bacteria is lower than in the case of Gram-positive bacteria.²⁵ The generally lower susceptibility of Gram-negative pathogens like *Enterobacteriaceae*, *Acinetobacter*, and *Pseudomonas* species is due to their cell membrane. Compared to Gram-positive bacteria, which have a single membrane, Gram-negative bacteria exhibit an inner and an outer membrane (OM) separated by the periplasm.^{26,27} The OM represents a low-permeability barrier that can be very efficient in combination with efflux pumps, especially in *P. aeruginosa*.^{26,28,29} The low permeability of the OM is caused by porin channels that allow the relatively fast influx of small hydrophilic drugs.^{30–32} This situation is different for *P. aeruginosa* and *Acinetobacter* species. They do not exhibit the classical trimeric porins as they can be found, for instance, in *Escherichia coli*, but porins that form a much narrower channel resulting in the extremely low permeability of the OM known for *P. aeruginosa*.^{29,33}

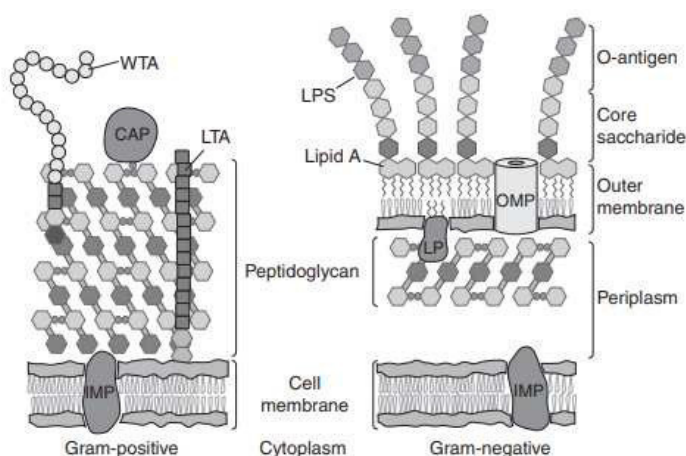


Figure 1: Schematic illustration of the cell envelope of Gram-positive and Gram-negative bacteria. CAP = covalently attached protein; IMP = integral membrane protein; LP = lipoprotein; LPS = lipopolysaccharide; LTA = lipoteichoic acid; OMP = outer membrane protein; WTA = wall teichoic acid.³⁴

In the last 10-15 years, multidrug-resistant *A. baumannii* attracted attention as it became a common human pathogen in hospitals worldwide.³⁵⁻³⁷ Unlike MRSA that causes mainly skin infections,⁷ *A. baumannii* infections can concern blood, the urinary tract, the respiratory tract and also the central nervous system with significant rates of morbidity and mortality.^{7,35,38} Besides intrinsic resistance of *A. baumannii* to several antibiotics like ampicillin, amoxicillin, clavulanic acid, cefotaxime, ceftriaxone, ertapenem, trimethoprim, and fosfomycin, its acquisition of further resistances made this pathogen even more alarming in the last years.³⁹⁻⁴¹ After the occurrence of *A. baumannii* has become common in hospital settings, community-acquired *A. baumannii* infections are still rare but their reports increased in the last years.⁴² Another Gram-negative pathogen, which became a severe threat, is *P. aeruginosa*. Like *A. baumannii*, *P. aeruginosa* is intrinsically resistant to a number of antibiotics. These include chloramphenicol, kanamycin, neomycin, trimethoprim + sulfamethoxazole, and tetracyclines in addition to the antibiotics *A. baumannii* is resistant to.⁴¹ In the case of *P. aeruginosa*, which can cause bloodstream infections and pneumonia, the acquisition of antibiotic resistance is often connected to biofilm formation.^{43,44} Despite the rather fast development of antibiotic resistance of *P. aeruginosa*, community-acquired infections remain rare.⁴⁴

Actinobacterial pathogens

The pathogens presented here may suggest that Gram-negative human pathogens state a more severe threat to health compared to Gram-positive ones. This might be true regarding the acquisition of antibiotic resistance but not regarding the dangers of the infections they cause in general. Leprosy and tuberculosis belong to the severest infectious diseases worldwide, and both are caused by Gram-positive bacteria, *Mycobacterium leprae*^{45,46} and *Mycobacterium tuberculosis*,^{47,48} which belong to the phylum *Actinobacteria*. The latter one causes more than 1.5 million deaths per year and thus more than any other infectious disease.⁴⁹

In 2020, the Centre for Disease Control and Prevention (CDC) estimated the number of people carrying *Mycobacterium tuberculosis* to be approximately 2 billion, which represents one fourth of the global population that can potentially develop tuberculosis.⁵⁰ As a bacterial infection, tuberculosis can be treated with antibiotics. One treatment regime for pulmonary (affecting the lungs) and extrapulmonary (not primarily located in the lungs) tuberculosis is represented by a combination therapy consisting of four antibiotics (rifampin, isoniazid (Figure 2, 1), pyrazinamide,

and ethambutol (Figure 2, **2**) during intensive phase and two antibiotics (rifampin and isoniazid) during maintenance phase.⁵¹⁻⁵⁴ The circumstance that these antibiotics are used for a rather long anti-tuberculosis therapy with a duration of up to several months,⁵¹ even though rifampin⁵⁵ and isoniazid^{56,57} show hepatotoxicity (chemical-driven liver damage), further illustrates the seriousness of infectious diseases caused by *M. tuberculosis*.⁵⁸ The combination of a treatment that lasts several months and a daily intake of 4 tablets (body weight >50 kg) results in high rates of non-compliance, which in turn results in the development of resistance.^{59,60} Thus, MDR, XDR, and even TDR strains of *M. tuberculosis* have already occurred.^{59,60}

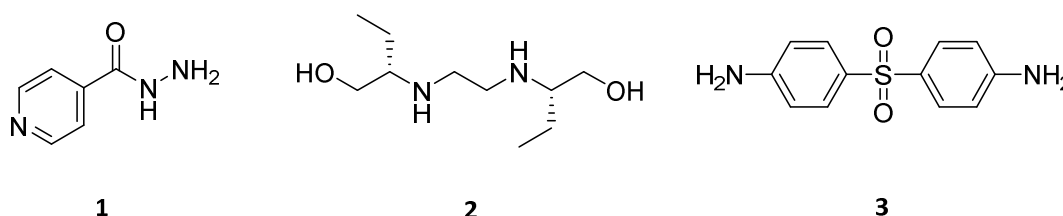


Figure 2: Chemical structures of isoniazid (**1**),⁶¹ ethambutol (**2**)⁶² and dapsone (**3**).⁶³

Leprosy represents a chronic infectious disease caused by *M. leprae*.⁴⁶ By the year 2015, this human pathogen caused approximately 200 000 new infections annually within the last 8 years.^{64,65} Unlike tuberculosis, leprosy can be cured by combination therapy of rifampicin, clofazimine, and dapsone (Figure 2, **3**).^{65,66}

Due to a rather long treatment of 6-9 months, hepatotoxicity of rifampicin and dapsone states a problem. Nevertheless, regimen dosages given by the World Health Organization (WHO) of once per month for rifampicin and clofazimine and daily doses for dapsone, and potentially clofazimine reduces the risk of non-compliance compared to the treatment of tuberculosis, lowering the possibility of the development of antibiotic resistance. Nevertheless, the exact treatment regimens depend on the degree of severity like the presence of single or multiple skin lesions.⁶⁶⁻⁶⁸

1.1.3. The advance of antibiotic resistance

The situation regarding the increasing occurrence of antibiotic resistance in bacterial pathogens worsens as simultaneously the number of novel drug approvals drastically decreases. Compared to the middle of the 20th century, the discovery of novel anti-infective agents, especially antibiotics, and their approval as drugs significantly decreased in the last decades (Figure 3). Within 30 years, the number of antimicrobial agents approved by the Food and Drug Administration declined to only one fourth.⁶⁹

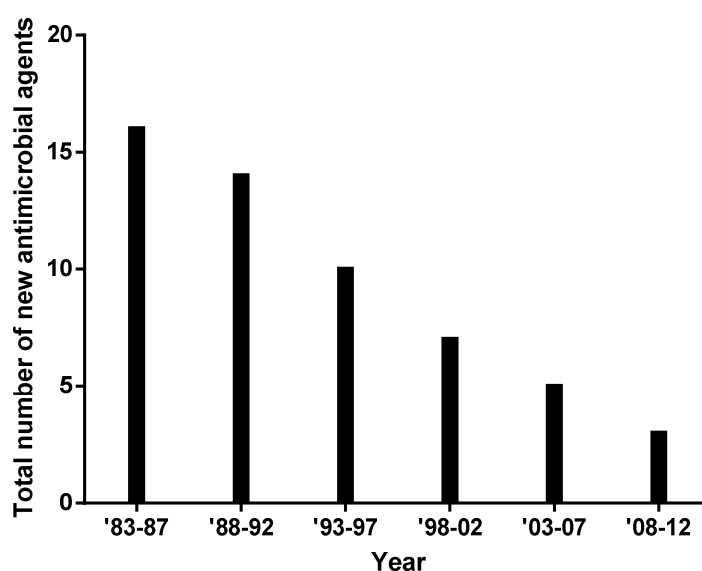


Figure 3: Antimicrobial agents approved by the Food and Drug Administration from 1983-2012.⁶⁹

The increase in antibiotic resistance is based on different reasons concerning different parts of life. An argument that is commonly addressed for its major contribution to antibiotic resistance is the misuse of antibiotics in hospital settings and prescriptions. This statement includes the wrong duration (too short; too long) of antibiotic treatments but also the overprescription and prescription of wrong antibiotics.^{70,71}

Infectious diseases caused by Gram-negative bacteria should not be treated with antibiotics that are only effective against Gram-positive ones and *vice versa*. Also the unnecessary prescription of broad-spectrum antibiotics is a frequent argument.⁷¹ Another fact, which strongly contributes to the development of antibiotic resistance, is non-compliance. Non-compliance, which simply means that a dose of antibiotic is not taken especially in the case of orally administered ones, can reduce the success rates of antibiotic treatment by 50 %.⁷² Here, aspects like the duration of antibiotic treatment, the age of the patient as well as the frequency of antibiotic administration per day are crucial.^{72,73} In addition to aspects of the health care sector, the contribution of the usage of antibiotics in agriculture cannot be neglected.⁷⁴ In agriculture, antibiotics are used to *e.g.* prevent the spread of infectious diseases within a population of animals kept for meat production and for growth stimulation.⁷⁵ Even though, this is necessary to ensure the global demand on affordable meat, especially the accumulation of antibiotics within the food chain with humans as “final consumer” is a questionable price to pay.⁷⁶ The permanent uptake of low doses of antibiotics in the region of sub-inhibitory concentrations in food can contribute to the development of antibiotic resistance. A specific capability of bacteria, the so-called horizontal gene transfer (HGT), plays an important role within these processes. In fact, HGT strongly contributes to antibiotic resistance as it allows bacteria to gain genes encoding for antibiotic resistance without being in contact with the antibiotic.^{77,78} This is of particular interest when it involves both, a non-pathogenic and a pathogenic strain. By HGT, it is possible that the capability of resistance is transferred from the non-pathogenic to the pathogenic strain whereby only the latter represents a problem. The DNA segment that is transferred during HGT by either conjugation, transformation or transduction is called mobile genetic element (MGE). As MGEs can be transferred among taxa, HGT contributes to bacterial evolution but also to antibiotic resistance.^{77,79,80}

A very important mechanism connected to HGT, is the production of so-called virulence factors. Per definition, “virulence” is the ability of a microorganism to infect a host organism.⁸¹ The virulence factor is a molecule of bacterial,⁸¹ fungal,⁸² viral⁸³ or protozoal⁸⁴ origin that increases the effectiveness of a pathogen to cause an infectious disease.^{81,82} This increased virulence is due to effects of the virulence factor on, among others, the colonization of the host,⁸⁵ immunosuppression of the host’s immune system, and effects on cell invasion.⁸¹ Even though virulence factors strongly contribute to the pathogenicity of microorganisms, they are not exclusively “pathogen-associated” but can be found in non-pathogens as well.⁸⁶ A prominent example for the involvement of virulence factors to increase its virulence is *S. aureus*.⁸⁷ *S. aureus* uses a variety of membrane-damaging toxins

as virulence factors that cause the hemolytic capability of this pathogen.^{87,88} Also the virulence of *E. coli* O157:H7, a human pathogen, is caused by virulence factors, which increase the ability of the strain to colonize human hosts.⁸⁹

To overcome the problem of antibiotic resistance, a change regarding their application has to take place. This concerns all areas, which apply antibiotics, like agriculture, clinical settings but also their supervised application to overcome non-compliance. This might reduce the development of further multidrug-resistant pathogens in the future, but the challenge to deal with the MDR pathogens that have appeared during the last decades remains a global challenge.

1.2. *Actinobacteria* as specialized metabolites producers

To accomplish this challenge of finding novel anti-infective agents, different approaches are used. One possibility is the classical approach of antibiotic research, which means the (bioactivity-guided) isolation and characterization of novel specialized metabolites. This approach has been successfully applied for decades with its start in the “golden age” of antibiotic discovery in the 1940s and 50s. For this purpose, the phylum *Actinobacteria* and the genus *Streptomyces* in particular, are applied due to the chemical diversity of their specialized metabolites.^{90,91} *Actinobacteria* are Gram-positive bacteria that can be found in a vast variety of terrestrial and aquatic habitats.^{92,93} With cell counts of 10^6 - 10^9 cells per gram of soil, *Actinobacteria* are most abundant in soil whereas *Streptomyces* species are predominant with an account of 95 %.^{92,93} Further, these bacteria can be found as endophytic living organisms in *e.g.* plants, as well.⁹⁴ As endophytes, the bacteria live inside the so-called host (*e.g.* the plant) without causing apparent harm to the host organism.^{95–97} Besides *Actinobacteria*, also Gram-negative bacteria including pathogenic strains of *E. coli* and *Salmonella* species can be found as endophytes in plants, which can represent a problem in agriculture.^{98,99} The symbiosis between endophyte and host can be expressed by diverse effects of the microbial endophyte to the plant. This may include the microbial production of compounds that may, among others, promote plant growth, serve as insecticides, degrade contaminants or facilitate nitrogen assimilation, which makes endophytes an interesting and promising source for potentially novel bioactive specialized metabolites.^{98,100,101}

Besides the usefulness in natural product research, the application of endophytes in agriculture represents a potential way to reduce the appearance of plant diseases without the need for antibiotics.¹⁰² Here, endophytic specialized metabolites with antifungal or insecticidal properties can replace the application of antibiotics and pesticides to ensure the global demand on food without harming the environment.^{103,104} Nevertheless, the focused application of endophytes in agriculture has to take place without a potential harm to the final consumer, which is mainly the humankind.

Like in soil, *Actinobacteria* can be found in a huge diversity in association with a wide range of plants.^{105,106} The diverse distribution of *Actinobacteria* may be due to the relatively high guanine-cytosine (G+C) content of their DNA of up to 70 %, which results in a better thermal stability compared to other bacteria.^{93,107–109} Thus, thermal treatment can be applied to the selective isolation of *Actinobacteria* from *e.g.* soil samples beside the application of appropriate antibiotics to suppress the growth of Gram-negative bacteria, and fungi.^{110,111}

Even though the phylum *Actinobacteria* with its six classes and 53 families has been a rich source for biologically active specialized metabolites for a long time, the decreasing discovery of novel NPs in combination with the increase of antibiotic resistance make new approaches necessary.¹¹² This importance of *Actinobacteria* can be illustrated as by the end of 2002, 45 % of in total 22000 biologically active NPs known to this date, was produced by this phylum.¹¹³ 80 % of these actinobacteria-derived NPs was produced by *Streptomyces* species, making this genus the most important genus within *Actinobacteria* concerning the production of specialized metabolites.^{113,114} For decades, the classical approach for the exploitation of actinobacterial chemical diversity and the isolation of specialized metabolites has included a bioactivity-guided workflow (Figure 4).

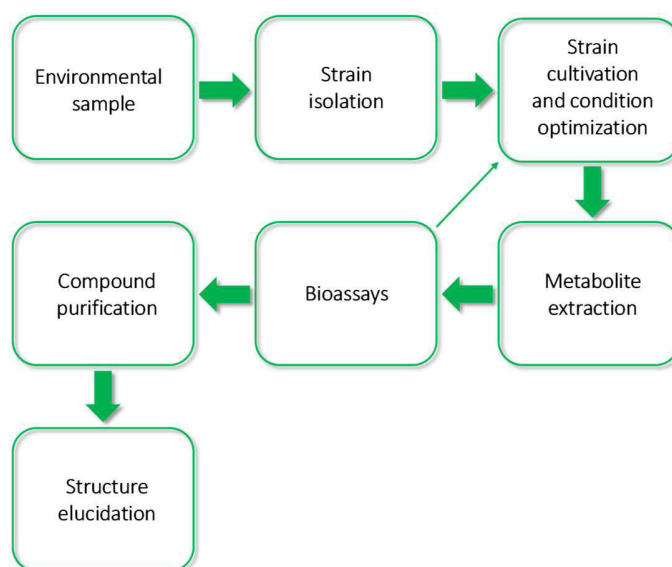


Figure 4: Classical bioactivity-guided workflow for NP isolation from *Bacteria*.^{115,116}

Using this approach, an enormous diversity of NPs of bacterial origin was discovered. These actinobacterial and actinobacteria-derived NPs include the aminoglycosides like streptomycin (produced by *Streptomyces griseus*),¹¹⁷ and kanamycin A (isolated from *Streptomyces kanamyceticus*)¹¹⁸ as well as its semi-synthetic derivatives netilmicin (Figure 5, 4)¹¹⁹ and amikacin.^{117,120} Moreover, the macrolide antibiotics erythromycin (produced by *Saccharopolyspora erythraea*)¹²¹ and pikromycin (Figure 5, 5),¹²² which belong to the 14-membered macrolides, and the 16-membered macrolides tylosin (isolated from *S. fradiae*)¹²³ and carbomycin (isolated from

Streptomyces thermotolerans).¹²⁴ Further, chloramphenicol (produced by *Streptomyces venezuelae*)¹²⁵ and rifamycin (isolated from *Amycolatopsis mediterranei*).¹²⁶

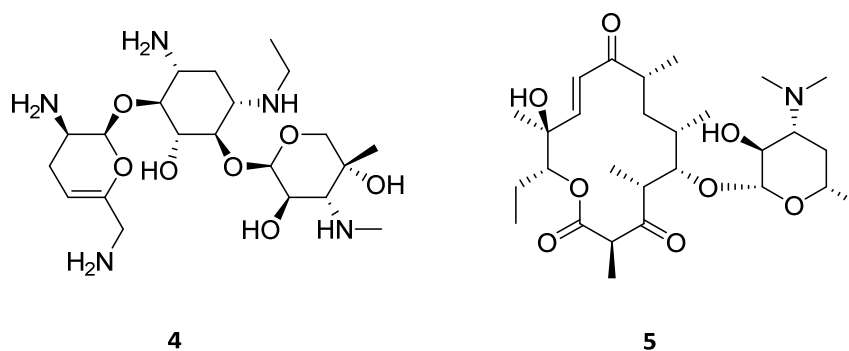


Figure 5: Chemical structures of netilmicin (**4**)¹²⁷ and pikromycin (**5**).¹²⁸

Despite this vast diversity of biologically active NPs, the increase in antibiotic, and antimicrobial resistance in human pathogens, strengthens the need either to discover novel NPs including completely new chemical entities or to develop a new strategy for the treatment of infectious diseases also apart from novel antibiotics.

After decades of antibiotic research, *Actinobacteria* are now used for the search for a more diverse range of activities (e.g. anticancer or anti-HIV). Some more recently discovered actinobacterial specialized metabolites that were published within the last 5 years are shown below.

Jiang *et al.* isolated the two anticancer agents huanglongmycin A (Figure 6, **6**), produced by *S. sp.* CB09001,^{129,130} and xiakemycin A, which is produced by *S. sp.* CC8-201.¹³¹ Another example, published by Axenov-Gibanov *et al.* in 2016, is the antibiotic chaxalactin B (Figure 6, **7**), produced by *S. sp.* IB 2014/I/78-8.¹³²

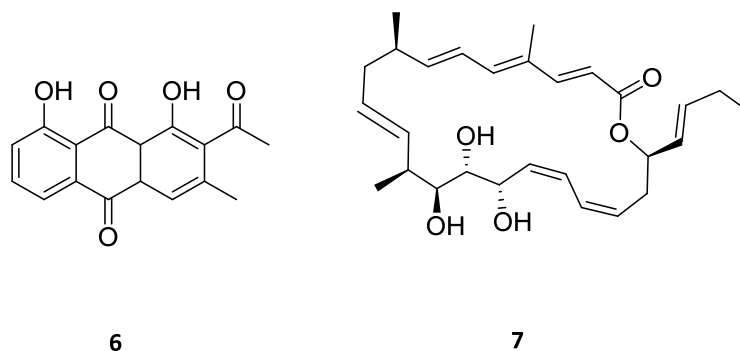


Figure 6: Chemical structures of huanglongmycin A (**6**) and chaxalactin B (**7**).¹²⁹

In the same year, Zhang and co-workers published two new but biologically inactive specialized metabolites produced by *S. so. ZZ388* searching for novel anti-tumor agents.¹³³ Lentzeoside A-F (Figure 7), six new specialized metabolites produced by *Lentzea sp. H45*, showed *in vitro* anti-HIV integrase activity and thus interference with virus replication.¹³⁴

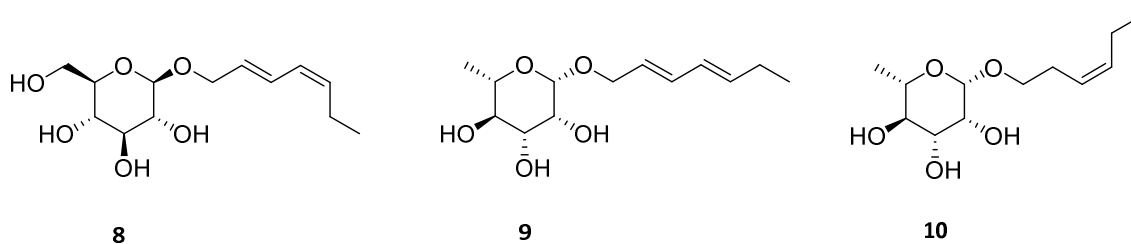


Figure 7: Chemical structures of lentzeoside C (**8**), D (**9**) and E (**10**).¹³⁴

The ongoing discovery of new anticancer and anti-HIV agents compared to novel antibiotics might be caused by the fact that the pharmaceutical industry almost completely abandoned the field of antibiotic research. Compared to drugs for the treatment of *e.g.* cancer, diabetes or other chronic diseases, antibiotics are less profitable.^{125,135–137} Especially novel anti-HIV agents have a high-profit potential, as they are not used to cure the infection (as it is the case for antibiotics) but to suppress the virus in the body. This can expand the lifespan of infected adults to approach the lifespan of uninfected ones, but it also means the daily uptake of appropriate medication.¹³⁸ It is apparent that the prescription of a drug for several decades is more profitable compared to several weeks (*e.g.*

for antibiotics). The threat by HIV infection is further illustrated by the introduction of pre-exposure prophylaxis for the prevention of acquiring HIV infection. Like the treatment of HIV, pre-exposure prophylaxis also requires the daily intake of drugs, which is in turn very profitable for the pharmaceutical company that produces these drugs.¹³⁹ Such examples clearly illustrate the rather small role of antibiotics and their discovery for big pharmaceutical companies.

Although, antibiotic research is now mainly restricted to facilities apart from the big pharmaceutical enterprises and mainly done in universities and institutes, the development of new approaches and tools for antibiotic discovery continues. Compared to the procedures and tools, which have been used for decades, recent approaches changed to a more efficient way of research especially concerning the throughput of screening and data analysis.

This includes the (late-stage) modification of known NPs for medical use as well as the application of computer and software-based tools.

Latter ones (especially in combination with high-throughput screening (HTS)) can be used to accelerate NP research. Using HTS, it is possible to process a high number of samples simultaneously, yielding an accordingly big amount of data.^{140,141} Without the possibility to handle this data efficiently, the time gained by HTS is lost due to manual analysis. Molecular networking represents such a possibility. Molecular networking is a tool based on grouping MS² data corresponding to their similarities.¹⁴² As MS² fragmentation is connected to the chemical structure of a compound, this approach can be used for a fast dereplication of larger data sets where manual dereplication would be very time-consuming.¹⁴³ An important web-based platform for molecular networking is Global Natural Products Social Molecular Networking (GNPS) that provides the ability to analyze (*e.g.* automatic dereplication) own MS and MS² data sets and also to compare it to other data.¹⁴⁴ Visualization of molecular networks can be done either directly using GNPS or by *e.g.* Cytoscape, an open source software that can create molecular networks with data exported from GNPS.^{143–146} The major advantage of this procedure, beside the possibility to handle, process, and analyze large data sets, is the circumstance that all needed tools and software are open access or open source.^{144,146}

The idea behind the modifications of known NPs is their further diversification and the improvement of physico-chemical, pharmacokinetic and biopharmaceutical effects on target binding.¹⁴⁷ Modifying NPs avoids the very time-consuming discovery, isolation and structure elucidation process of NP

discovery and thus represents a promising way to new bioactive agents. Besides the rather historical procedures like enzymatic catalysis, more recent approaches apply hydroxy group derivatization using electrophilic reagents, C-H bond functionalization followed by oxidation or amination reactions and olefin functionalizations.¹⁴⁸ As NPs are structurally complex molecules with a wide diversity of functional groups, such modifications have to be highly specific to yield the desired product.^{148–150}

Using these approaches, the growing diversity of natural, semi-synthetic or synthetic compounds can be applied to the search of novel bioactive agents to reduce the impacts of life-threatening infections.

At the end of 2019, the WHO listed 32 antibiotic agents in clinical trials. 11 of these 32 agents showed bioactivity against carbapenem-resistant Gram-negative pathogens (*A. baumannii*, *Enterobacteriaceae*, *P. aeruginosa*) and another 12 showed activity against “other priority pathogens”. Only one agent, which is currently in phase 1 clinical trials, cannot be assigned to a known antibiotic class and thus may represent a new chemical scaffold.¹⁵¹

1.3. Natural products in infectious disease therapy

Even though *Actinobacteria* still represent a promising field of research for NP scientists, the drastically decreasing number of novel biologically active antimicrobial agents highlights the need for alternatives.¹⁵² The difficulties NP scientists have to face include high rediscovery rates of already known specialized metabolites but also low expectations regarding potential profit. The latter caused the abandonment of this research area by many companies, as novel antibiotics are usually kept as “agents of last resort” instead of prescribing them.^{135,153} Furthermore, unlike *e.g.* anticancer agents, antibiotics are comparatively cheap, which additionally lowers the potential profit of a novel antibiotic.^{136,137}

Alternatives to overcome these problems apart from the ones mentioned above include, among others, the usage of other phyla like *Cyanobacteria*,^{154,155} the attempt to activate so-called silent gene clusters by the application of the OSMAC (One Strain-Many Compounds) approach,¹⁵⁶ genetic approaches^{155,157} as well as combination therapy.¹⁵⁸ In contrast to the other approaches, the application of combination therapy “skips” the part of discovery of novel specialized metabolites by combining already discovered NPs and analyzing a potentially enhanced biological activity. This can be convenient as especially the process of approval and clinical trials for novel compounds can be time-consuming and cost-intensive.¹⁵⁹

Studies showed that for Gram-negative pathogens in particular, combination therapy can yield a significant decrease in mortality. Zarkotou and co-workers presented the advantage of combination therapy over monotherapy to treat bloodstream infections caused by *Klebsiella pneumoniae*, which produces *K. pneumoniae* carbapenemase (KPC).¹⁶⁰ The enzyme KPC is able to degrade penicillin, cephalosporin as well as broad-spectrum β -lactam antibiotics, which results in a more complicated treatment of infections caused by KPC-producing Gram-negative pathogens.¹⁶¹ Nevertheless, Zarkotou *et al.* showed that the combination of tigecycline with, among others, colistin, gentamicin, carbapenem or amikacin reduced mortality to 0%. Monotherapy with colistin, tigecycline or carbapenem on the other side showed mortalities of 67, 40, and 100%.¹⁶⁰ In this study, the real number of patients has to be compared rather than the infection mortality given in percentage. In total, 20 patients received combination therapy treatment and 15 patients were treated with a monotherapy approach. Nevertheless, the overall infection mortality remained 0% in the case of combination therapy but 47% for monotherapy, which shows the advantage of combination therapy over monotherapy.¹⁶⁰ Another example for the positive outcome of combination therapy

over conventional monotherapy is shown by Batirel and co-workers in regard of an XDR *Acinetobacter* bloodstream infection.¹⁶² Compared to an in-hospital mortality of 72 % for patients treated with a colistin monotherapy, the mortality decreased to 52 % for combination therapy of colistin combined with carbapenem or sulbactam.¹⁶² Further studies, for example by Tumbarello *et al.*¹⁶³ or Tzouveleki *et al.*¹⁶⁴ also indicate the superiority of combination therapy over monotherapy in regard to the treatment of MDR Gram-negative infections.

All these studies used the pairing of two antibiotics (congruous approach)¹⁶⁵ including colistin, a polypeptide antibiotic that is known for its inhibitory bioactivity against several MDR Gram-negative pathogens.¹⁶⁶ Colistin was already discovered in the 1940s but its use was reduced due to its toxicity.^{166,167} Nowadays, colistin is seen as an antibiotic of last resort to treat infections by MDR *P. aeruginosa*, *A. baumannii*, and *K. pneumoniae*.^{166,168}

Besides this congruous approach, the combination of an antibiotic with a non-antibiotic, a so-called “adjuvant molecule”, is possible.¹⁶⁹ The usage of adjuvant molecules (syncretic approach) increases the effectiveness of the antibiotic.^{165,170,171} In general, antibiotic adjuvants can be divided into the two classes I and II, whereas class I can be further divided into I.A and I.B. Class I.A adjuvants inhibit active antibiotic resistance. This is *e.g.* performed by inactivating efflux mechanisms or enzymes like β -lactamases. Adjuvants of Class I.B are represented by non-antibiotic compounds that inactivate intrinsic resistance mechanisms like biofilm formation. Class II adjuvants, on the other side, increase the ability of the host organism, thus the organisms infected with the pathogen, to kill the pathogen.^{165,171}

The potential synergism of two compounds can be confirmed using the checkerboard assay to obtain the FICI (Fractional Inhibitory Concentration Index).^{158,165,172} The FICI is calculated as the sum of the FIC values of the combined drugs. For two drugs, A and B, the FIC for drug A is determined using the values for the minimum inhibitory concentration (MIC) as $\text{MIC(A in combination)}/\text{MIC(A)}$.¹⁷² Synergism between two compounds is indicated by a $\text{FICI} \leq 0.5$ whereas a $\text{FICI} \geq 4.0$ means that there is an antagonistic effect.^{158,165}

Using this approach in combination with established natural products databases might result in the discovery of interesting compound combinations, which could be used against infectious diseases caused by MDR, XDR, and TDR human pathogens.

1.4. Aim of this thesis

The aim of this PhD thesis was the isolation and characterization of novel anti-infective specialized metabolites from *Actinobacteria* using a bioactivity-guided approach. For this purpose, actinobacterial strains from the Tübingen actinomycetes strain collection as well as strains of Moroccan origin were applied. Latter ones included endophytic bacteria that have been isolated from different red, brown, and green macroalgae in the course of this thesis as well as endophytic strains isolated from Moroccan aromatic plants by the Moroccan project partners before.

The general procedures included the application of the OSMAC approach to exploit the chemical diversity of the strains and a variety of extraction techniques. For the isolation of specialized metabolites, analytical and semi-preparative HPLC-UV were used. Characterization and structure elucidation was performed using HPLC-MS, 1D and 2D NMR experiments as well as Marfey's analysis for the determination of the absolute configuration of isolated compounds.

Tübingen actinomycetes strain collection

For the strains of the Tübingen actinomycetes strain collection, a reporter-based bioassay was applied as part of the bioactivity-guided approach. The reporter-based bioassays were performed by project partners of the Eberhard Karls University in Tübingen. The aim of the reporter-based assay was to obtain information about the mode of action of potentially novel bioactive specialized metabolites in the beginning of the bioactivity-guided procedure. This included the search for compounds that interfere with the biosynthesis of DNA, RNA, proteins, fatty acids, and the cell wall using genetically modified strains of *B. subtilis* 1S34.

Microorganisms from Moroccan ecosystems

This project was in cooperation with project partners of the Cadi Ayyad University in Marrakesh, Morocco. The investigated endophytic bacteria included 10 strains, which have been isolated from different macroalgae, and 115 strains from Moroccan aromatic plants. For the bioactivity-guided approach, all strains and generated samples were screened for their inhibitory bioactivity against five multidrug-resistant bacterial human pathogens: methicillin-resistant *S. aureus*, imipenem-resistant *A. baumannii*, ceftazidime-resistant *P. aeruginosa*, and *K. pneumoniae* and *E. coli* both resistant to "extended spectrum".

2. Materials and methods

Unless it is stated otherwise, all experiments and analyses were performed by the author of this thesis. MS data were acquired by Prof. Timo Niedermeyer, Steffen Breinlinger or Markus Schwark throughout the whole thesis.

Detailed information regarding materials and devices that have been used as part of this thesis can be found in chapter 3 and 4 of the appendix. This information includes the providers of chemicals as well as the manufacturers of the used instruments and devices.

2.1. Applied bacterial strains

The work was comprised of two main parts, the investigation of a) actinobacterial strains from the actinomycetes strain collection of the Eberhard Karls University in Tübingen (Table 1), and b) *Actinobacteria* of Moroccan origin (Tables 2 and 3). The latter ones included strains that were isolated within the course of this PhD work.

Tübingen actinomycetes strain collection

The strains provided by the Eberhard Karls University in Tübingen were chosen due to their interesting biological activity targeting different parts of the bacterial metabolism. This information was obtained by the project partners in Tübingen before the start of this thesis using a reporter-based bioactivity assay indicating the presence of compounds interfering with the biosynthesis of DNA, RNA, cell wall, or proteins.

Table 1: Applied strains from the actinomycetes strain collection of the Eberhard Karls University in Tübingen and the biological activity they were selected for. This information was obtained by the project partners in Tübingen before the start of this thesis.

Applied strain [Tü #]	Targeting biosynthesis of
12	cell wall
6448, 6457	protein
12, 27	RNA
39, 102, 108, 735, 2401, 2445, 2471, 4011, 6448	DNA

Except the strain Tü 6448, which belongs to the genus *Micromonospora*, all used strains of the Tübingen actinomycetes strain collection are *Streptomyces* species. Further information down to the species level is available for the strains Tü 12 (*S. echinatus*), Tü 27 (*S. fradiae*), Tü 39 (*S. fradiae*), Tü 735 (*S. albus*), and Tü 2471 (*S. flaveolus*).

Bacterial strains of Moroccan origin

The endophytic bacteria of Moroccan origin included 10 strains that have been isolated from different macroalgae as part of this thesis, as well as 115 strains isolated from Moroccan aromatic plants by the Moroccan project partners before.

The bacterial strains were isolated from different red, brown, and green macroalgae, which were collected at the west coast of Morocco (32°03'02.0"N 9°20'27.6"W), as shown in Figure 8. The macroalgae were stored at 4 °C within 4 hours after sampling and processed within 24 hours.



Figure 8: Sampling place for the macroalgae at the west coast of Morocco (32°03'02.0"N 9°20'27.6"W). The pictures show (from left to right) the sampling location on a map of Morocco, the sampling location itself and a water basin containing the macroalgae.

The microbial strains as well as the corresponding host macroalgae species are shown in Table 2. The classification of the macroalgae species (Figure 9) as well as the final purification of the microbial strains using the streak plate technique were performed by the Moroccan project partners. Detailed information on the isolation of the endophytes can be found in chapter 2.3.

Table 2: Applied bacterial endophytes isolated from macroalgae from Moroccan ecosystems and their host organism.

Applied strain [MiMo_ALe#]	Host
1	<i>Codium elongatum</i>
2	<i>Codium elongatum</i>
3	<i>Cystoseira ericoide</i>
4	<i>Cystoseira tamariscifolia</i>
5	<i>Calliblepharis jubata</i>
6	<i>Calliblepharis jubata</i>
7	<i>Bryopsis balbisia</i>
8	<i>Halopteris scoparia</i>
9	<i>Halopteris scoparia</i>
10	<i>Cystoseira tamariscifolia</i>

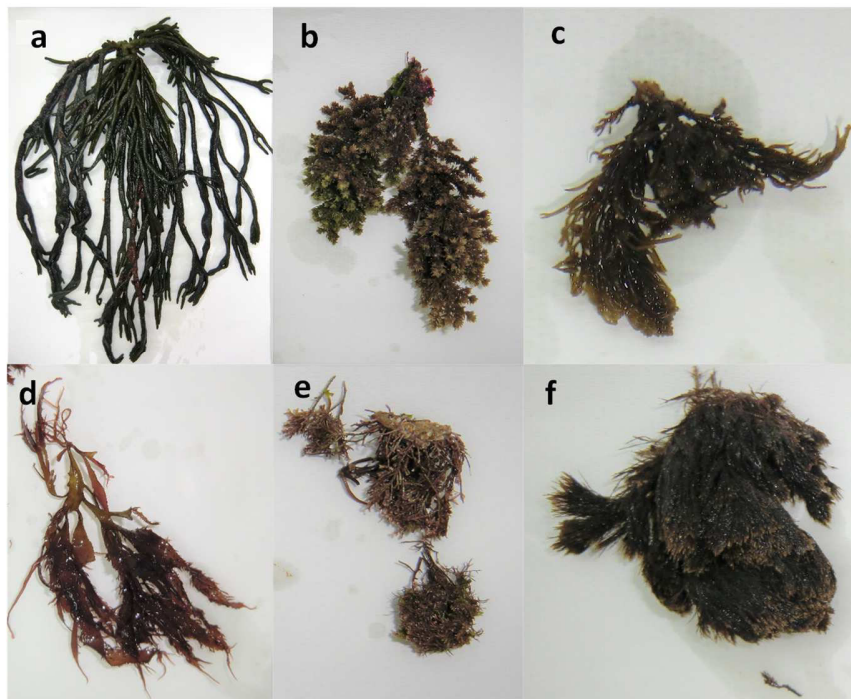


Figure 9: Different macroalgae used for the isolation of endophytic bacteria: (a) *Codium elongatum*, (b) *Cystoseira ericoide*, (c) *Cystoseira tamariscifolia*, (d) *Calliblepharis jubata*, (e) *Bryopsis balbisia*, and (f) *Halopteris scoparia*. Classification was done by the Moroccan project partners.

Furthermore, bacterial strains isolated from Moroccan aromatic plants were screened for inhibitory bioactivity against MDR strains. This screening, which was performed by the author of this thesis together with the Moroccan project partners in their laboratories, resulted in 16 strains that were applied to further work due to their inhibitory bioactivity. Table 3 shows information on these strains including the host plant, the part of the host, which was used for isolation, and the sampling region.

Table 3: 16 bacterial endophytes isolated from Moroccan aromatic plants including sampling side and (part of the) plant they were isolated from. The strain code is composed as follows: VW-XYZ and a number. VW are the initials of the host plant, X is the first letter of the sampling side, Y is the first letter of the part of the plant that was used for the isolation (R = root, L = leaf, S = stem), and z is an additional information on the isolation medium (y = YECD medium, w = WYEA medium). These strains have been isolated by the Moroccan project partners before.

Strain code	Sampling side	Host (part of the plant)
BH-ER11	Essaouira	<i>Ballota hirsuta</i> (root)
BH-ER12	Essaouira	<i>Ballota hirsuta</i> (root)
RA-ER35	Essaouira	<i>Rhus albida</i> (root)
RA-ER45	Essaouira	<i>Rhus albida</i> (root)
AM-EL53	Essaouira	<i>Asphodelus microcarpus</i> (leaf)
AH-TS86	Tata	<i>Anastatica hierochuntica</i> (stem)
ZG-TR94	Tata	<i>Zygophyllum gaetulum</i> (root)
ZG-TR96	Tata	<i>Zygophyllum gaetulum</i> (root)
PT-TS107	Tata	<i>Pergularia tomentosa</i> (stem)
PT_TS114	Tata	<i>Pergularia tomentosa</i> (stem)
PT-TS115	Tata	<i>Pergularia tomentosa</i> (stem)
CS-TS81	Tata	<i>Crotalaria saharae</i> (stem)
CS-TS85	Tata	<i>Crotalaria saharae</i> (stem)
HS-TRy87	Tata	<i>Haloxylon scoparium</i> (root)
HS-TRw87	Tata	<i>Haloxylon scoparium</i> (root)
PA-OR21	Oukaimeden	<i>Paronychia argentea</i> (root)

Monitor strains

The bacterial monitor strains that were used in the course of the bioactivity-guided approach are listed below.

For the MiMo_ALe project the following multidrug-resistant monitor strains were employed: *A. baumannii* resistant to imipenem (ABRi), *S. aureus* resistant to methicillin (MRSA), *P. aeruginosa* resistant to ceftazidime (PARc), and *K. pneumoniae* (KPR) and *E. coli* (ECR) both multi-resistant to extended spectrum (this term was introduced by the Moroccan project partners and is used in this thesis). The extended spectrum for ECR and KPR included β -lactam (amoxicillin, ceftazidime, and ticarcillin), aminoglycoside (netilmicin), sulfonamide (sulfamethoxazole) and fluoroquinolone (norfloxacin) antibiotics. These strains are clinical isolates, which have been isolated by the project partners in the hospital of Marrakesh, Morocco. The complete antibiogram for each MDR strain obtained by the Moroccan project partners can be found in chapter 2.1 of the appendix.

For the reporter-based bioassay that was performed by the project partners in Tübingen for the strains of the Tübingen actinomycetes strain collection, different mutants of a genetically modified *B. subtilis* 1S34 strain were employed. The mutants were genetically modified by the project partners based on the work of Piggot¹⁷³ with a certain promoter in combination with *lacZ*, which is being expressed in the case of promoter induction. The following promoters were used: *yorB* concerning DNA biosynthesis, *pps* concerning RNA biosynthesis, *yheI* concerning protein biosynthesis, *lial* concerning cell wall biosynthesis, and *fabH* concerning fatty acid biosynthesis. To prioritize, which samples may be of interest for the application in the reporter-based bioassay, samples were tested for inhibitory bioactivity against *B. subtilis* ATCC6051 first.

2.2. Analysis

High-resolution electrospray ionization mass spectrometry (HRESIMS) data were acquired using a Q Exactive Plus mass spectrometer (Thermo Fisher Scientific) equipped with a heated ESI interface coupled to an UltiMate 3000 HPLC system (Thermo Fisher Scientific). Analytical and semi-preparative HPLC separations were performed using an UltiMate 3000 HPLC system (Thermo Fisher Scientific) connected to a diode array detector (Thermo Fisher Scientific) and a low temperature evaporative light scattering detector (LT-ELSD) (Sedere). HPLC-UV data were analyzed with Chromeleon™ 7 (Thermo Fisher Scientific). HPLC-MS data were processed using FreeStyle™ 1.5 (Thermo Fisher Scientific). NMR experiments were performed on a Bruker Avance-II spectrometer operating at 600 MHz (^1H) or 150 MHz (^{13}C). NMR data were analyzed with ACD/Structure Elucidator Suite (2018.2). NMR data acquisition was performed by Andrea Porzel at the Leibniz-Institute for plant biochemistry in Halle (Saale).

Samples for the acquisition of NMR data were dissolved in 750 μL hexadeuterodimethyl sulfoxide ($\text{DMSO-}d_6$) or trideuteroacetonitrile ($\text{ACN-}d_3$) and transferred into a 5 mm NMR tube. To avoid contamination, the deuterated solvents were taken from ampoules containing 750 μL of solvent each. Thus, every NMR sample was dissolved in solvent from a separate and freshly opened ampoule.

For sample preparation for HPLC-UV and HRMS, all samples were either filtrated or dried under reduced pressure and dissolved in HPLC grade methanol with a certain mass concentration followed by centrifugation at 14000 rpm for 10 min. The supernatant was then used for analysis. For filtration, which was necessary for culture supernatants, multi-well plates (Pall Corporation) and a 96-well plate vacuum manifold (Phenomenex®) were employed.

Table 4 contains information on the HPLC method parameters (column dimensions and type, method parameters) for common screenings including the methods used for time-based micro-fractionation (N^o 1) and the method employed for HPLC-HRMS analysis (N^o 3).

Table 4: Frequently used HPLC methods for screenings, micro-fractionation, and HPLC-HRMS analyses.

Nº	Stationary phase	Mobile phase	Time [min]	Flow rate [mL/min]	T [°C]
1	Phenomenex® Luna (5 µm) C-18, 250x4.6 mm ID	5-100 % acetonitrile in water (0.1 % (v/v) formic acid each)	30	1.5	25
2	Phenomenex® Kinetex (2.6 µm) C-18, 100x3.0 mm ID	5-100 % acetonitrile in water (0.1 % (v/v) formic acid each)	12.5	0.6	50
3	Phenomenex® Kinetex (2.6 µm) C-18, 50x2.1 mm ID	5-100 % acetonitrile in water (0.1 % (v/v) formic acid each)	12.5	0.6	50

For dereplication of larger amounts of HPLC-HRMS data, I applied GNPS followed by data processing with the open source software platform Cytoscape.^{142,143,146} For this purpose, I used the following procedure: raw MS data were converted into mzXML format using MSconvert from the open source platform ProteoWizard with a binary encoding precision of 64-bit. Additionally two filters were applied. The filter “Peak Picking” was set to “Vendor” and the desired polarity (positive or negative ion mode) was set for the filter “Subset”. Using the GNPS online workflow, the mzXML data were clustered with a precursor ion mass tolerance and a fragment ion mass tolerance of 0.02 each and a minimum pairs cosine of 0.6 yielding the Cytoscape data that was applied to create a hit list based on molecular networking.

2.3. Isolation of endophytic *Bacteria* from macroalgae

For the isolation of endophytic *Bacteria*, the different macroalgae species, which were sampled at the west coast of Morocco, were washed with seawater still at the sampling place, and processed within 24 h. For the isolation of endophytic *Actinobacteria* from the different macroalgae species, two approaches were applied. For both approaches, the macroalgae were cut into pieces with approximately 0.5-2 cm in size followed by surface-sterilization. This was mandatory to assure the isolation of endophytic and not epiphytic bacterial strains.

For this purpose, the fragments were successively dipped into ethanol (95 %) for 1 min, sodium hypochlorite (1.25 %) for 4 min, and another ethanol solution (70 %) for 0.5 min. Then, the fragments were dipped into sterile water for 5 min to remove traces of the other three solutions, as they would inhibit bacterial growth in the next step.

For the first approach, the surface-sterilized fragments were air-dried, placed on YECD (yeast extract-casein hydrolysate) agar plates (yeast extract (0.3 g), K_2HPO_4 (2 g), casamino acids (0.3 g), and agar (15 g) per 1 L deionized water) and incubated at 30 °C (Figure 10). The YECD agar was modified with nalidixic acid (20 mg/L) and cycloheximide (80 mg/L) to suppress the growth of Gram-negative bacteria (suppressed by nalidixic acid)¹¹⁰ and fungi (suppressed by cycloheximide)¹¹¹. As negative control, the washing solution of the last step was used. After successful surface-sterilization, the final water solution was not supposed to contain any microorganisms. The endophytes were observed as colonies growing in the surrounding of the macroalgae fragments.



Figure 10: YECD agar plates with surface-sterilized macroalgae fragments for the macroalgae *Laurentia pinnatifida*, *Cystoseira tamariscifolia*, and *Ulva lactuca* (from left to right).

The second approach included a chemical as well as a high temperature treatment. For this purpose, the surface-sterilized fragments of the macroalgae were placed in 250 mL Erlenmeyer flasks containing 100 mL of a sterile solution for chemical treatment (sodium chloride (9 g), sodium dodecyl sulfate (0.02 g), glutamine (0.3 g), and calcium carbonate (0.5 g) per 1 L of deionized water) each. The flasks were incubated at 25 °C for 24 h. After this time, the temperature was increased to 55 °C for 30 min to kill bacteria that are more sensitive to higher temperature and thus less likely to be *Actinobacteria*, which are less affected by high temperature due to the high G+C content in their DNA. For the isolation of the bacteria that survived this treatment, 0.1 mL of the solution in the Erlenmeyer flasks as well as a 10-fold dilution were used to inoculate YECD agar plates containing nalidixic acid (20 mg/L) and cycloheximide (80 mg/L). The agar plates were then incubated at 30 °C.

In total, 10 endophytic bacterial strains were isolated using these two approaches. The final purification of the microbial strains was performed by the Moroccan project partners using the streak plate technique.

Microscopic and macroscopic analyses

The 10 endophytic strains were analyzed microscopically as well as macroscopically. For this purpose, the strains were cultivated on LB agar plates. Macroscopic pictures were acquired with a Stemi 508 microscope (Zeiss) equipped with an AxioCam MRc5 (Zeiss) and processed with ZEN 2.3 lite, blue edition (Zeiss). Microscopic analyses were performed using a Leica DM2000 LED microscope (Leica) and processed with LAS V4.2 (Leica).

2.4. Bacteria cultivation and extraction

For the used bacterial strains, the OSMAC approach was applied using different media for liquid fermentation.¹⁷⁴ For the evaluation of relevant fermentation conditions like fermentation medium and length, culture samples (1 mL each) were withdrawn on a daily basis and tested for bioactivity. For the strains of the Tübingen actinomycetes strain collection, the culture samples were tested in the reporter-based bioassays by the project partners in Tübingen whereas samples from the Moroccan strains were screened for inhibitory bioactivity against MDR strains. The latter was either performed by the author of this thesis, the Moroccan project partners or both. For the relevant fermentation conditions, medium extracts were generated and tested for the bioactivity that was observed for the culture samples.

Bacteria cultivation in small and larger scale

For small-scale cultivation in liquid fermentation medium, the bacterial strains were cultivated using 500 mL Erlenmeyer flasks containing 100 mL of liquid fermentation medium each. Incubation was carried out at 28 °C and shaking at 120 rpm. For inoculation, 30 µL of glycerol stock were used per 500 mL flask. For the preparation of the glycerol stocks, a sterile glycerol/water solution (1:1) was inoculated with an equal volume of either a well-grown bacterial culture or a suspension of bacterial aerial mycelium in sterile water. Both procedures yielded a final overall glycerol concentration of 25 % of the glycerol stock.

For larger scale fermentation with up to 12 L of liquid fermentation medium, 5 L Erlenmeyer flasks were employed containing 1 L of medium each. Fermentation conditions and media ingredients were the same as for small-scale fermentation. For inoculation of larger scale setups, small-scale pre-cultures were prepared with the same fermentation conditions (fermentation medium, temperature, shaking speed) used for the larger scale culture. The pre-culture was inoculated with 30 µL of glycerol stock. After 3-5 days of cultivation, 5 mL of pre-culture were used for the inoculation of each 5 L flask.

The used fermentation media for liquid fermentation were **Bennett** (beef extract (1 g), D-(+)-glucose (10 g), N-Z amine A (2 g), yeast extract (1 g), pH 7.3), **ISP2** (yeast extract (4 g), malt extract (10 g), D-(+)-glucose (4 g), pH 7.2),¹⁷⁵ **ISP3** (oatmeal (20 g), trace elements solution (5 mL), pH 7.3),¹⁷⁵ **NL19** (D-(+)-mannitol (20 g), full-fat soy flour (20 g), pH 7.5), **NL200** (D-(+)-mannitol (20 g), corn steep solids (20 g), pH 7.5), **NL300** (D-(+)-mannitol (20 g), cotton seed (20 g), pH 7.5), **NL333** (D-(+)-glucose (5 g), soluble starch (10 g), malt extract (10 g), yeast extract (3 g), Bacto peptone (3 g), ammonium nitrate (3 g), calcium carbonate (2 g), pH 7.2), **NL400** (D-(+)-glucose (10 g), soluble starch (20 g), Bacto peptone (3 g), beef extract (3 g), yeast extract (5 g), calcium carbonate (3 g), pH 7.0), **NL410** (D-(+)-glucose (10 g), glycerol (10 g), oatmeal (5 g), full-fat soy flour (10 g), yeast extract (5 g), Bacto casamino acids (5 g), calcium carbonate (1 g), pH 7.0), **NL500** (soluble starch (10 g), D-(+)-glucose (10 g), glycerol (10 g), fish flour (15 g), sea salts (10 g), pH 8.0). The trace elements solution contained $\text{CaCl}_2 \cdot 2\text{H}_2\text{O}$ (3 g), Fe-(III)-citrate (1 g), $\text{MnSO}_4 \cdot \text{H}_2\text{O}$ (200 mg), ZnCl_2 (200 mg), $\text{CuSO}_4 \cdot 5\text{H}_2\text{O}$ (25 mg), $\text{Na}_2\text{B}_4\text{O}_7 \cdot 10\text{H}_2\text{O}$ (20 mg), $\text{CoCl}_2 \cdot 6\text{H}_2\text{O}$ (4 mg), and $\text{Na}_2\text{MoO}_4 \cdot 2\text{H}_2\text{O}$ (10 mg).

The amounts of all ingredients are given for 1 L of deionized water. The pH was adjusted ± 0.2 using NaOH (2 M) or HCl (2 M). It is recommended not to use solutions of NaOH or HCl with higher concentrations as these may cause the change of medium components leading to non-reproducible results.

General procedure for the extraction of liquid fermentation broths

Small-scale extraction of liquid bacterial cultures was carried out in 50 mL centrifuge tubes and performed as follows: 20 mL of the liquid fermentation broth were withdrawn and centrifuged at 5000 rpm for 10 min to separate the supernatant from insoluble medium components and the bacterial biomass. Then, the pH of the supernatant was adjusted to 5.0 ± 0.2 using NaOH (2 M) or HCl (2 M). For extraction, organic solvent was added in a 1:1 (v/v) ratio. The organic solvent was either ethyl acetate (EtOAc), 1-butanol (1-BuOH) or dichloromethane (DCM). After the mixtures were kept in an overhead shaker for 30 min, phase separation was achieved by centrifugation at 5000 rpm for 5 min. After separation of the organic and the aqueous layers, the organic layer was dried under reduced pressure to obtain the medium extract.

For the extraction of larger scale fermentation broths, the culture broth was filtered through Celite® 545 and the pH of the filtrate was adjusted to 5.0 ± 0.2 using NaOH (2 M) or HCl (2 M). The filtrate was extracted with the desired organic solvent by stirring for 1 hour (Figure 11). After phase separation, the aqueous layer was employed for an additional extraction two more times. The volume of organic solvent used for each extraction was 1/3 of the total culture volume. Thus, in the end the ratio of culture volume and the volume of organic solvent used for extraction ended up being 1:1 (v/v). The combined organic layers were then dried under reduced pressure to obtain the medium extract. The desired solvent for larger scale extraction was ethyl acetate due to the hazardous properties of DCM and the high boiling point of 1-BuOH (118 °C).¹⁷⁶

The medium extracts were stored at -20 °C.



Figure 11: Setup for the extraction of larger scale fermentation culture broths.

2.5. Additional extraction of medium extracts

Due to the complexity of actinobacterial medium extracts, I performed an additional extraction and enrichment step before I isolated compounds of interest using semi-preparative HPLC. The direct isolation of compounds from the medium extract is usually not possible. The workflow of this additional extraction step is shown in Figure 12 and is used to separate crude bases, neutral compounds, and crude acids from each other.

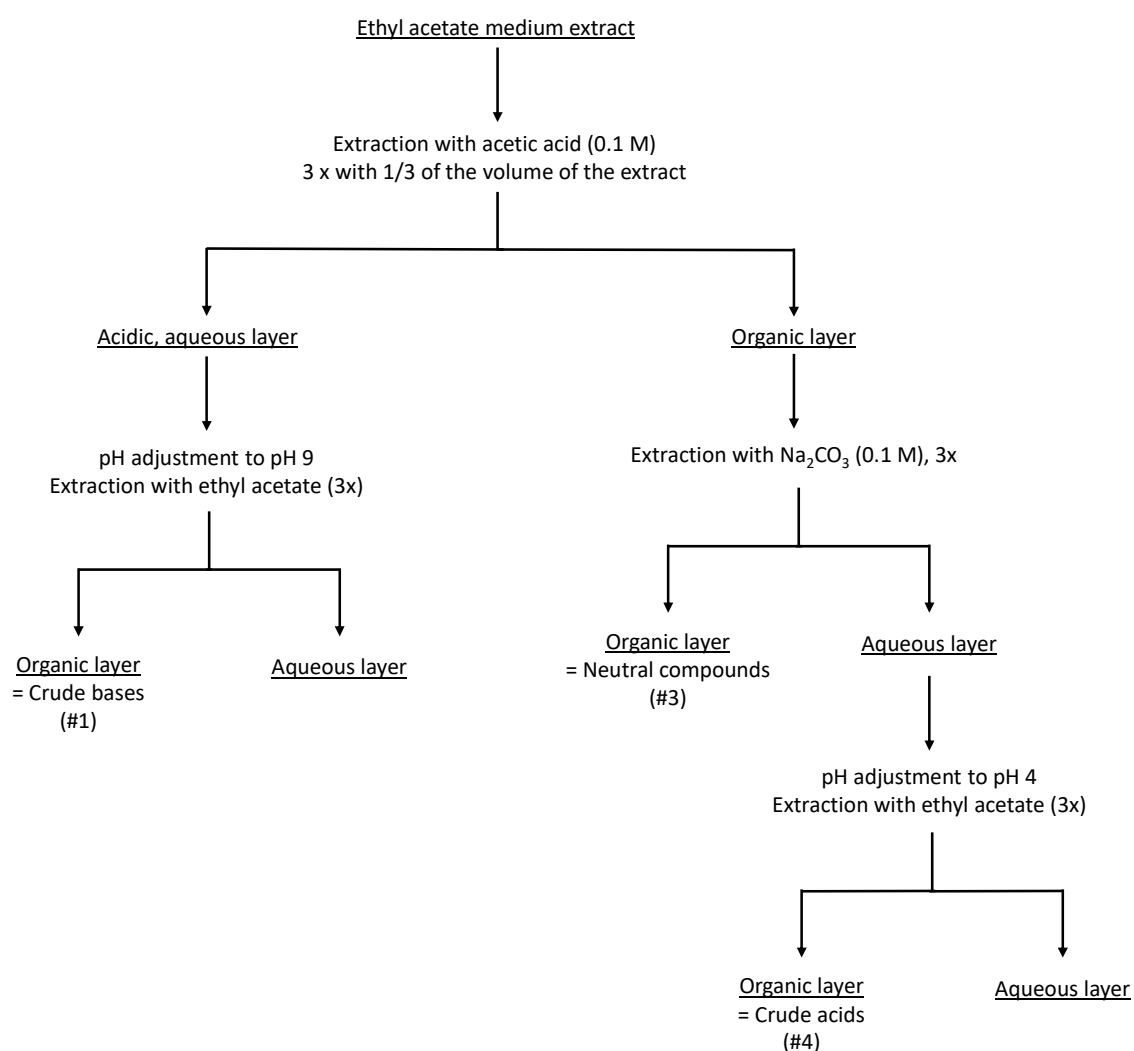


Figure 12: Workflow of the additional extraction procedure of medium extracts.

First, the medium extract is dissolved in the same solvent that was used for its generation. The volume to do this should be as small as possible but enough to properly dissolve the extract. The dissolved medium extract is then extracted with acetic acid (0.1 M). After phase separation, the organic layer is extracted another two times with acetic acid (0.1 M). For each extraction, the applied volume of acetic acid was one third of the volume that was used to dissolve the medium extract. Thus, the ratio of organic solvent and acetic acid sums up to be 1:1 (v/v). The pH of the combined aqueous layers was adjusted to 9.0 ± 0.2 followed by extraction with ethyl acetate. The extraction was performed in the same way as in the first step. The resulting combined organic layer contains the crude bases present in the initial medium extract. The corresponding aqueous layer can be discarded. The organic layer that was obtained from the extraction with acetic acid was extracted with Na_2CO_3 (0.1 M) in the same way as in the first step. The resulting organic layer contains the neutral compounds of the initial medium extract. The pH of the aqueous layer was adjusted to 4.0 ± 0.2 and extracted with EtOAc in the same way as before. The resulting organic layer contains the crude acids of the initial medium extract whereas the aqueous layer can be discarded.

For all extraction steps, I used centrifugation bottles and overhead shakers.

2.6. Antibacterial bioactivity assay

Tests for antibacterial bioactivity comprised the following assays: the test for inhibitory bioactivity against MDR pathogens, and non-pathogenic monitor strains, the report-based bioassays using different mutants of *B. subtilis* 1S34, and the test for synergistic antimicrobial activity against *B. subtilis* ATCC6051.

All performed inhibitory bioactivity assays were based on agar diffusion and performed using either LB medium (tryptone (10 g), yeast extract (5 g), sodium chloride (5 g), pH 7.0) or MH medium (beef infusion solids (2 g), soluble starch (1.5 g), casein hydrolysate (17.5 g), pH 7.4). The amounts of all ingredients are given per 1 L of deionized water. As ready-to-use media were employed, pH adjustment was not necessary.

For *B. subtilis* as monitor strain, LB medium was used whereby for the bioactivity assays targeting inhibition of MDR strains, MH medium was chosen.

2.6.1. Reporter-based bioassay

To evaluate, which samples are of interest to be used in the reporter-based bioassay, I screened them for inhibitory bioactivity against *B. subtilis* ATCC6051 first. For this purpose, molten LB agar was inoculated using an overnight culture of the monitor strain whose OD₅₄₆ was adjusted to 1.3 (0.1 mL of bacterial suspension was used per 10 mL agar). The OD₅₄₆ adjustment was carried out by dilution with LB medium. The overnight culture was incubated at 37 °C and shaking at 90 rpm. Samples were tested using the filter discs method (disc diameter 6 mm) applying 15-20 µL of the dissolved sample with a mass concentration of 40 mg/mL.

The reporter-based bioassay used for the strains of the Tübingen actinomycetes strain collection was performed by Katharina Wex, a PhD student of the group of Prof. Heike Brötz-Oesterhelt of the Eberhard Karls University in Tübingen and is based on the work of Urban *et al.*¹⁷⁷ Reporter-based bioassays were performed to obtain information regarding the mode of action (MOA) of bioactive compounds in the tested samples at the beginning of the bioactivity-guided workflow. The application of this reporter-based bioassay revealed the presence or absence of compounds interfering with the biosynthesis of DNA, RNA, proteins or the bacterial cell wall depending on the promoter used for the genetic modification of the *B. subtilis* strain.

The work of Urban *et al.* can be summarized as follows:¹⁷⁷ By screening an antibiotics library, they analyzed gene expression after antibiotic treatment. They were interested in genes that were being upregulated when an antibiotic interfered with one specific metabolic pathway like *e.g.* transcription, replication or protein biosynthesis. As the MOA of the different antibiotics were known, they were able to state a relation between the mode of action and the upregulation of gene expression. Then, the promoter regions of these genes were ligated to the reporter (in our case *lacZ*) that can be easily detected when expressed. Thus, every time the gene is expressed, also the reporter that is connected to the gene's promoter is expressed and can be detected.¹⁷⁷ In the case of *lacZ*, coding for the production of β-galactosidase, the expression can be easily detected when the medium contains X-Gal (5-bromo-4-chloro-3-indolyl-β-D-galactopyranoside). In the presence of β-galactosidase, X-Gal is hydrolyzed into the colorless products galactose and 5-bromo-4-chloro-3-hydroxyindole whereas the latter one is spontaneously being transformed by dimerization and oxidation into the blue pigment 5,5'-dibromo-4,4'-dichloro-indigo, which can be detected (Figure 13).^{178,179}



Figure 13: Illustration of the blue induction in the reporter-based assay (here caused by the positive control (rifampicin) from a screening of micro-fractions of Tü 27 for RNA biosynthesis interfering properties).

This blue pigment is formed at the interphase between the inhibition zone and the growth zone of the monitor strain. This is the case, as the monitor strain does not grow within the inhibition zone and thus there is no production of LacZ (there is actually no production at all, as the monitor strain does not grow within the inhibition zone). At the interphase, the monitor strain still “senses” the test compound but in concentrations that allow the monitor strain to survive (in agar diffusion assays, the concentration of a test compound decreases with increasing distance from the middle of the inhibition zone where the compound was applied). Thus, the monitor strain can survive even if a specific biosynthesis is disturbed, which causes the expression of *lacZ* that is ligated to the promoter of the biosynthetic pathway, which is disturbed by the sample.

For the reporter-based bioassay, agar diffusion assays were employed using 2-5 μL of sample with a mass concentration of 40 mg/mL for medium extracts and micro-fractions. The samples were dissolved in DMSO and directly given onto the agar without filter discs or drilled holes.

2.6.2. Test for synergistic antimicrobial activity

The test for a potential synergistic antimicrobial activity of pure compounds in combination with different antibiotics was performed by agar diffusion assays. For this purpose, the MIC values of actinomycin D, and tetracycline for *B. subtilis* were determined using LB agar medium. The antibiotics were dissolved in DMSO yielding a mass concentration of 1 mg/mL. After sterile filtration, the antibiotic solution was given to liquid agar medium before pouring the agar plates. In total, antibiotic concentrations ranged from 23.5 ng/mL to 50 µg/mL. The highest antibiotic concentration that still allowed visible growth of the monitor strain was chosen as sub MIC. 4 µg/mL was chosen for tetracycline and 0.047 µg/mL for actinomycin D.

For testing potential synergistic antimicrobial activity, the compound of interest was dissolved in DMSO (10 mg/mL) and directly given onto the test agar plates (1 µL). The agar plates were prepared as follows: after inoculation of the molten agar with the antibiotic in the sub MIC, the plates were poured. After solidification, the monitor strain was spread with a sterile swap covering the whole surface of the agar plate. The compound of interest was then given onto the agar without filter discs or drilled holes. All test plates were incubated at 37 °C for 16 h. Concentrations of interest were prepared as triplicates including a positive control (monitor strain spread on LB agar without any antibiotic) and a negative control (LB agar medium without monitor strain).

2.6.3. Test for inhibitory bioactivity against MDR strains

Unlike the bioactivity assays using *B. subtilis* as monitor strain, the MDR strains were not used to inoculate the molten agar medium as part of the preparation of the bioassay agar plates. The procedure that was used is as follows: In advance of every assay, the MDR strains were refreshed from conservation at -80 °C by inoculation of MH agar plates and incubation at 36 °C overnight. In the meanwhile, the MH agar plates that were used for the assay were prepared. For this purpose, new agar plates were poured and 45 holes (5 rows with 9 holes each) were drilled into each agar plate after solidification. After this, the MDR strains were spread onto these agar plates with a sterile swap covering the whole surface.

The results of the bioassays were evaluated by eye after incubation at 36 °C overnight. Figure 14 shows an MH agar plate as it was used. The sample (30 µL), which was tested for inhibitory activity, was given into the holes.



Figure 14: An MH agar plate with drilled holes to test supernatants of bacterial cultures for inhibitory bioactivity against ceftazidime-resistant *P. aeruginosa*. The lower left corner represents the positive control (10 µL of an apramycin solution with a mass concentration of 5 mg/mL in water).

The screening of different antibiotics (ampicillin, apramycin, chloramphenicol, kanamycin, fosfomicin, rifampicin, and tetracycline), revealed that apramycin was suitable as positive control for all used MDR strains (10 µL of a 5 mg/mL solution).

2.7. Cytotoxicity assay

Cytotoxicity assays were performed by Paul Barac, Martin-Luther-University Halle-Wittenberg. The analysis, visualization, and discussion of the results were carried out by the author of this thesis.

For the evaluation of cytotoxicity, the standard sulforhodamine B (SRB) colorimetric assay was used. Sulforhodamine B is a fluorescent dye that can be used, among others, for the quantification of cultured cells. The SRB assay was adapted from Vichai and Kirtikara and was performed as follows:¹⁸⁰

HeLa cells were maintained in Dulbecco's modified Essential Medium (DMEM) supplemented with Roticell-glutamine-solution (1 % (v/v), 2 mM) and heat-inactivated (60 °C for 30 min) fetal bovine serum (FBS, 10 % (v/v)). The used phosphate-buffered saline (PBS 10x) contained KCl (2 g), Na₂HPO₄·xH₂O (14.2 g), KH₂PO₄ (2.4 g) per 1 L deionized water and was diluted tenfold before use. All incubation steps were carried out in a humidified atmosphere containing 5 % (v/v) CO₂ at 37 °C.

The medium was removed and the cell monolayer was washed with PBS as soon as the confluence reached >80 %. After the addition of trypsin followed by incubation for 5 min, medium was added to resuspend the cells for their transfer into a reaction tube. After centrifugation (7 min at 150 rpm), the supernatant was removed and the cells were resuspended in medium. This cell suspension was transferred to a reaction tube. After the addition of Trypan Blue, the cell suspension was analyzed using an EVE™ cell counter, and the cell concentration was adjusted to 2.5x10⁵ cells/mL. The cell suspension with the adjusted cell concentration was then dispersed in a 96-well plate and incubated for 24 h. The compound, which was tested for cytotoxic activity was dissolved in DMSO and applied to the wells. DMSO with the same final concentration was used as negative control and either 5-fluorouracil, hygromycin B or doxorubicin served as positive control. After incubation for 48 h, the cells were fixed, stained, and analyzed by OD measurements. Cell fixation was performed by the addition of cold (4 °C) trichloroacetic acid (TCA, 10 %) followed by incubation at 4 °C for 1 h. Then, the medium and the TCA were discarded and the remaining cells were washed with water. Viable cells were fixed whereas dead cells were removed by the washing steps. The plates were dried with compressed air followed by staining with SRB solution (0.057 % solution in 1 % acetic acid) and incubated at 4 °C for 30 min. The staining solution was discarded and the fixed cells were washed with water similar to the previous step. After drying, the cells were prepared for the OD measurement. For this purpose, 2-amino-2-(hydroxymethyl)-1,3-propanediol (Tris base, 10 mM, pH 10.5) was added to each well. OD measurements were carried out at 510 nm using a Tecan-infinite

200 Pro (TECAN) with a shaking duration of 600 s and a shaking amplitude of 1 mm. Data were processed using i-control V2 (TECAN). For data illustration, GraphPad Prism 6 (GraphPad Software Inc.) was used.

The applied concentrations for the cytotoxicity assays ranged from 3-694 μM for leucine hydrazone, 0.19-3 mM for hygromycin B, 0.1-29 μM for G418, and 0.04-0.16 μM for actinomycin D.

Fractional Inhibitory Concentration Index

The determination of the FICI was carried out using the checkerboard assay.¹⁸¹ The checkerboard assay was performed in triplicates to obtain the information if the cytotoxic effect of the combination of leucine hydrazone and hygromycin B is synergistic ($\text{FICI} \leq 0.5$) or additive ($0.5 < \text{FICI} < 1.0$). Table 5 shows the different combinations of leucine hydrazone and hygromycin B, which were used.

Table 5: Template for the checkerboard assay including the used concentrations of leucine hydrazone, and hygromycin B.

		Concentration of leucine hydrazone in [μM]								
		694	347	174	87	43	22	11	5.4	0
Concentration of hygromycin B in [mM]	3									
	1.5									
	0.74									
	0.38									
	0.19									
	0									

For both compounds, stock solutions in DMSO (95 mM for hygromycin B and 69 mM for leucine hydrazone) were prepared. For normalization, the minimal value (0 % cell viability) was obtained for medium without cells and the maximum value (100 % cell viability) for cells with medium without hygromycin B or leucine hydrazone.

2.8. Molecular biology

Isolation of genomic DNA

The isolation of bacterial genomic DNA was performed using the kit NucleoSpin®Tissue (Machery Nagel) in accordance to the associated user manual. For sample preparation, aerial mycelium of a well-grown culture cultivated on agar medium was used.

PCR and gel electrophoresis

The obtained genomic DNA was amplified by polymerase chain reaction (PCR) using a 96 universal peqSTAR thermocycler (PEQLAB Biotechnology GmbH). The master mix contained 5xbuffer (250 µL/mL), dNTPs (10 mM with 2.5 mM each, 25 µL/mL), DMSO (37.5 µL/mL), MilliQ water (537.5 µL/mL), and Taq polymerase (25 µL/mL) as well as two primers specific for *Actinobacteria* (10 µM, 62.5 µL/mL each). The primers were ordered from eurofins Genomics (fD1: (5'→3') AGAGTTTGATCCTGGCTCAG and rP2: (5'→3') ACGGCTACCTTGTTACGACTT,¹⁸² and 8F (5'→3'): AGAGTTTGATCCTGGCTCAG and 1510R (5'→3'): GGTTACCTTGTTACGACTT¹⁸³). The PCR program included an initial denaturation (96 °C for 2 min) and 30 cycles of denaturation (96 °C for 45 s), annealing (56 °C for 30 s), extension (72 °C for 2 min) followed by a final extension (72 °C for 5 min).¹⁸²

Gel electrophoresis was carried out using an agarose gel (1.5 % (m/v)) at 135 V. The gel was prepared by dissolving agarose in TAE buffer (0.5x). The TAE (50x) buffer contained tris(hydroxymethyl)aminomethane (tris, 242.2 g), ethylenediaminetetraacetic acid (EDTA, 100 mL, 0.5 M, pH 8), and acetic acid (57.1 mL).¹⁸⁴ This solution was adjusted to 1 L with deionized water. For gel electrophoresis, a 100-fold dilution of the 50x TAE buffer was prepared.

Rotistain® (50 µL/L) was applied for staining and 6xloading buffer represented 1/6 of total sample volume for gel electrophoresis. GeneRuler DNA Ladders (Thermo Fisher Scientific) were used as ladders.

The results were analyzed using a Syngene G:BOX gel documentation system (VWR).

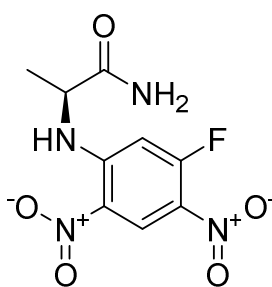
Extraction of pure DNA

After gel electrophoresis, extraction of pure DNA was carried out using the GeneJET Gel Extraction Kit (Thermo Fisher Scientific) using the procedure as it is described in the associated user manual.

The extraction of amplified DNA from the gel electrophoresis gel was preferred over its isolation from the PCR mix as the former procedure usually yields purer DNA compared to the latter one.

2.9. Determination of the absolute configuration using Marfey's reagent

The principle of the determination of stereochemistry using Marfey's reagent (FDAA: 1-fluoro-2,4-dinitrophenyl-5-L-alanine amide; Figure 15, **11**) is based on the different retention times observed using HPLC analysis of the corresponding D- and L- amino acids after derivatization using FDAA. Underivatized D- and L-stereoisomers of an amino acid have the same retention time when being analyzed with HPLC of RP₁₈ columns. The difference after derivatization with Marfey's reagent is due to hydrogen bonding that differs in dependence of the stereochemistry of the derivatized amino acid. This difference in hydrogen bonding causes differences in the interaction of the amino acid derivative with the packing material of the HPLC column and thus causes different retention times.¹⁸⁵



11

Figure 15: Chemical structure of FDAA (**11**).¹⁸⁵

Compared to the method described in the literature, modifications were made regarding the derivatization using Marfey's reagent as well as the HPLC analysis.^{185,186}

The compounds (1.0 mg each) were hydrolyzed in hydroiodic acid (1 mL, 48 %). The reaction mixture was maintained in a sealed reaction vessel at 110 °C for 16 h. As hydroiodic acid is a stronger acid compared to HCl, hydroiodic acid was used for hydrolysis to ensure a complete hydrolysis of the compounds and the present hydroxy-ornithin moieties.

After drying under a stream of nitrogen at 105 °C, FDAA solution in acetone (50 µL, 0.04 M) and NaHCO₃ (100 µL, 1 M) were added to each reaction vessel. The reaction mixture was kept at 80 °C for 3 min, cooled down to room temperature and acidified with HCl (50 µL, 2 M). After the addition

of ACN/water (200 μ L, 1:1), the FDAA-amino acid derivatives of the hydrolysates were analyzed and compared with standard FDAA-amino acid derivatives by HPLC analysis:

Phenomenex® Kinetex C-18 RP (2.6 μ m) 100x3 mm was applied as stationary phase. As mobile phase, a combination of acetonitrile and water (with 0.1 % (v/v) FA each) was used. The gradient that was used for separation was 5 % ACN to 45 % ACN within 20 min with a flow rate of 0.6 mL/min at 50 °C. Detection was carried out at 340 nm.

The absolute configuration of each amino acid was determined by comparing the obtained retention times of the derivatized hydrolysates of the compounds with authentic standards of the respective derivatized D- and L-amino acids.

3. Results and discussion

3.1. Tübingen actinomycetes strain collection

The aim of the work investigating strains from the Tübingen actinomycetes strain collection was the identification and isolation of novel biologically active specialized metabolites followed by structure elucidation. The reporter-based bioassay, which was performed by the project partners in Tübingen for these strains, was supposed to reveal the mode of action of a potentially new NP in the beginning of the bioactivity-guided workflow.

For this purpose, 280 strains of the Tübingen actinomycetes strain collection that were screened in previous projects, resulted in 13 strains of interest that were chosen for further investigation in the course of this thesis. These investigations, which included, among others, the application of the OSMAC approach, resulted in the dereplication of pactamycin, which can be seen as a proof of concept regarding the applied reporter-based bioassay. Furthermore, I isolated a novel NP produced by *S. fradiae* Tü 27.

3.1.1. Concept verification by rediscovering pactamycin from Tü 6448

The application of the strain *Micromonospora* Tü 6448 using the reporter-based bioassay revealed the presence of protein biosynthesis interfering compounds in the ethyl acetate medium extract of this strain. The dereplication of the known biosynthesis inhibiting pactamycin (Figure 18, 12) was performed using HPLC-HRMS (Figure 16). Pactamycin was dereplicated applying the elemental composition analysis tool of FreeStyle® 1.5 using a mass difference of 1 ppm. Pactamycin is an aminocyclopentitol-derived specialized metabolite produced by *Streptomyces pactum*.^{187–189} The compound was obtained by fermentation of Tü 6448 in liquid ISP2 medium. Incubation was carried out at 27 °C and shaking at 90 rpm. After 7 days, the pactamycin-containing ethyl acetate medium extract was generated.

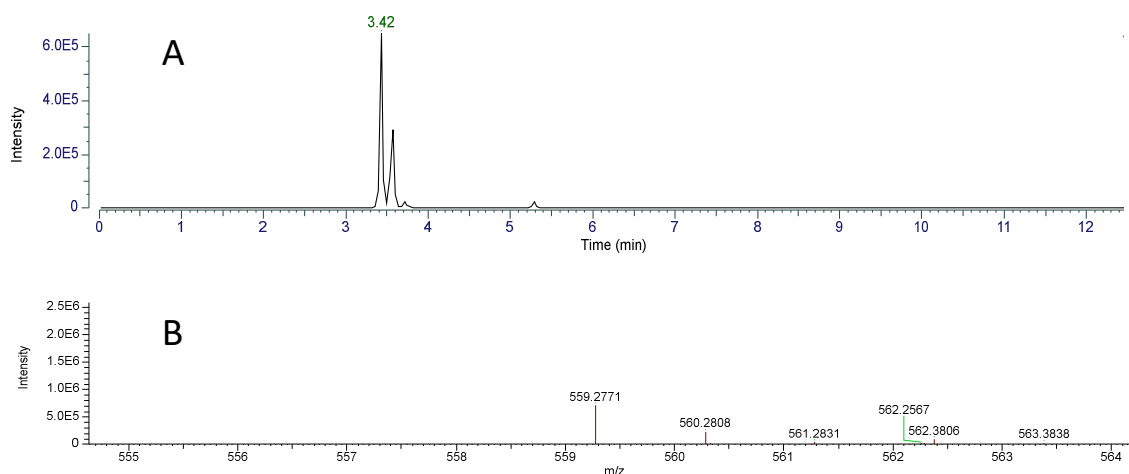


Figure 16: (A) Extracted ion chromatogram of the ethyl acetate medium extract of Tü 6448. The signal at 3.42 min belongs to pactamycin. (B) The mass spectrum showing the signal at m/z 559.2771 caused by pactamycin obtained in positive ion mode.

Figure 17 shows the results of the reporter-based bioassay as it was obtained for the ethyl acetate and 1-butanol medium extracts of Tü 6448 and Tü 6457 after fermentation for 72 and 168 h. In this case, the used *B. subtilis* strain was genetically modified to indicate the presence of protein biosynthesis interfering compounds. The blue induction that can be observed for all 8 samples indicates the presence of such compounds.

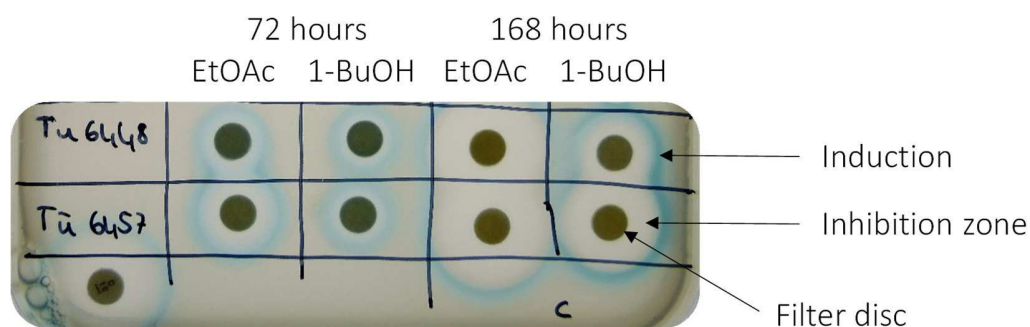
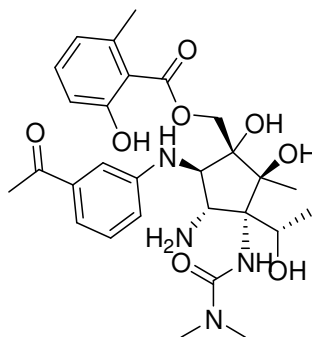


Figure 17: Reporter-based bioassay for the medium extracts of Tü 6448 and Tü 6457 generated after 72 and 168 h. For this agar plate, *B. subtilis* 1S34 modified with an *yheI* promoter was employed to screen for protein biosynthesis interfering compounds.

The observation of protein biosynthesis interfering bioactivity (in our case with a reporter-based bioactivity assay applying a *B. subtilis* 1S34 strain that was genetically modified with an *yheI* promoter) of a medium extract containing pactamycin is in accordance to literature. Pactamycin is known to inhibit the synthesis of proteins in *Archaea*, *Bacteria* (both Gram-positive and Gram-negative), and *Eukarya*.^{187,190}



12

Figure 18: Chemical structure of pactamycin (12) with the sum formula $C_{28}H_{38}N_4O_8$.^{187,188}

Even though pactamycin, which might be most likely responsible for the observed bioactivity, is an already known NP, its dereplication can be seen as a proof of concept for the reporter-based bioassay.

3.1.2. *Streptomyces fradiae* Tü 27

The strain *S. fradiae* Tü 27 was one of 13 strains that were applied as part of this thesis. Previous reporter-based bioassays suggested the presence of an RNA biosynthesis interfering compound produced by Tü 27.

To obtain information on relevant fermentation conditions for Tü 27 that cause the production of the specialized metabolite with the RNA biosynthesis interfering bioactivity, the OSMAC approach was applied using 7 different fermentation media (NL19, NL200, NL300, NL333, NL400, NL410, and NL500). For this purpose, I screened the culture broths that were withdrawn on a daily basis over a period of 14 days for inhibitory bioactivity against *B. subtilis* ATCC6051. Then, the samples inhibiting the growth of *B. subtilis* ATCC6051 were employed for the reporter-based bioassay searching for RNA biosynthesis interfering compounds.

The results of the screening for inhibitory bioactivity against *B. subtilis* ATCC6051 are shown in Table 6.

Table 6: Results of the bioassays of the withdrawn culture samples obtained from the OSMAC approach for Tü 27 against *B. subtilis* ATCC6051. (-) indicates no observed inhibitory bioactivity. The numbers represent the diameter of the inhibition zone in cm.

Day \ Medium	NL19	NL200	NL300	NL410	NL500
1	-	-	-	-	-
2	-	-	-	-	-
3	1.2	1.1	1.0	-	-
4	1.1	1.7	1.6	1.5	-
6	1.8	1.8	1.6	1.4	1.5
7	1.6	1.7	1.5	1.3	1.5
8	1.5	1.5	1.4	1.2	1.4
9	1.5	1.5	1.6	1.3	1.4
14	1.6	1.5	1.6	1.2	1.4

The results of the reporter-based bioassay are shown in Table 7. Withdrawn culture broths of Tü 27 cultivated in NL333, and NL400 did not show any inhibitory bioactivity against *B. subtilis* ATCC6051 and were thus not tested in the reporter-based bioassay.

Table 7: Results of the reporter-based bioassay performed by the project partners in Tübingen targeting RNA biosynthesis of the withdrawn culture samples that showed inhibitory bioactivity against *B. subtilis* ATCC6051. The intensity of inhibition/induction is illustrated by “+” and “++”. “+++” means there was a stronger inhibition/induction observed than when “+” is used. “±” means no relevant inhibition/induction and “n.d.” means “not determined”.

Day \ Medium	NL19	NL200	NL300	NL410	NL500
3	+/+	+/+	+/+	n.d.	n.d.
4	+/+	++/+	+/+	+/+	n.d.
6	++/+	++/+	+/+	+/+	+/+
7	++/+	+/+	+/+	+/+	++/+
8	++/+	+/+	+/+	+/±	+/±
9	++/+	+/+	+/+	+/+	+/+
14	++/+	+/+	+/+	+/+	+/+

Based on these results, I chose NL19 as fermentation medium, and a cultivation length of 14 days as fermentation conditions for the production of the compound of interest. Besides the results of the bioactivity assay, NL19 was further chosen as its extraction could be carried out without major difficulties like problematic phase separation. Further, unlike *e.g.* ISP3, NL19 does not contain heavy metals like copper ($\text{CuSO}_4 \times 5\text{H}_2\text{O}$) or cobalt ($\text{CoCl}_2 \times 6\text{H}_2\text{O}$), which makes it less hazardous to handle in larger amounts for larger scale fermentation.¹⁷⁵

For further analysis, the strain was cultivated applying the fermentation conditions mentioned above, and medium extracts using 1-BuOH, DCM, and EtOAc were generated. After micro-fractionation with HPLC, the medium extracts as well as their corresponding micro-fractions were tested in the reporter-based bioassay for RNA biosynthesis interfering bioactivity. Even though only the 1-BuOH medium extract showed the expected bioactivity among the three medium extracts, the bioactivity was observed for certain micro-fractions of each of the three medium extracts. Additionally, the pattern of bioactive micro-fractions was congruent for all three medium extracts. Thus, we suggested that the same biologically active compound was present in all three medium extracts even though the bioactivity could be observed neither for the DCM nor EtOAc medium extract. It might be possible that the ethyl acetate medium extract and the dichloromethane medium extract contain compounds that interfere with the bioactivity of the RNA

biosynthesis interfering compound. This would explain the circumstance that the RNA biosynthesis interfering bioactivity was not observed for these medium extracts.

As Tü 27 is a known actinomycin D producer, we were aware of the possibility that the observed bioactivity might be caused by this antibiotic, which interferes with RNA biosynthesis.¹⁹¹ However, HPLC-MS analysis of the biologically active medium extracts and micro-fractions did not confirm the presence of actinomycin D.

Furthermore, Tü 27 is known to produce tetracyclines, which interfere with protein biosynthesis and are thus not supposed to induce the *ppS* promoter.^{177,192} Thus, tetracyclines should not be responsible for the induction in the reporter-based bioassay targeting RNA biosynthesis interfering compounds.

For further analyses, Tü 27 was cultivated in 12 L scale, and the corresponding ethyl acetate medium extract was generated. Ethyl acetate was chosen due to its lower boiling point (77 °C) compared to 1-butanol (118 °C), which facilitates the evaporation of the solvent to obtain the medium extract. The aim was to isolate and characterize the compound that is responsible for the initially observed bioactivity.

Additional extraction

To facilitate the isolation of compounds with semi-preparative HPLC, the additional extraction procedure was used for purification and enrichment of the ethyl acetate medium extract (43 g) obtained from the 12 L culture of Tü 27.

Compared to small-scale fermentation, the HPLC-UV chromatogram of the ethyl acetate medium extract of the 12 L culture (Figure 19) shows more hydrophilic compounds. This is due to an incomplete phase separation during the extraction of the 12 L culture causing the presence of more water and thus more hydrophilic compounds in the organic layer.

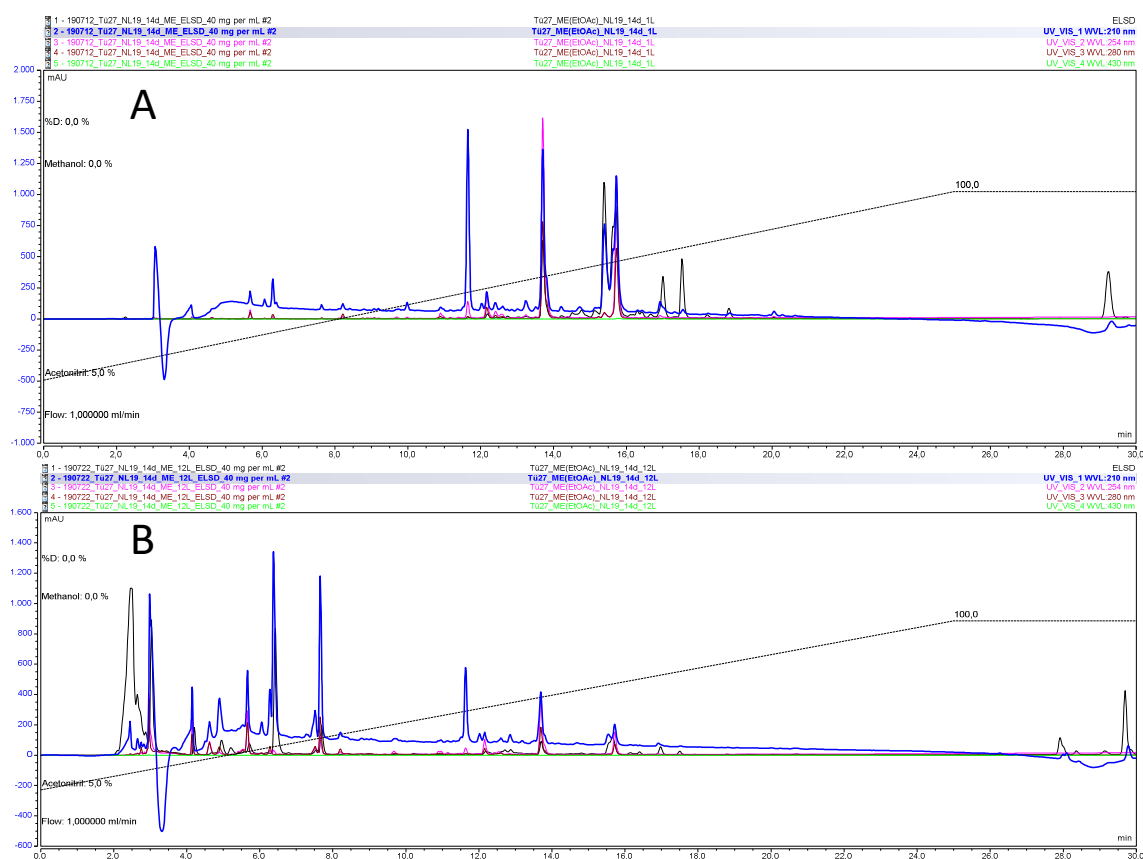


Figure 19: HPLC-UV chromatograms of ethyl acetate medium extracts obtained from (A) the 1 L culture and (B) the 12 L culture of Tü 27 after fermentation in NL 19 for 14 d. The detection was done at 210 nm (blue), 254 nm (magenta), 280 nm (brown), 430 nm (green), and with the ELSD (black).

In total, three fractions were obtained after the additional extraction: crude acids, crude bases, and neutral compounds. Focusing on rather lipophilic compounds, the aqueous layers were analyzed using HPLC-UV and discarded. The comparison of the HPLC-UV chromatograms (Figure 20) of these three fractions showed that several compounds were present in all of them, especially the compounds with the retention times 14, and 16 min. This might be due to either the presence of several functional groups, making them not only acidic or basic under the extraction conditions or due to a non-quantitative extraction. The HPLC-UV analyses of the aqueous fractions showed that the additional extraction procedure separated the hydrophilic compounds of the medium extract from the lipophilic compounds, which were of interest. Two of the three obtained fractions were used for direct isolation of compounds using semi-preparative HPLC.

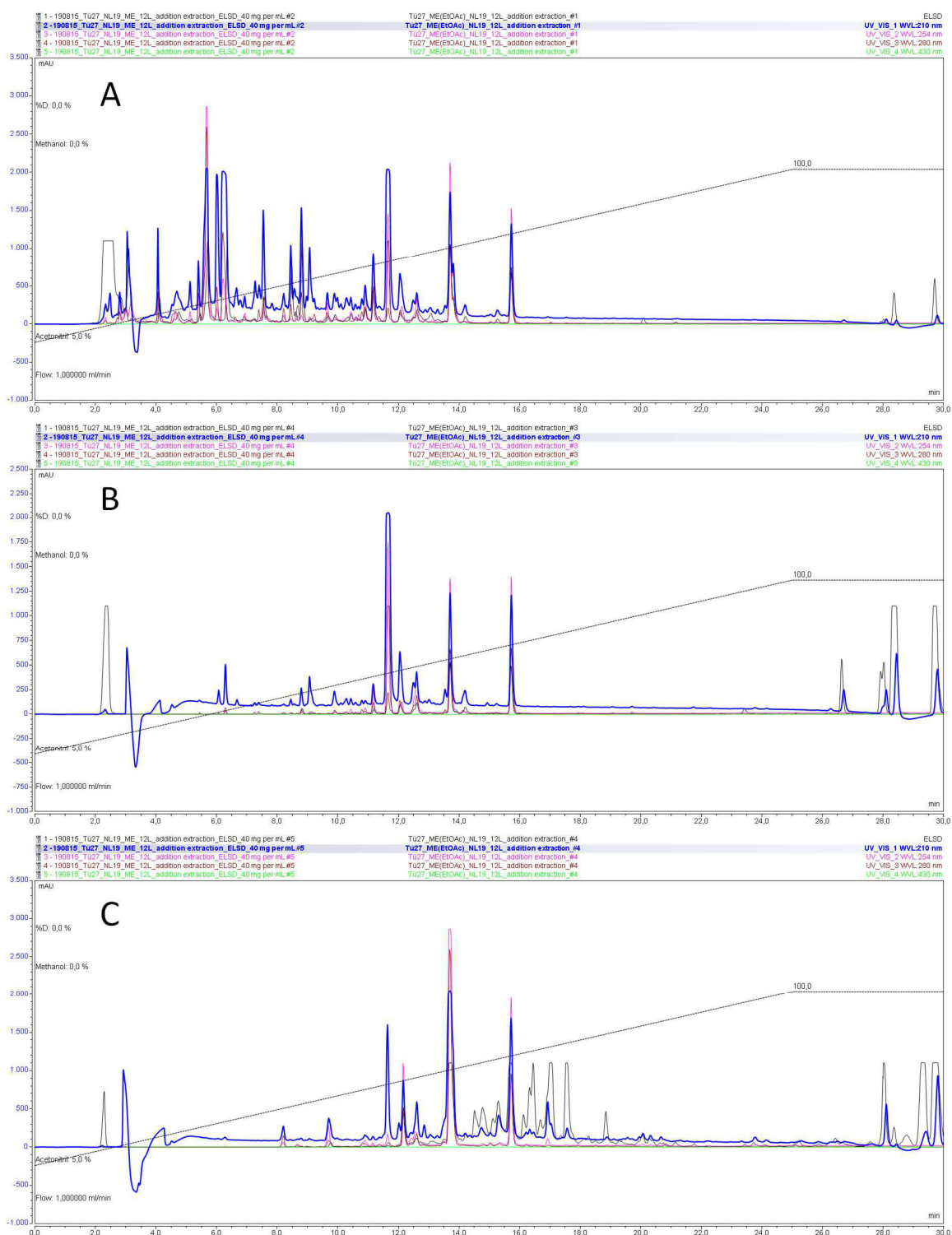


Figure 20: HPLC-UV chromatograms of the fractions containing (A) crude bases, (B) neutral compounds, and (C) crude acids after the additional extraction. Detection was carried out at 210 nm (blue), 254 nm (magenta), 280 nm (brown), 430 nm (green), and with the ELSD (black).

3.1.3. Isolation and structure elucidation

The fraction that was used for the isolation of compounds by HPLC was the fraction containing the basic compounds of the ethyl acetate medium extract. The first step was the application of different HPLC columns to evaluate the best combination of stationary phase (C-18, pentafluorophenyl (PFP), or phenylhexyl (PH)) and mobile phase for an adequate compound separation.

This included the following HPLC columns: Luna (5 μ m) C-18, 250x4.6 mm; Luna (5 μ m) PFP, 250x4.6 mm; and Luna (5 μ m) PH, 250x4.6 mm.

The tested variations of the mobile phase included two different organic solvents (methanol (MeOH) or acetonitrile (ACN)) as well as the performance with or without the addition of formic acid (0.1 % (v/v)) to both the organic solvent and the water. Hence, every column was tested for its suitability to separate the compounds by the performance of four different HPLC methods each:

1. MeOH as organic solvent and addition of FA (0.1 % (v/v)) to MeOH and water,
2. MeOH as organic solvent without adding FA to MeOH and water,
3. ACN as organic solvent and addition of FA (0.1 % (v/v)) to ACN and water,
4. ACN as organic solvent without adding FA to ACN and water.

This revealed PFP to be the most suitable stationary phase in combination with MeOH with added FA (0.1 % (v/v)) as mobile phase. After the most suitable stationary and mobile phase were obtained, gradient optimization was carried out. This optimization step resulted in the optimized method shown in Table 8, which was used for compound isolation.

Table 8: Optimized HPLC method for compound isolation from the basic fraction obtained from the ethyl acetate medium extract of Tü 27.

Stationary phase	Mobile phase gradient (MeOH + 0.1 % FA (v/v))	Time [min]	Flow rate [mL/min]	T [°C]
Phenomenex® Luna (5 µm) PFP, 250x4.6 mm ID	5-60 %	0-13	1.0	21
	60 %	13-17		
	60-80 %	17-24		
	80-100 %	24-26		
	100 %	26-31		

For the isolation, a corresponding semi-preparative HPLC column (Luna (5 µm) PFP, 250x10 mm ID) was used. The flow rate of the optimized method was adjusted to 4.7 mL/min while the other parameters were retained. The compounds were collected using an automated peak-based fraction collection. As pool wrapping was disabled, fractions of the same compound were combined afterwards. The HPLC-UV chromatogram of the compound isolation is shown in Figure 21. The collected compounds are highlighted in blue.

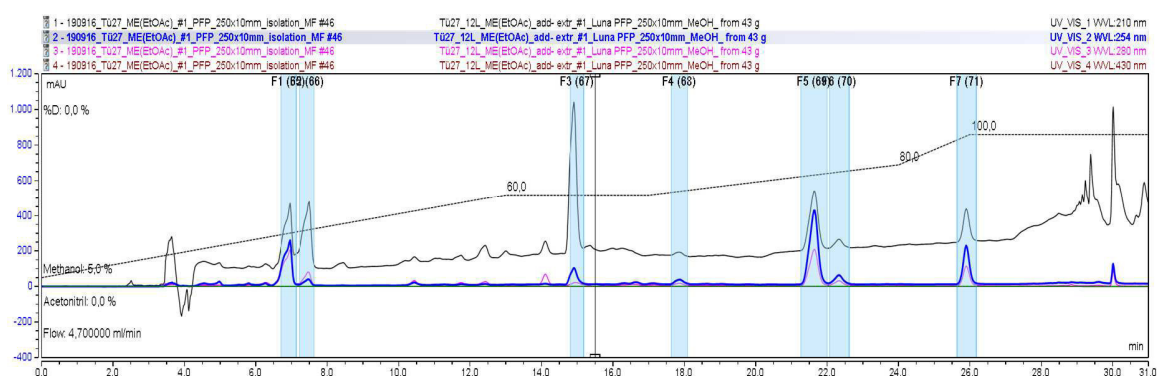


Figure 21: HPLC-UV chromatogram of the optimized isolation method for fraction 1, basic compounds. The signals corresponding to the isolated compounds are highlighted in blue. The detection was done at 210 nm (black), 254 nm (blue), 280 nm (magenta), and 430 nm (brown).

The two compounds at a retention time of approximately 7 min were collected due to completeness as they are strongly overlapping at higher injection volumes as they were applied to compound isolation. At lower injection volumes that were used for method optimization these compounds appeared properly separated. As these compounds were not of main interest, the fact that they were not well-separated at higher injection volumes was ignored for compound isolation, which focused on compounds with higher retention times.

After the isolation, the combined fractions were dried under reduced pressure to obtain the isolated compounds. Methanol was removed using rotary evaporators. The remaining water/FA mixture was dried by lyophilisation to avoid damage or the destruction of the isolated compounds by high FA concentrations and thus low pH at the end of drying. This would be the case using rotary evaporators or vacuum centrifuges as FA has a slightly higher boiling point (100.8 °C) than water (100.0 °C).

I evaluated the purity of the isolated compounds (Table 9) using HPLC-UV and HPLC-MS data and pure compounds were submitted for NMR analysis. NMR data were acquired by Andrea Porzel at the Leibniz-Institute for plant biochemistry in Halle (Saale) and included ^1H , ^{13}C (when the isolated amount was sufficient), HSQC, COSY, HMBC, and TOCSY.

Table 9: Isolated compounds and estimated sum formulae.

compound name	isolated mass [mg]	estimated sum formula*
P3	0.5	$\text{C}_{12}\text{H}_{23}\text{O}_4\text{N}$
P4 (leucine hydrazone)	3.8	$\text{C}_6\text{H}_{12}\text{O}_2\text{N}_2$
P5	0.1	$\text{C}_{21}\text{H}_{20}\text{O}_8$
P6 (daidzeine)	2.0	$\text{C}_{15}\text{H}_{10}\text{O}_4$
P7	5.8	$\text{C}_{16}\text{H}_{12}\text{O}_5$
P8	0	$\text{C}_{15}\text{H}_{10}\text{O}_5$

* Molecular formulae were estimated using FreeStyle® and high-accuracy HPLC-MS data.

The amount of the isolated compounds might be incorrect due to the used balance.

3.1.3.1. Dereplication of daidzeine

Compound P6 was shown to be daidzeine, a compound that can be isolated from soy. As the fermentation medium for Tü 27 contained soy flour, this finding is unfortunate but not unreasonable. 1D and 2D NMR data as well as HRMS analysis confirmed these findings.¹⁹³

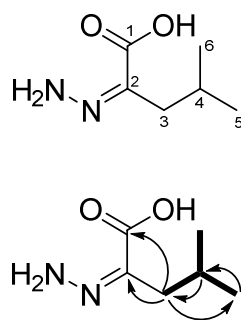
3.1.3.2. Hydrazone derivatives of amino acids

Hydrazone derivative of leucine

Leucine hydrazone (Figure 22, **13**) was isolated as a colorless solid. HRESIMS in positive ion mode revealed a signal at m/z 145.0970 $[M+H]^+$. Using this HRESIMS data, the molecular formula of leucine hydrazone was established as $C_6H_{12}N_2O_2$ with a corresponding exact mass of 144.0891 g/mol. The UV spectrum obtained from HPLC-UV showed a maximum at 211 nm. The 1H -NMR spectrum of the compound in $DMSO-d_6$ (Table 10) shows a broad singlet of the carboxylic acid moiety [δ_H 11.54 ppm (1H, br s)], one methylene group [δ_H 2.35 ppm (2H, d, 7.34 Hz)], one methine group [δ_H 1.91 ppm (m)], two methyl groups [δ_H 0.83 ppm (d, 6H), 6,79 Hz] and two hydrogens of an amino group [δ_H 7.09 and 7.20 ppm (s, 1H each)]. The ^{13}C -NMR revealed one carbonyl carbon (δ_C 165.8 ppm), one quaternary carbon (δ_C 153.3 ppm), and four sp^3 hybridized carbon atoms (δ_C 22.6, 25.6, and 31.6 ppm).

Table 10: 1H (600 MHz) and ^{13}C (125 MHz) NMR spectroscopic data of leucine hydrazone in $DMSO-d_6$.

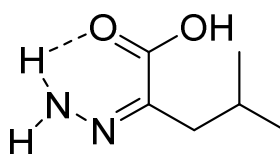
Position	δ_H (ppm), multiplicity (J [Hz])	δ_C (ppm), type
1	-	165.8, C
2	-	153.3, C
3	2.35, d (7.34)	31.6, CH ₂
4	1.91, m	25.6, CH
5, 6	0.83, d (6.79)	22.6, CH ₃
-N=	-	-
NH₂	7.09 and 7.20, s	-
COOH	11.54, br s	-



13

Figure 22: Chemical structure of leucine hydrazone and HMBC (arrows) and ^1H - ^1H COSY (bold bars) correlations.

Detailed analysis of the ^1H -NMR spectrum revealed the two singlets of the NH_2 group. This can be explained as hydrogen bonding can occur between one hydrogen atom of the NH_2 group and the oxygen of the carbonyl moiety causing a six-membered ring structure that usually exhibits stabilizing properties (Figure 23).¹⁹⁴ This hydrogen bonding causes the two NH_2 hydrogens to be non-equivalent and thus causing two separate signals in the ^1H -NMR spectrum.



13

Figure 23: Illustration of possible hydrogen bonding (dashed line) between a hydrogen atom of the NH_2 group and the oxygen of the carbonyl moiety in leucine hydrazone causing magnetic inequivalence of the two NH_2 hydrogens in the ^1H -NMR spectrum.

The elucidated structure clearly shows that the compound is, from a structural point of view, a hydrazone derivative of the proteinogenic amino acid leucine.

Even though MS^2 data were acquired, it is challenging to state a characteristic fragmentation pattern. This is, among others, because MS^2 data for hydrazones can hardly be found.^{195–197}

Together with hydrazines and hydrazides, hydrazones belong to the rather scarce category of nitrogen-nitrogen bond containing NPs (N2NP), which are known since the 1950s.¹⁹⁸ Since this time, several organisms were found to produce these N2NPs including actinomycetes, filamentous fungi and mushrooms, plants, and marine organisms like sponges.¹⁹⁹

Hydrazones and hydrazides of microbial origin are, among others, produced by bacteria of the genus *Streptomyces* like *S. sp.* IFM 11299, producing the hydrazone katorazone (Figure 24, **14**),²⁰⁰ and *S. sp.* 11307, producing the hydrazone yoropyrazone (Figure 24, **15**).²⁰¹ Additional examples for microbial N2NPs include negamycin (Figure 24, **16**), produced by *S. purpeofuscus*,^{202–204} the antibiotic FR-900137, produced by *S. unzenesis*,²⁰⁵ the antibiotic XK-90, produced by *S. sp.* MR-90,^{206,207} and fosfazinomycin A and B, produced by *S. lavendofoliae*.²⁰⁸

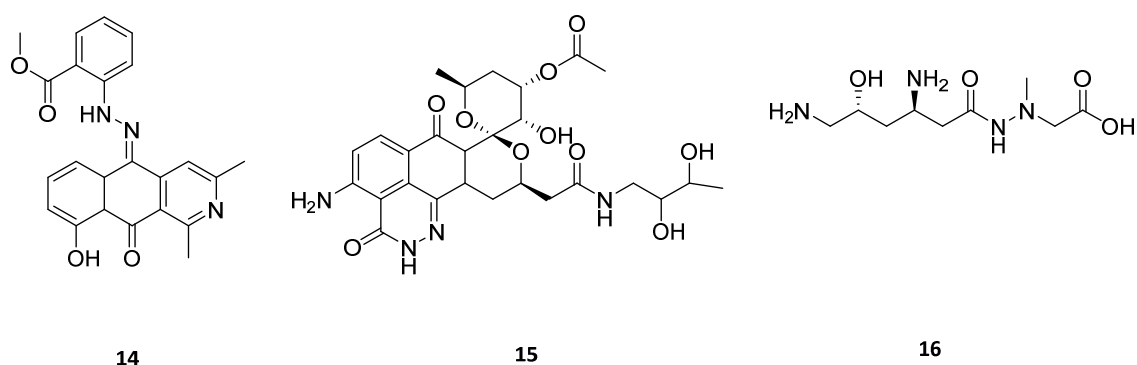


Figure 24: Chemical structures of katorazone (**14**)²⁰⁰, yoropyrazone (**15**)²⁰¹ and negamycin (**16**).²⁰⁴

Besides remarkable structural diversity, these compounds can exhibit a variety of biological activity *e.g.* as antimicrobial, antifungal, anticancer, antioxidant, and antigenotoxic agents, which make them interesting for drug discovery.^{209,210} The hydrazones katorazone and yoropyrazone, for instance, show anticancer activity.^{200,201} Hydrazides with antimicrobial properties are represented by negamycin and its derivatives,²⁰⁴ as well as XK-90²⁰⁷ and FR-900137.²⁰⁵ Antifungal bioactivity can be observed for fosfazinomycin.²⁰⁸ As it is the case for the hydrazides geralcin D, and E that were isolated from *Streptomyces sp.* LMA-545 antimicrobial or cytotoxic activity do not necessarily have to be observed.²¹¹

Regarding biosynthetic considerations, the enzymes involved in the nitrogen-nitrogen bond formation are still unknown.¹⁹⁹ It is suggested that primary amines serve as precursor molecules and that the enzymatic reactions include N-hydroxylation as well as N-nitrosation reactions.¹⁹⁹ Although

every amino acid can potentially be transformed into a N2NP, only a few N2NPs derived from α -amino acids are known. These N2NPs include valanimycin that is produced by *S. viridifaciens* MG456-hF10 and is composed of the L-stereoisomers of valine and serine.^{199,212} Referring to the work of Le Goff *et al.*,¹⁹⁹ and Garg *et al.*,²¹² the nitrogen-nitrogen bond of valanimycin (Figure 25, **17**) is formed between the α -amino groups of both amino acids *via* several biochemical reactions that are not mentioned. The N2NP azaserine (Figure 25, **18**), produced by *S. fragilis*, and its derivative thrazarine (Figure 25, **19**), produced by *S. coerulescnes*, include the amino acid serine, but its amino group is not involved in the nitrogen-nitrogen bond formation.¹⁹⁸

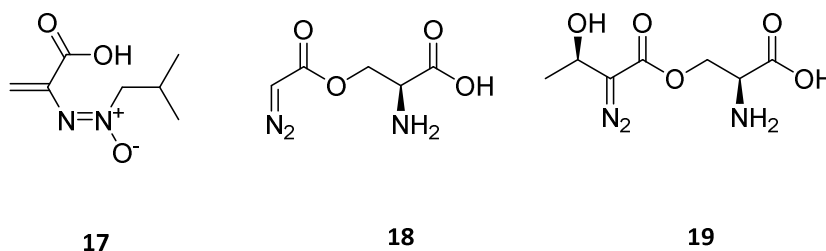


Figure 25: Chemical structures of valanimycin (**17**),¹⁹⁹ azaserine (**18**)¹⁹⁸ and thrazarine (**19**).¹⁹⁸

Compared to NP research, in chemical synthesis with its variety of nitrogen-nitrogen bond containing compounds, NMR and MS analyses are mainly used to verify (instead of elucidate) the structure and molecular mass of the synthesized product without the need for information on fragmentation. Thus, MS² data is usually not acquired. But also for the small number of hydrazone NPs, MS² data can hardly be found.^{195–197}

In addition to the poor amount of literature including MS² data of hydrazones, it is difficult to state general fragmentation patterns for hydrazones, as the fragmentation is highly dependent on the chemical structure of the whole molecule and not just the hydrazone moiety. A terminal hydrazone moiety indicates that the formation of a NH₃ or a N₂H₄ fragment may be reasonable but also the cleavage of HCN may be possible.¹⁹⁵ Besides this, no further general fragments can be stated as, for instance, a hydrazone compound containing aryl groups might cause C₆H₆ fragments that cannot be observed for hydrazones without a corresponding group. This complicates the identification of hydrazone moieties in dereplication workflows based on MS and MS² data.¹⁹⁵

Regarding leucine hydrazone, the only fragment that was successfully used for elemental composition prediction revealed a signal at m/z 100.0760 in positive ion mode suggesting a chemical formula of C_5H_9NO . Regarding the chemical formula of the initial compound, this means a loss of CH_3NO that corresponds to a formamide moiety.

Presence of hydrazone derivatives of further α -amino acids

Since the compound represents a hydrazone derivative of the α -amino acid leucine, I suggested that Tü 27 might produce hydrazone derivatives of other α -amino acids, as well. For this purpose, I used the HPLC-HRMS data of the ethyl acetate medium extract of the larger scale culture of Tü 27, which was also used for the isolation of leucine hydrazone. However, the presence of further hydrazone derivatives of α -amino acids could not unambiguously be proven.

3.1.3.3. Test for cytotoxic and inhibitory bioactivity of leucine hydrazone

All cytotoxicity assays were performed by Paul Barac. The analysis and visualization of the cytotoxicity data were carried out by the author of this thesis. Leucine hydrazone was assayed for cytotoxic and antibiotic activity. For both, the compound was tested alone as well as in combination with known antibiotics, and cytotoxic compounds. Leucine hydrazone did not show significant cytotoxicity as its IC_{50} value was about 174-347 μ M compared to IC_{50} values of cytotoxic compounds found in literature, which are in the sub- μ M or even in the nM range.^{213,214}

Nevertheless, we observed increased cytotoxicity when it was combined with the cytotoxic aminoglycoside antibiotics hygromycin B (Figure 27, **20**) or G418 (geneticinsulfate, Figure 27, **21**). The performance of the checkerboard assay followed by the calculation of the FICI revealed an additive effect for the combination of leucine hydrazone with hygromycin B. Further, there was no observed increase in cytotoxicity when it was combined with actinomycin D (Figure 27, **22**). There was no increased antimicrobial bioactivity on *B. subtilis* when the compound was combined with actinomycin D or tetracycline.

Cytotoxicity of leucine hydrazone

The results of the cytotoxicity assay of leucine hydrazone using HeLa cells are shown in Figure 26. The y-axis shows the cell viability depending on the leucine hydrazone concentration that is shown on the x-axis. The assumption for the following text is that a cell viability of 50 % corresponds to the IC_{50} value of a compound.

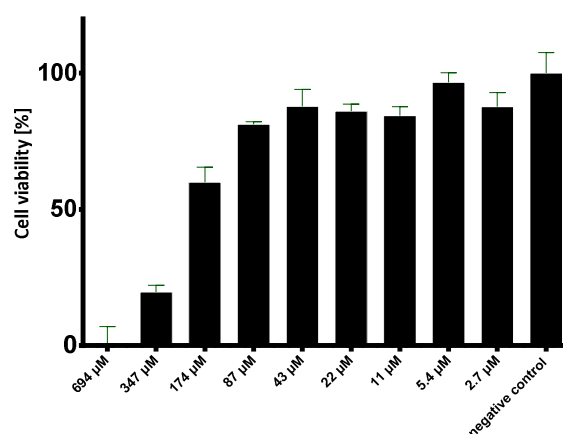


Figure 26: Results of the cytotoxicity assay of leucine hydrazone using HeLa cells (normalized data).

Synergistic effects of leucine hydrazone in combination with different compounds

As there was no significant cytotoxicity of leucine hydrazone itself, we tested for a synergistic or additive effect when the compound is combined with either one of the two cytotoxic aminoglycoside antibiotics hygromycin B, and G418, as well as actinomycin D, which are all produced by *Actinobacteria*.^{215–217} Hygromycin B is produced by *Streptomyces hygrosopicus*,²¹⁸ G418 is produced by *Micromonospora rhodorangea*²¹⁵, and actinomycin D is produced by a magnitude of *Streptomyces* species like for instance *Streptomyces costaricanus*.²¹⁷

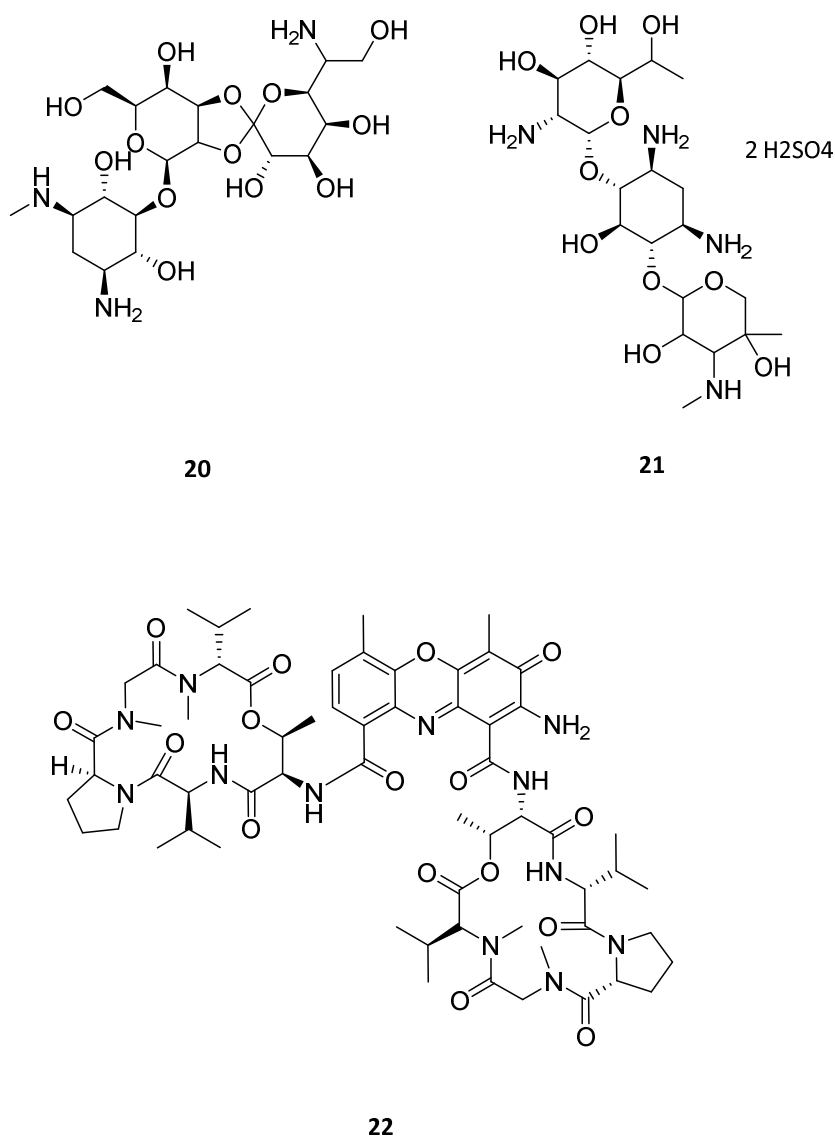


Figure 27: Chemical structures of hygromycin B (**20**),²¹⁸ G418 (**21**),²¹⁹ and actinomycin D (**22**).²²⁰

Combination of leucine hydrazone with hygromycin B

The performance of an initial screening for cytotoxicity and a potential synergistic effect of the combination of leucine hydrazone with either hygromycin B or G418 indicated a synergistic effect of the combinations.

The results of the cytotoxicity assay for the combination of leucine hydrazone with hygromycin B are shown in Figure 28. The graph includes the results of a cytotoxicity assay of the compound (left), of hygromycin B (middle), and of a combination of both (right). Figure 28 illustrates the cell viability (y-axis) depending on the compound concentration (x-axis).

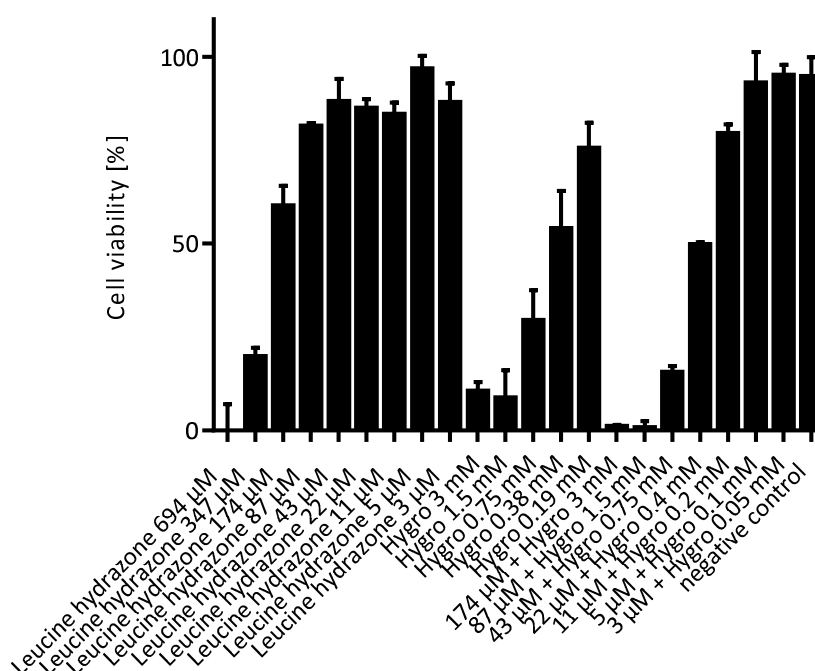


Figure 28: Results of the cytotoxicity assay of leucine hydrazone using HeLa cells as well as the test for synergistic effects with hygromycin B (normalized data).

When the IC_{50} values of leucine hydrazone and hygromycin B are being compared, no increase in cytotoxicity of hygromycin B can be seen when leucine hydrazone is added. For both, hygromycin B alone and in combination with the compound (22 μ M), the IC_{50} value is 0.4 mM. Nevertheless, the addition of leucine hydrazone (43 μ M) to hygromycin B (0.75 mM) decreases the cell viability from 29 % for hygromycin B alone (0.75 mM) to 15 % for the combined compounds indicating a synergistic effect.

So far, an enhancement of bioactivity for hygromycin B in combination with chromate as a second compound is known concerning antifungal activity against, among others, the fungal pathogen *Candida albicans*.^{221,222} The mechanism of this synergistic effect is based on the competition between sulfate (SO_4^{2-}) and chromate (CrO_4^{2-}) concerning their uptake into the cell, causing an inhibition of sulfate-uptake. Due to this inhibition, which is likely to be based on the structural similarity of SO_4^{2-} and CrO_4^{2-} , sulfur-containing amino acids like cysteine and methionine cannot be synthesized in the cell, which causes errors in protein biosynthesis.^{221,223}

This synergistic effect cannot be observed when these amino acids are present in the cultivation medium as they are being taken up by the fungus and thus have not to be synthesized in the cell.²²¹ Another study, by Vallière and co-workers,²²² showed synergistic antifungal activity when hygromycin B is combined with quinine that is known for its anti-malaria bioactivity.^{222,224} As in the case of the combination of hygromycin B with chromate, its combination with quinine is based on amino acid depletion as well. They suggest that quinine competes with tryptophan uptake resulting in tryptophan depletion causing errors in protein biosynthesis.^{222,225} In both studies, neither antibacterial nor anti-mammalian cell bioactivity was observed for the combinations, which showed synergistic antifungal activity. In these studies, it is suggested that the combination of an aminoglycoside antibiotic like hygromycin B, and compounds like chromate or quinine, which all interfere with protein biosynthesis, have led to the synergistic effect. Nevertheless, this effect was antifungal-specific.^{221,222}

Based on these studies, the additive cytotoxic effect of hygromycin B in combination with leucine hydrazone may be based on amino acid depletion as well. As leucine represents an essential amino acid,²²⁶ the uptake of its hydrazone derivative instead of leucine into the cell may cause errors in protein biosynthesis. As hygromycin B interferes with protein biosynthesis as well,²¹⁶ the combination with an adjuvant molecule with effects on protein biosynthesis may be the reason for the increased cytotoxic bioactivity.

Combination of leucine hydrazone with G418

Figure 29 contains the results of the cytotoxicity assay of leucine hydrazone in combination with G418. The graph includes the results for leucine hydrazone (left), G418 (middle), and for a combination of both compounds (right).

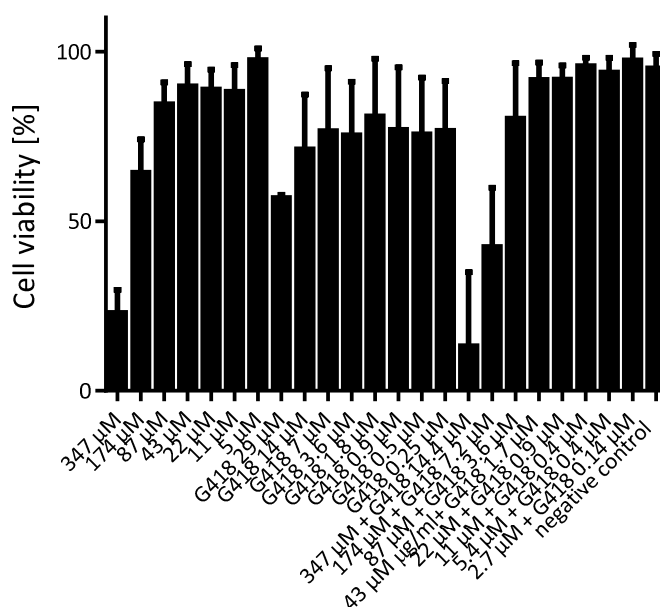


Figure 29: Results of the cytotoxicity assay of leucine hydrazone using HeLa cells as well as the test for synergistic effects with G418 (normalized data).

The assay revealed an IC_{50} value for G418 of 29 μ M with a corresponding cell viability of 56 %. As in previous assays, the IC_{50} value of leucine hydrazone is between 174 and 347 μ M. When both compounds are combined, a synergistic cytotoxic effect was observed. The combination of leucine hydrazone (174 μ M) and G418 (7.2 μ M) yielded a cell viability of 42 % compared to 77 % for G418 (7.2 μ M), and 64 % for leucine hydrazone (174 μ M) when these compounds are tested alone. The combination of leucine hydrazone (347 μ M) and G418 (14.4 μ M) resulted in a cell viability of only 13 % compared to 71 % for G418 (14.4 μ M), and 23 % for leucine hydrazone (347 μ M). Although, leucine hydrazone (347 μ M) already caused a cell viability of 23 %, the combination with G418 (14.4 μ M) lowers the value by another 10 %, which indicates a synergistic effect between the two compounds. Even though the concentrations of leucine hydrazone needed for these results are high, it is worth to be mentioned, as the compound itself does not have relevant cytotoxic effects.

To evaluate if the effect of the combined compounds is either synergistic or additive, the checkerboard assay was performed for the combination of leucine hydrazone with hygromycin B.

Combination of leucine hydrazone with actinomycin D

As Tü 27 is a known producer of actinomycin D, leucine hydrazone was tested for potential synergistic cytotoxic activity in combination with actinomycin D. Figure 30 shows the results for actinomycin D (0.1 μM), the combination of leucine hydrazone (120 μM) and actinomycin D (0.1 μM), and leucine hydrazone (120 μM). Compared to actinomycin D (0.1 μM), and leucine hydrazone (120 μM) that yielded cell viabilities of 5 %, and 78 %, the combination of both yielded a cell viability of 15 %. This suggests an antagonistic effect for the combination of these two compounds as the addition of leucine hydrazone (120 μM) to actinomycin D (0.1 μM) increases the cell viability compared to actinomycin D (0.1 μM) alone.

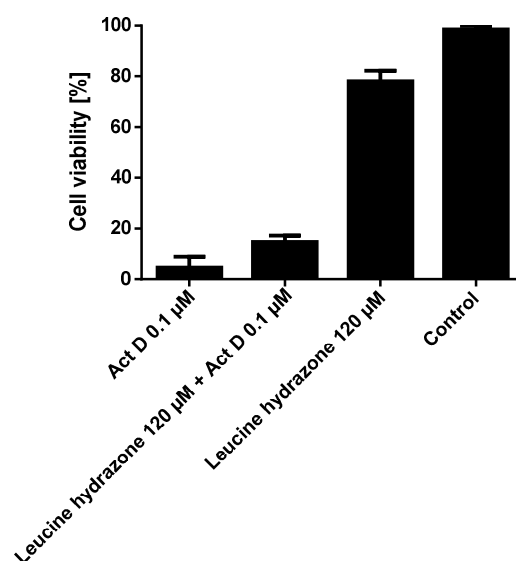


Figure 30: Results of the cytotoxicity assay of leucine hydrazone, and actinomycin D using HeLa cells as well as the test for synergistic effects with actinomycin D (normalized data).

Fractional Inhibitory Concentration Index

The checkerboard assay followed by the calculation of the FIC_{50} index revealed an additive effect when leucine hydrazone is combined with hygromycin B. The FIC_{50} index for this combination, which yielded a cell viability of approximately 50 %, has been calculated. The results of the assay are shown in Figure 31.

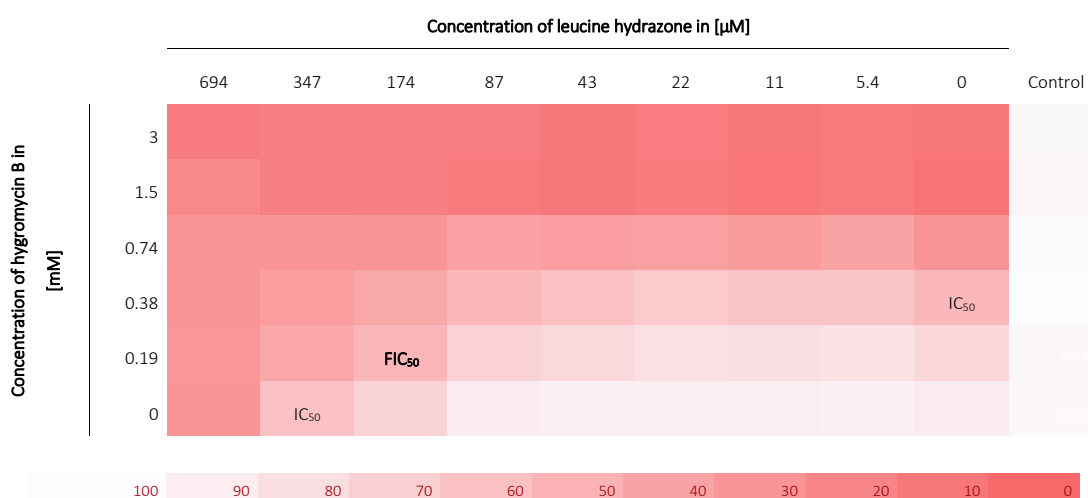


Figure 31: Results of the checkerboard assay of the combination of leucine hydrazone and hygromycin B including the legend of the checkerboard assay indicating the cell viability from 0-100 % and the corresponding color code.

The IC_{50} values for leucine hydrazone and hygromycin B correspond to the concentration of each individual substance that yields approximately 50 % cell viability. The FIC_{50} was calculated for the combination of leucine hydrazone (174 μM) and hygromycin B (0.19 mM) to be 1.0. Thus, this combination shows additive effects concerning cytotoxicity.

Inhibitory antibacterial activity

Additionally, leucine hydrazone was tested for inhibitory bioactivity against *B. subtilis* wt 168 and *P. fluorescens* DSM50090 as well as in the reporter-based bioassay. The latter was performed by the project partners in Tübingen. The compound did not show inhibitory bioactivity against *B. subtilis* wt 168 or *P. fluorescens* DSM50090 nor in the reporter-based bioassay investigating different promoters (*ppS*, *yorB*, and *yheI*). Furthermore, I tested if the compound increases the antimicrobial activity of actinomycin D or tetracycline as these antibiotics are produced by Tü 27. Thus, the increase of their antibacterial bioactivity would be a reason for the production of leucine hydrazone by Tü 27.

There was no antibacterial activity observed in any of the tested strains. Also no synergistic antimicrobial activity in combination with actinomycin D or tetracycline could be detected.

3.2. MiMo_ALe project

3.2.1. Macroscopic and microscopic characterization

The endophytic microbial strains that were isolated from different macroalgae species in cooperation with the Moroccan project partners were analyzed in regard to their macroscopic and microscopic appearance. Concerning their macroscopic appearance like colony color, shape, and growth behavior, the strains MiMo_ALe#2, 4, and 6-9 were estimated to be identical. However, this has to be proven by analyses on the genomic level. The following section describes the microscopic and macroscopic appearance of the strains when grown on solid medium.

MiMo_ALe#1

When the strain MiMo_ALe#1 is grown on LB agar, it forms a white mycelium (Figure 32 A). Furthermore, substrate mycelium, which surrounds the colony center with its aerial mycelium, can be observed. The filamentous properties with the long, branching and overlapping filaments are shown on a microscopic level in B, and C of Figure 32.

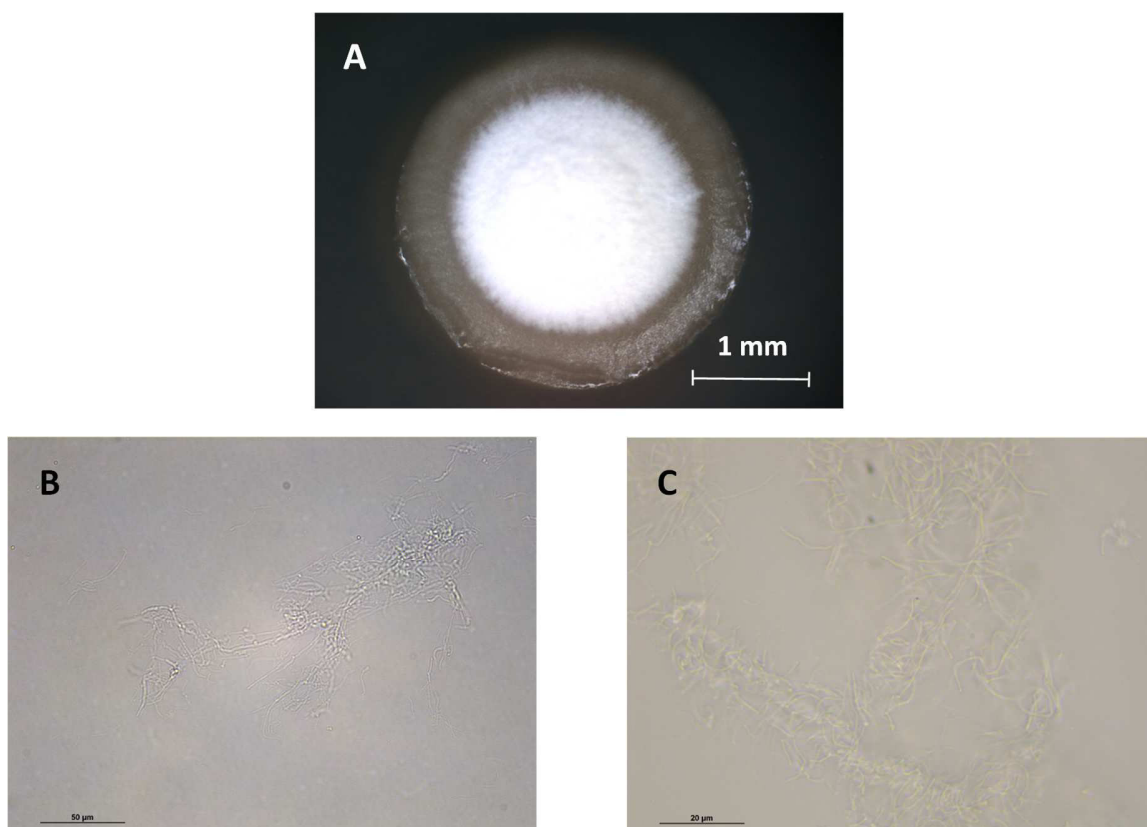


Figure 32: **A**: Macroscopic picture of a well-separated colony MiMo_ALe#1. **B** (measure bar 50 μm), and **C** (measure bar 20 μm): microscopic pictures of this strain.

MiMo_Ale#3

The filamentous growth of MiMo_Ale#3 with its white and yellowish aerial mycelium can be seen in the macroscopic picture of a well-separated colony in Figure 33 A. In addition to the filamentous growth, the microscopic pictures (Figure 33 B and C) show the presence of spores, formed from the aerial mycelium, which is known for *Actinobacteria* and especially the genus *Streptomyces*.^{175,227,228}

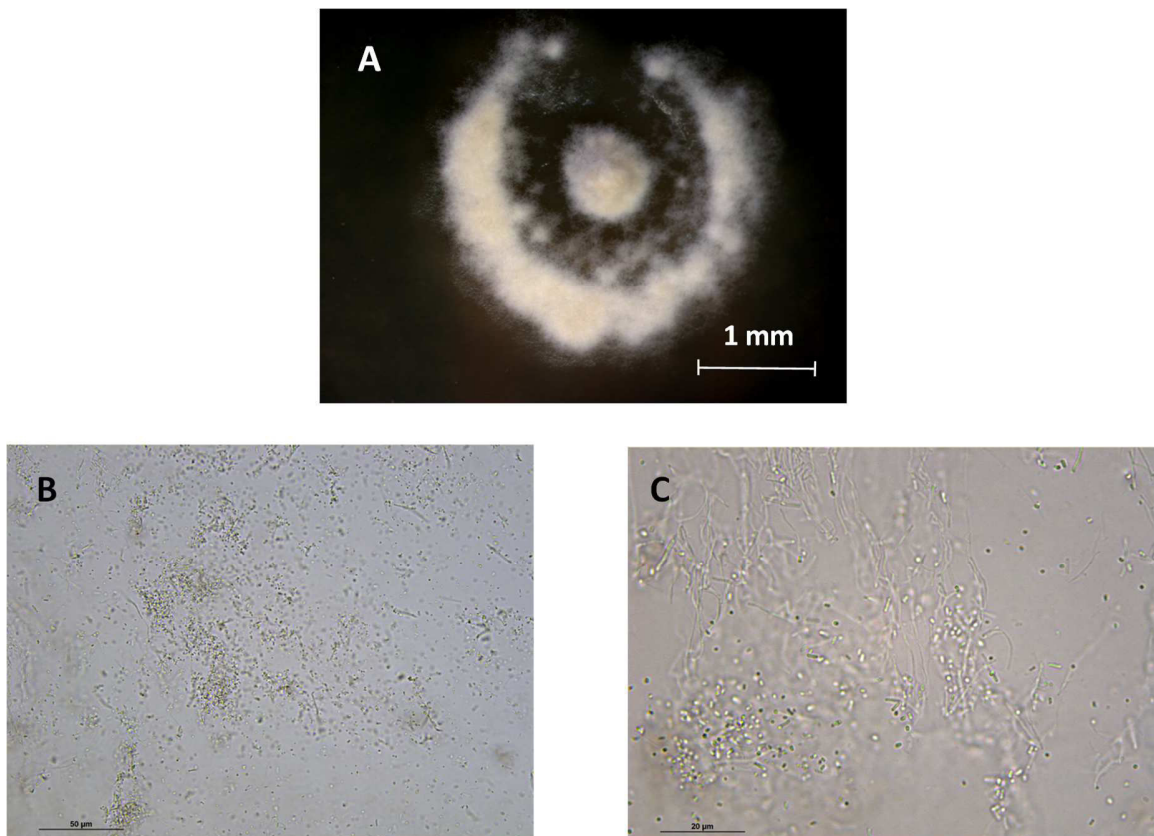


Figure 33: **A**: Macroscopic picture of a well-separated colony MiMo_Ale#3. **B** (measure bar 50 µm), and **C** (measure bar 20 µm): microscopic pictures of this strain.

MiMo_ALe#5

For MiMo_ALe#5, the filamentous growth can be observed macroscopically (Figure 34 A) as well as microscopically (Figure 34 B, and C). On agar, the strain forms distinct colonies with a white and greyish color and the aerial mycelium is surrounded by substrate mycelium.

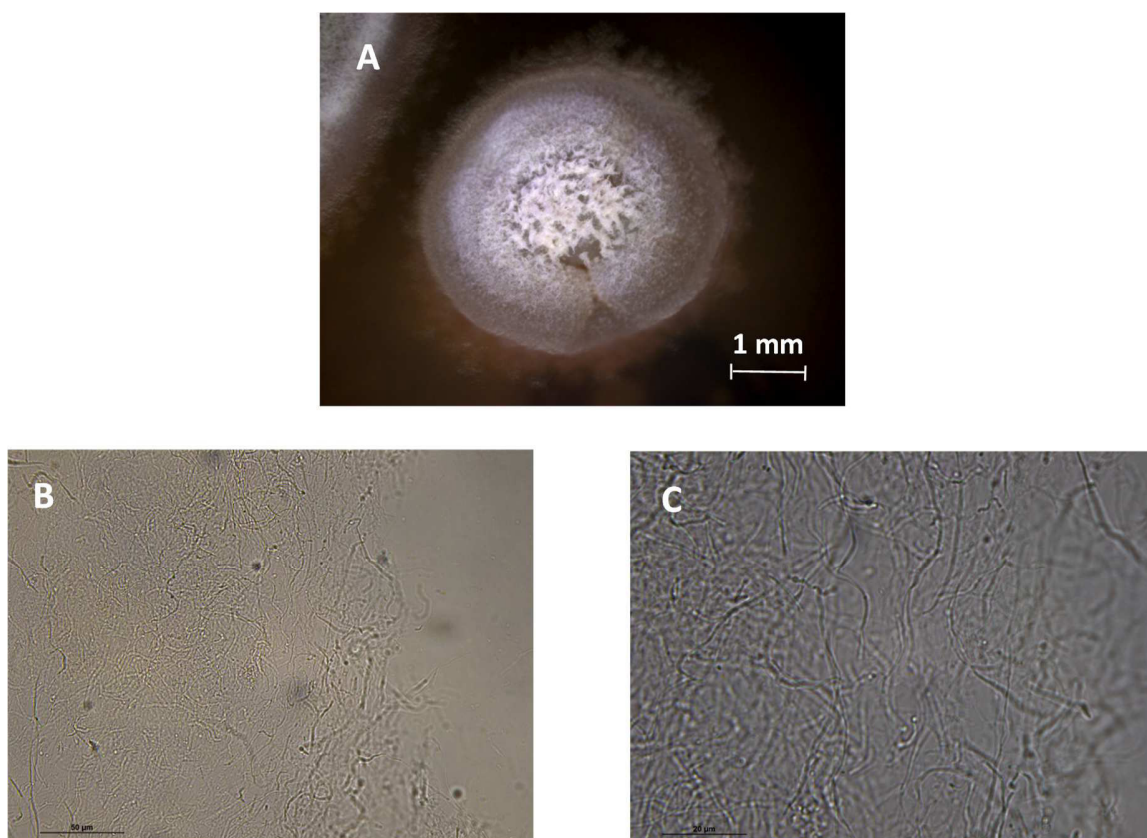


Figure 34: **A**: Macroscopic picture of a well-separated colony MiMo_ALe#5. **B** (measure bar 50 μm), and **C** (measure bar 20 μm): microscopic pictures of this strain.

MiMo_ALe#7

Regarding the morphology and growth behavior like growth speed and color change, we suggested that the strains MiMo_ALe#2, 4, and 6-9 are either identical or closely related to each other. These strains show the formation of white aerial mycelium for the first days of incubation, which changes to a dark green mycelium afterwards. In Figure 35 A, the remains of this white aerial mycelium can be seen as a white top of the green colony. On the microscopic level (Figure 35 B and C), spores can be seen instead of filamentous growth.

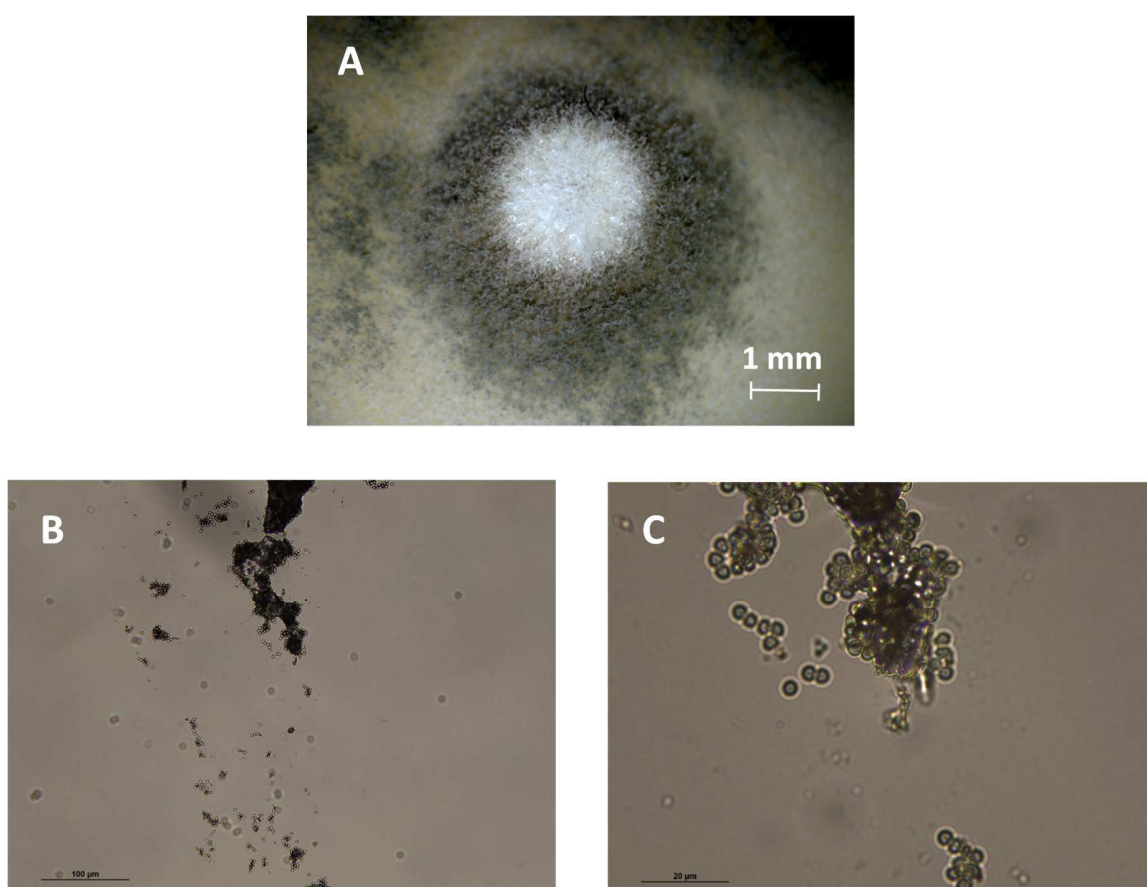


Figure 35: **A**: Macroscopic picture of a well-separated colony MiMo_ALe#7. **B** (measure bar 100 μm), and **C** (measure bar 20 μm): microscopic pictures of this strain.

MiMo_ALe#10

MiMo_ALe#10 forms distinct colonies with a white aerial mycelium surrounded by substrate mycelium (Figure 36 A). The presence of filamentous growth can be seen on the microscopic level as well (Figure 36 B, and C).

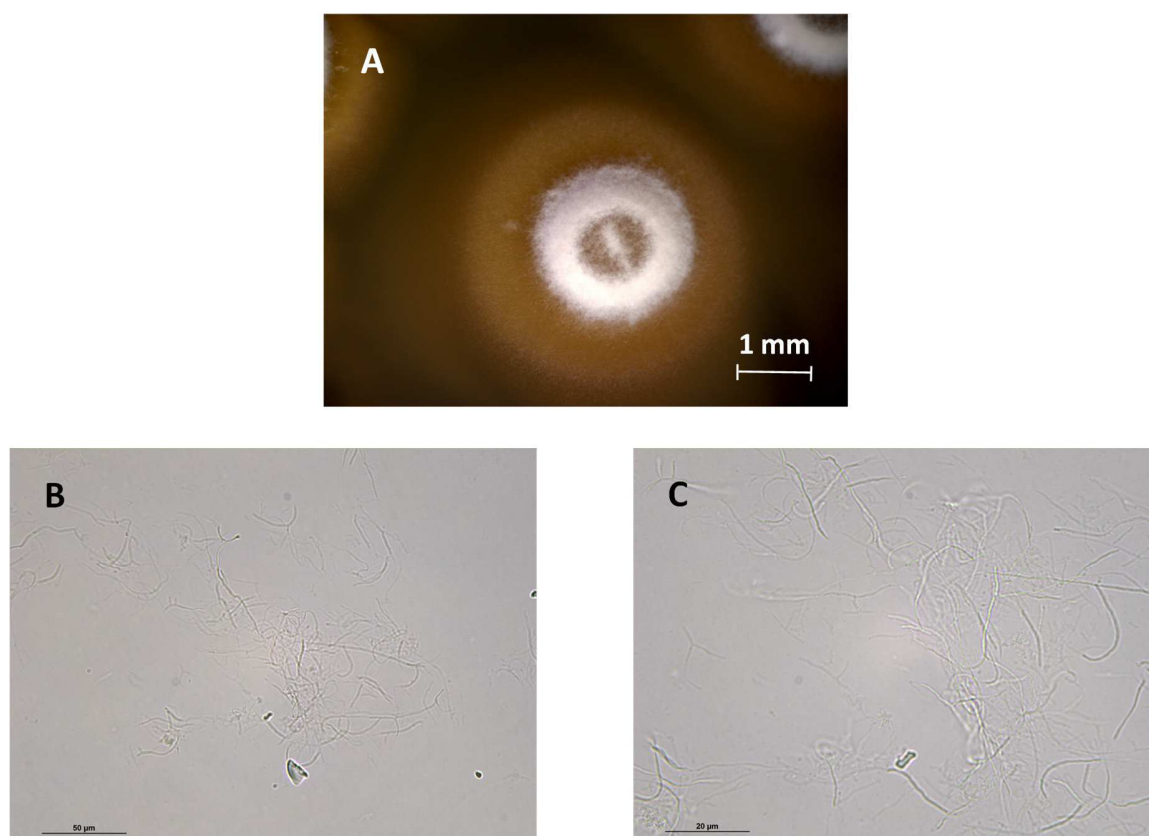


Figure 36: **A**: Macroscopic picture of a well-separated colony MiMo_ALe#10. **B** (measure bar 50 μm), and **C** (measure bar 20 μm): microscopic pictures of this strain.

In summary, it can be stated that all isolated endophytes exhibit the formation of filamentous aerial mycelium on the macroscopic level, which is a known characteristic of filamentous bacteria. The strains MiMo_ALe#3, and 7 additionally show spores on the microscopic level.

3.2.2. Isolated endophytes – primary screening

Endophytes from Moroccan aromatic plants

The endophytic bacteria that have been isolated from Moroccan aromatic plants by the Moroccan project partners before the start of this project were screened for their inhibitory bioactivity against 5 MDR strains (MRSA, ABRI, KPR, ECR, and PARc). This screening was performed as agar plug assay by the author of this thesis together with the Moroccan project partners in their laboratories. Due to the lower availability of chemicals and consumables in the laboratories of the project partners, the screening was performed without replicates or positive controls.

This screening of in total 115 strains revealed 16 strains that were chosen for further investigation due to their inhibitory bioactivity against at least one MDR strain. These strains and the observed inhibitory bioactivity are shown in Table 11. Bioactivity was marked as “static”, when bacterial growth was slowed down within a certain zone around the agar plug but not completely inhibited. Bioactivity was seen as inhibiting, when “shiny” agar was observed within the inhibition zone, compared to the turbid appearance in the case of static or no inhibition.

Table 11: Bacterial endophytes from Moroccan aromatic plants that were selected to further work due to their antibacterial activity against MDR bacteria. The index “static” means there was only a static inhibition. The composition of the strain-code can be found in chapter 2.1, Table 3. This screening was performed by the author of this thesis together with the Moroccan project partners in their laboratories.

Strain-code	inhibited MDR strain (diameter of inhibition zone [cm])
BH-ER11	MRSA (1.5)
BH-ER12	MRSA (3.2)
PA-OR21	MRSA (2.4)
RA-ER35	MRSA (2.4), ECR (3.6) _{static}
RA-ER45	ECR (2.2) _{static}
AM-EL53	MRSA (2.5)
CS-TS81	MRSA (3.0) _{static}
CS-TS82	MRSA (1.8)
AH-TS86	MRSA (1.9)
HS-TRy87	MRSA (2.0) _{static}
HS-TRw87	ABRi (1.7), MRSA (3.6) _{static}
ZG-TR94	KPR (1.5) _{static}
ZG-TR96	MRSA (1.7)
PT-TS107	MRSA (1.2)
PT-TS114	MRSA (1.6)
PT-TS115	MRSA (1.4)

After the primary screening, the strains were transferred to Germany for further investigation. These investigations included the fermentation of the strains in liquid ISP2 and Bennett medium. After 8 days of cultivation, medium extracts using ethyl acetate, 1-butanol, and dichloromethane were generated. Furthermore, the biomass of each strain was extracted using acetone/methanol (1:1) to obtain the biomass extract. These extracts and biomass samples were tested for antibacterial activity by the Moroccan project partners. The results are shown in Table 12.

Table 12: Results of the bioactivity screening of medium extracts (ME) obtained from liquid fermentation in ISP2 medium of bacterial endophytes from Moroccan aromatic plants. The screening of the medium extracts was performed by the Moroccan project partners. The screening for the initial bioactivity was performed by the author of this thesis together with the Moroccan project partners in their laboratories.

Strain	Inhibitory bioactivity of ME against MDR strains			Initial bioactive against
	ME(EtOAc)	ME(DCM)	ME(1-BuOH)	
BH-ER11	-	-	-	MRSA
BH-ER12	MRSA	MRSA	MRSA	MRSA
PA-OR21	MRSA	MRSA	MRSA	MRSA
RA-ER35	-	-	ECR	MRSA, ECR
RA-ER45	-	-	ECR	MRSA, ECR
AM-EL53		MRSA	MRSA	MRSA
CS-TS81	MRSA	MRSA	-	MRSA
CS-TC82	-	MRSA	MRSA	MRSA
AH-TS86	MRSA	-	MRSA	MRSA
HS-TRy87	-	-	KPR	MRSA
HS-TRw87	-	-	KPR	MRSA
ZG-TR94	-	-	-	KPR
ZG-TR96	-	-	MRSA	MRSA
PT-TS107	-	-	MRSA	MRSA
PT-TS114	-	MRSA	-	MRSA
PT-TS115	-	-	MRSA	MRSA

Regarding the results of this screening, the strains RA-ER35, RA-ER45, HS-TRy87, and HS-TRw87 were chosen for further investigation as they showed inhibitory bioactivity against MDR Gram-negative pathogens. Compared to the initial agar plug assay, the medium extracts of the strains RA-ER35, HS-ER45, HS-TRy87, and HS-TRw87 did not show the same bioactivity. Thus, either the bioactive compounds of interest are produced when the strains are cultivated in liquid medium but not when the strains are grown on solid medium or the results of the initial agar plug screening were false positive. The latter has to be considered as no replicates were performed in screenings that were carried out by the Moroccan project partners.

As part of further investigations, I cultivated and extracted the strains RA-ER35, RA-ER45, HS-TRy87, and HS-TRw87 to verify the production of specialized metabolites that inhibit MDR Gram-negative pathogens. Compared to the results of the Moroccan project partners, the bioactivity was not observed anymore when I tested the medium extracts, withdrawn culture broths or micro-fractions of the medium extracts in laboratories in Germany.

The missing reproducibility of the results of the screenings performed in Germany and the results obtained by the Moroccan project partners might be caused by false positive results by the project partners due to missing replicates. As the assays in Germany were done in an almost 1000 fold concentration (40 mg/mL) compared to the assays performed in Morocco (50 µg/mL), the activity should have been observed. The performance of the assays in Germany in replicates compared to missing replicates by the project partners suggests the presence of false positive results rather than false negative ones.

Bacterial endophytes from macroalgae

In cooperation with the Moroccan project partners, we were able to isolate in total 10 bacterial endophytes from the collected macroalgae. The primary bioactivity screening of these strains was performed by the Moroccan project partners applying agar plug assays (Tables 13 and 14). The endophytic strains were screened for inhibitory bioactivity against the MDR strains as well as *S. aureus*, *Bacillus cereus*, *Micrococcus luteus*, *E. coli*, *P.aeruginosa*, *K. pneumonia* (Table 13), *Candida albicans*, *Candida glabrata*, *Candida krusei*, and *Candida parapsilopsis* (Table 14) as monitor organisms.

Table 13: Results of the primary bioactivity screening against non-MDR Gram-positive and Gram-negative bacteria performed by the Moroccan project partners. Results are given as diameter of inhibition zone in [cm]. *S. aureus* (Sa), *B. cereus* (Bc), *M. luteus* (Ml), *E. coli* (Ec), *P. aeruginosa* (Pa), *K. pneumoniae* (Kp). (-) means that no inhibitory bioactivity was observed. This screening was performed by the Moroccan project partners.

Strain [MiMo_ALe#]	Non-MDR Gram-positive bacteria			Non-MDR Gram-negative bacteria		
	Sa	Bc	Ml	Kp	Pa	Ec
1	1.1	1.1	1.3	-	1.2	-
2	1.9	1.8	1.8	-	1.2	-
3	-	-	-	-	1.4	-
4	-	-	1.8	-	-	-
5	-	1.6	-	-	-	-
6	-	1.8	-	-	1.4	-
7	-	-	-	-	2.0	-
8	2.1	-	1.2	1.1	1.7	-
9	-	-	1.4	-	1.1	-
10	2.0	1.9	1.3	-	1.2	-

Table 14: Results of the primary bioactivity screening of the isolated endophytes against fungi performed by the Moroccan project partners. *C. albicans* (L4), *C. glabrata* (L7), *C. krusei* (10), and *C. parapsilopsis* (L18). “+” means that there was inhibitory bioactivity but the inhibition zone was too small to be reasonably measured. “-” means no inhibitory activity was observed. This screening was performed by the Moroccan project partners.

Strain [MiMo_ALe#]	Fungi			
	L4	L7	L10	L18
1	-	-	-	+
2	-	-	1.1	+
3	-	-	-	+
4	-	-	-	-
5	2.1	1.7	1.9	1.3
6	-	-	-	-
7	-	-	-	-
8	1.1	-	-	-
9	-	-	-	-
10	-	-	-	-

None of the strains showed inhibitory bioactivity against the used Gram-negative MDR strains (data not shown) when they were tested by the Moroccan project partners using the agar plug assay. The strains MiMo_ALe#2, 5, and 10 showed inhibitory bioactivity against MRSA with inhibition zones of 1.2 cm, 1.2 cm, and 1.8 cm.

3.2.3. Secondary screening

After the transfer of the endophytic strains to Germany, I applied them to further investigation. For this purpose, the OSMAC approach using eight different liquid fermentation media was used. The supernatants of the culture broths that were withdrawn over a period of two weeks for every strain and medium were then tested for inhibitory bioactivity against the MDR strains.

In advance, I performed a screening for a suitable antibiotic serving as positive control. For this purpose, I tested seven antibiotics (ampicillin, apramycin, chloramphenicol, kanamycin, fosfomycin, rifampicin, and tetracycline) for their inhibitory activity against the five MDR strains (Table 15). As the bioassays, which were performed by the Moroccan project partners to obtain the antibiotic resistance profiles of the MDR strains, were not performed in replicates, a completely valid evaluation concerning the suitability of the tested antibiotics as positive control is not possible. The screening revealed that apramycin was suitable as positive control for all 5 MDR strains.

Table 15: Bioactivity assay against MDR strains using 7 different antibiotics (10 μ L of antibiotic dissolved in water with a mass concentration of 5 mg/mL followed by sterile filtration) to find an appropriate positive control for all 5 strains. (+) states inhibitory bioactivity, (-) states no inhibitory bioactivity. Static inhibition is not included in the table. The bioassay was performed in duplicate.

MDR strain	MRSA	ABRi	ECR	KPR	PARc
Antibiotic					
Ampicillin	+	-	-	-	-
Apramycin	+	+	+	+	+
Chloramphenicol	+	+	-	+	-
Kanamycin	-	-	-	+	-
Fosfomycin	-	-	-	-	-
Rifampicin	-	+	-	+	-
Tetracycline	-	-	-	+	-

Results of the secondary screening

Tables with the detailed results of the bioactivity screenings of the aforementioned supernatants from the strains MiMo_ALe#1-10 obtained from the OSMAC approach can be found in chapter 2.2 of the appendix. I performed all assays in duplicate.

None of the supernatants obtained from MiMo_ALe#1 showed inhibitory bioactivity against any of the used MDR strains. The supernatants of the remaining nine strains, MiMo_ALe#2-10, showed inhibitory bioactivity only against PARc even though none of the strains showed this inhibitory bioactivity in the primary screening that was performed as agar plug assay by the project partners. Thus, the production of the specialized metabolite that inhibits the growth of PARc only occurs when the strains are cultivated in liquid medium but not when grown on agar. It is known that cultivation conditions strongly influence the specialized metabolite production in *Actinobacteria*.^{156,229} In our case, this included the change from solid agar-containing MH medium to liquid medium that contained, among others, other carbon and nitrogen sources than MH medium.

As nine of 10 strains showed inhibitory bioactivity against PARc, it was suggested that the fermentation media might cause the bioactivity instead of specialized metabolites of the endophytes. This possibility was excluded, as there was no observed inhibitory bioactivity against PARc when the fermentation media were tested for their inhibitory bioactivity. Furthermore, if the media were responsible for the bioactivity against PARc, the samples of MiMo_ALe#1 would have been active as well.

We suggested that one or several compounds, which are produced by all strains, cause the observed bioactivity. With this assumption, one strain (MiMo_ALe#7) was chosen for further analysis and the application of molecular networking to detect the compounds that cause the bioactivity against PARc. The suggestion was supported by the fact that the strains were isolated from macroalgae species that were sampled within a range of approximately one kilometer. This increases the likelihood that the endophytic bacteria might be closely related to each other and thus show a similar specialized metabolite production.

For this purpose, HRMS data were acquired for the culture supernatants of the strain MiMo_ALe#7 for the fermentation in NL200, NL333, and NL400 after 4, 6, 11, and 13 days. All these samples showed inhibitory bioactivity against PARc. The combination of GNPS for HRMS data processing and Cytoscape for grouping of the data obtained from GNPS yielded the globomycins as possible active agents.

Globomycin is a peptide antibiotic consisting of L-allo-threonine, L-serine-glycine, and N-methylleucine-L-allo-iso-leucine (Figure 37). Its biological activity against Gram-negative but not Gram-positive bacteria, which is known from literature, supported the suggestion that globomycins are responsible for the observed bioactivity in the secondary screening.^{230, 231}

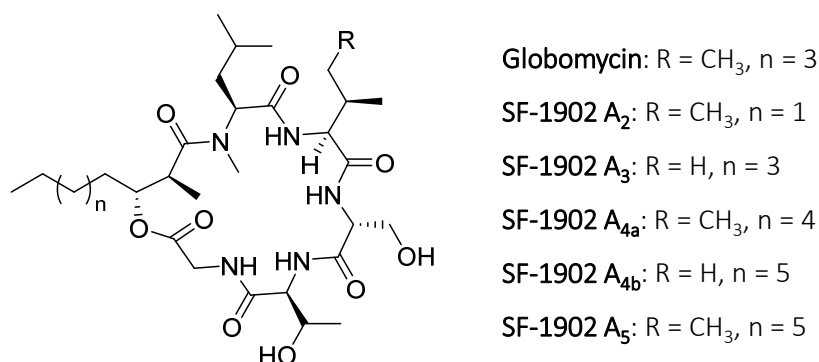


Figure 37: Chemical structure and formulae of globomycin and its derivatives.²³²

The observed bioactivity against PARc in this thesis is in accordance to the bioactivity of globomycins against Gram-negative bacteria found in literature.^{233,234} However, the sensitivity of PARc to globomycins cannot be explained with the antibiogram.

A possible explanation for these results is the circumstance that a compound, which inhibits the growth of a sensitive bacterial strain, does not necessarily inhibit the growth of the corresponding resistant strain. Furthermore, the fact that the applied strains ECR and KPR are resistant to extended spectrum (including β -lactam, aminoglycoside, sulfonamide and fluoroquinolone antibiotics) might explain their resistance to globomycins. The fact that there was no observed inhibitory bioactivity against ABRI was in accordance to literature as no bioactivity of globomycins against *Acinetobacter* species is mentioned in literature so far.²³³⁻²³⁵ To confirm the suggestion of globomycin production, all strains were cultivated in small-scale fermentation using liquid NL300 medium and 1-butanol and ethyl acetate medium extracts were generated after 3, and 7 days for each strain. The presence of globomycins in these extracts was analyzed by HPLC-UV and HPLC-MS analyses. Representative HPLC-UV chromatograms can be found in chapter 2.3 of the appendix.

Mass spectrometric analysis

In the following, the base peak chromatogram (Figure 38) and the extracted ion chromatograms (Figure 39) of the ethyl acetate medium extract of strain MiMo_ALe#2 after cultivation in NL300 medium for 3 days are shown. The HPLC-UV signals of the base peak chromatogram can be assigned to the globomycins as follows: SF1902A₂ ($t_R = 5.25$ min), SF1902A₃ ($t_R = 5.59$ min), SF1902A₁ ($t_R = 5.84$ min), and SF1902A_{4b} ($t_R = 6.15$ min).

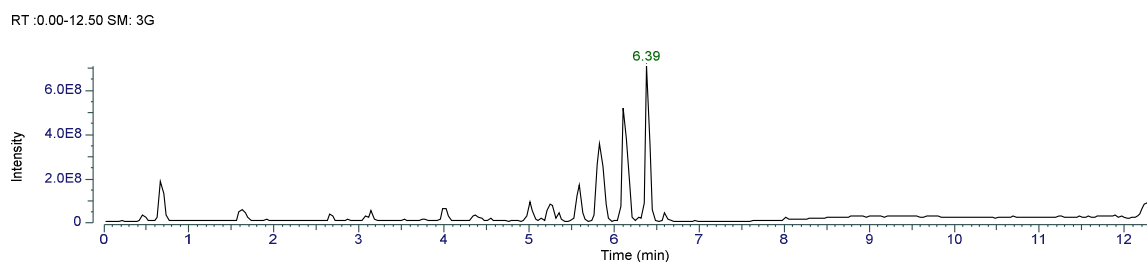


Figure 38: Base peak chromatogram of the ethyl acetate medium extract of MiMo_ALe#2 after cultivation in NL300 medium for 3 days. The signals can be assigned to the globomycins as follows: SF1902A₂ ($t_R = 5.25$ min), SF1902A₃ ($t_R = 5.59$ min), SF1902A₁ ($t_R = 5.84$ min), and SF1902A_{4b} ($t_R = 6.15$ min).

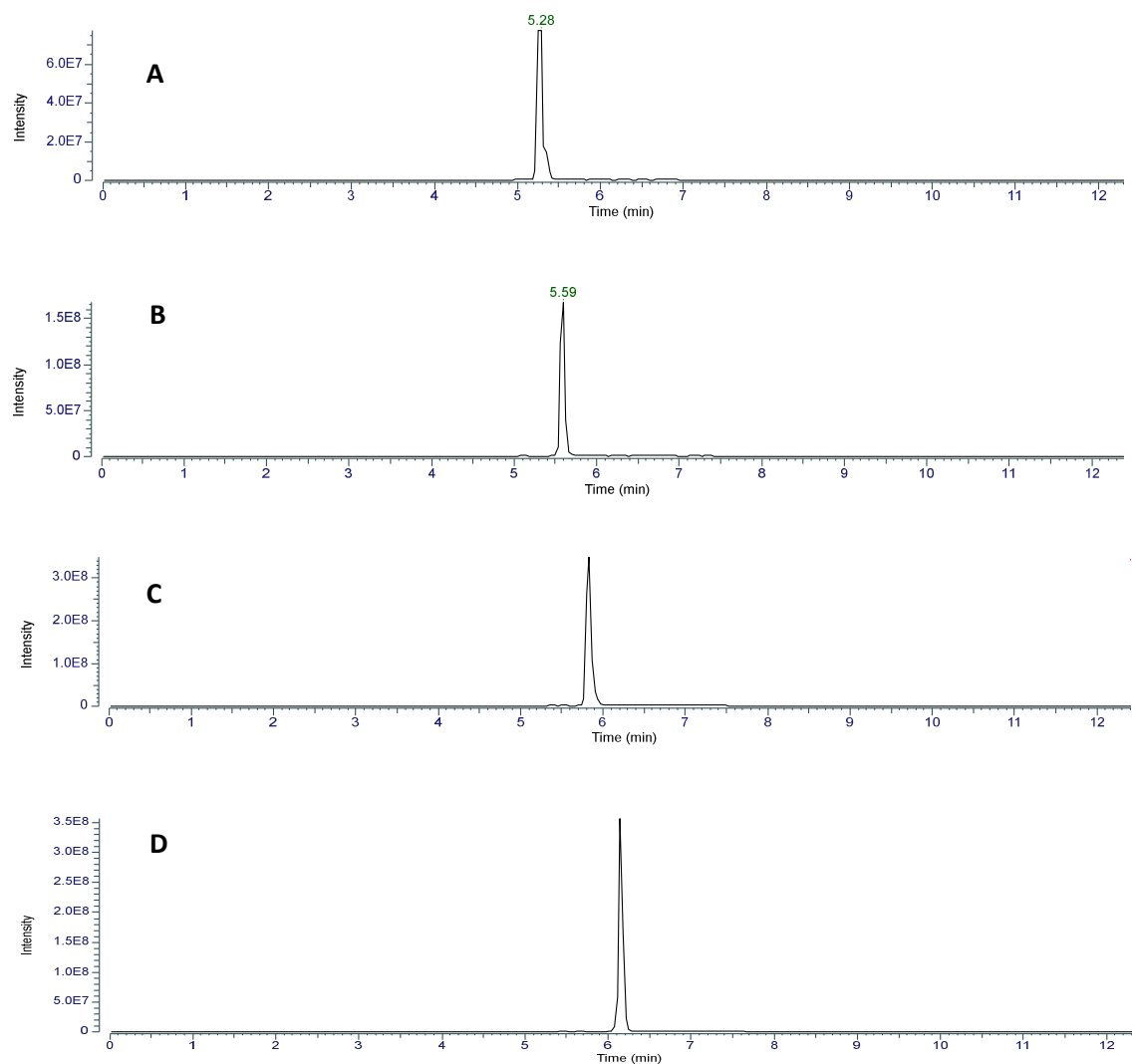


Figure 39: Extracted ion chromatograms of the ethyl acetate medium extract of MiMo_Ale#2 after cultivation in NL300 for 3 days. (A) SF1902A₂, (B) SF1902A₃, (C) SF1902A₁, and (D) SF1902A_{4b}.

The signals shown in the extracted ion chromatograms correspond to the different known globomycins SF1902A₁ (M = 655.42 g/mol; m/z 656.4209-656.4249), SF1902A₂ (M = 627.38 g/mol, m/z 628.3897-628.3935), SF1902A₃ (M = 641.40 g/mol; m/z 642.4054-642.4092), and SF1902A_{4a} (M = 669.43 g/mol; m/z 670.4366-670.4406). The chromatograms can be seen as representatives for the chromatograms of all 10 strains as HPLC-MS analyses revealed the presence of all 4 globomycins in every sample.

3.2.4. Verification of globomycin production

For the verification of globomycin production, HPLC-UV and HPLC-MS analyses were performed for all 10 strains. The acquired HPLC-UV data for both, ethyl acetate, and 1-butanol medium extracts after 3, and 7 days each, indicate that the specialized metabolite production of all strains is rather similar.

The HPLC-UV chromatogram in Figure 40 was obtained for the ethyl acetate medium extract of MiMo_Ale#1 after 7 days and can be seen as representative regarding the appearance of all obtained HPLC-UV chromatograms. Especially the signals at approximately 4.25 min and 7.0-8.5 min are present in all chromatograms.

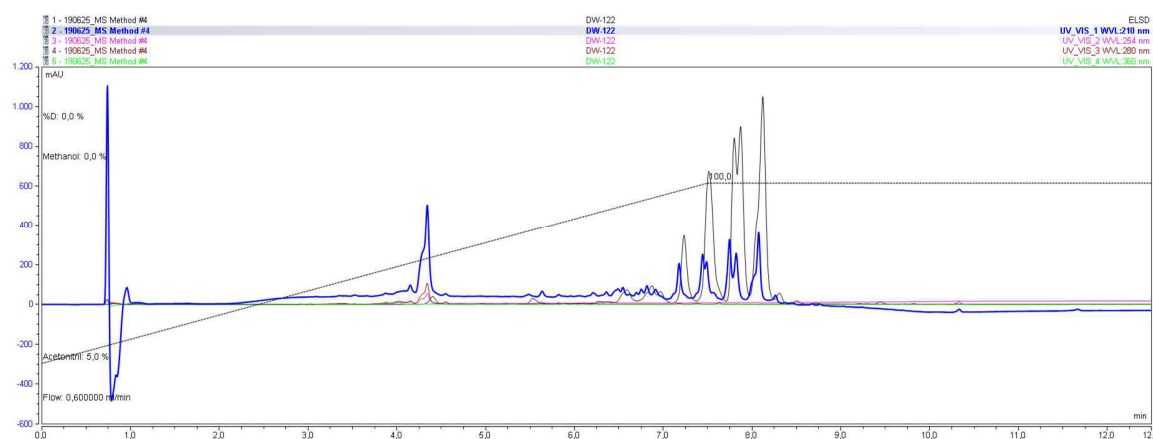


Figure 40: HPLC-UV chromatogram obtained for the ethyl acetate medium extract of MiMo_Ale#1 using a Phenomenex® Kinetex (2.6 μ m) C-18, 100x3.0 mm ID column at 50 °C. Detection was done at 210 nm (blue), 254 nm (magenta), 280 nm (brown), 430 nm (green), and with the ELSD (black).

An additional fact supporting the globomycins production is that in literature globomycins were extracted using ethyl acetate as in our case.²³⁶ For completeness, it should be mentioned, that the similarity concerning the HPLC-UV chromatograms was also observed for all 1-butanol medium extracts as well but with usually much lower signal intensities even though the injection volume and sample concentration were identical. This might be due to the lower solubility of globomycins in water in combination with the good miscibility of water and 1-butanol, which results in a lower concentration of globomycins in the 1-butanol medium extract than in the ethyl acetate medium extract.²³¹

As we suggested that the HPLC-UV signals between 7.0 and 8.5 min are caused by the globomycins, we performed micro-fractionation of an ethyl acetate medium extract and analyzed the respective micro-fractions with HPLC-MS. The analysis of the acquired HRMS data verified the assignment of the globomycins to the major signals with a $t_R > 7.0$ min. Using dereplication techniques, we assigned these compounds to globomycins with the accurate masses 627.38433, 641.39998, 655.41563, and 669.43128 g/mol that can be found in the DNP (Table 16).

Table 16: Experimentally observed retention times of globomycins in positive ion mode of HRMS analysis.

Name	Accurate mass of globomycin derivative		Retention time [min]
	[g/mol]		
	DNP	Experimental	
Globomycin (SF 1902A ₁)	655.41563	655.4148	5.8
SF 1902A ₂	627.38433	627.3840	5.3
SF 1902A ₃	641.39998	641.3991	5.6
SF 1902A _{4a}	669.43128	669.4303	6.2

After the verification of globomycins production based on HPLC-UV and HPLC-MS, I wanted to show the correlation with the observed inhibition of PARc. For this purpose, the strain MiMo_ALe#7 was cultivated in NL333 and NL400 medium for 4 days each to obtain the ethyl acetate, and 1-butanol medium extracts. Micro-fractions of the medium extracts were tested for inhibitory activity against PARc, and the active micro-fractions (15, 16, and 19-27) of the ethyl acetate medium extract were investigated. This revealed that all micro-fractions that inhibited the growth of PARc contained globomycins, strengthening our hypothesis that globomycins are responsible for the inhibitory bioactivity against PARc that was observed in the secondary screening. Table 17 shows the assignment of the different globomycins to the micro-fractions.

Table 17: Assignment of different globomycins to the micro-fractions of the ethyl acetate medium extract of MiMo_ALe#7 after cultivation in NL333 medium for 4 days.

Micro-fraction	Detected globomycins
15	SF1902A ₃
19	SF1902A ₂
	SF1902A ₃
20	SF1902A ₂
	SF1902A ₃
21	SF1902A ₃
	SF1902A ₁
22	SF1902A ₁
	SF1902A _{4b}
23	SF1902A ₁
	SF1902A _{4b}
24	SF1902A _{4b}
25	SF1902A _{4b}

16S rRNA sequencing that was performed to gain further information on the bacterial endophytes did not yield relevant results.

3.3. Determination of the absolute configuration of a siderophore

The determination of the absolute configuration using Marfey's reagent was used for two compounds (Figure 41, **23** and **24**) that were previously isolated in the research group.

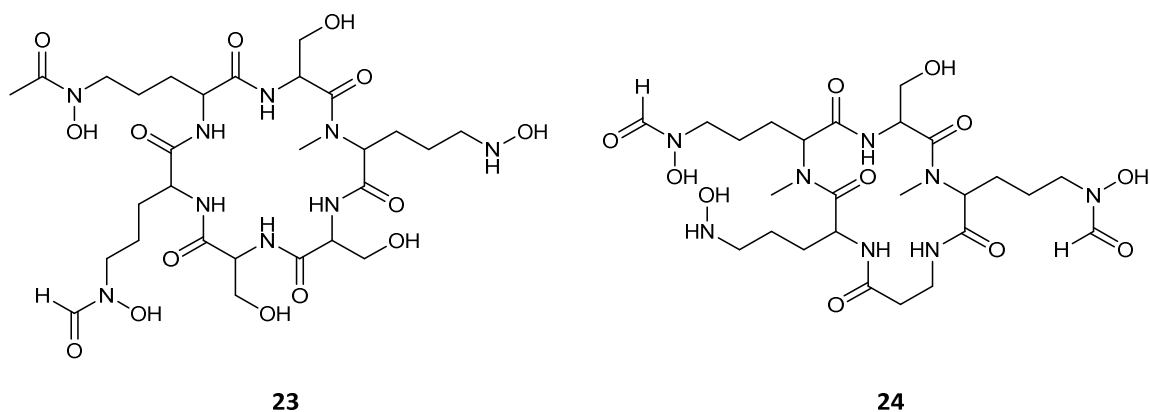


Figure 41: Chemical structures of compound 1 (**23**) and compound 2 (**24**) that were used for determination of the absolute configuration using Marfey's reagent.

The comparison of the HPLC-UV chromatograms of Marfey's derivatives of the hydrolysates of compound 1 (Figure 41, **23**) and 2 (Figure 41, **24**) with Marfey's derivatives of the authentic D- and L-Orn and D- and L-Ser indicates that compound 1 contains L-Orn as well as D- and L-Ser whereas compound 2 consists of only the L- enantiomers of Orn and Ser.

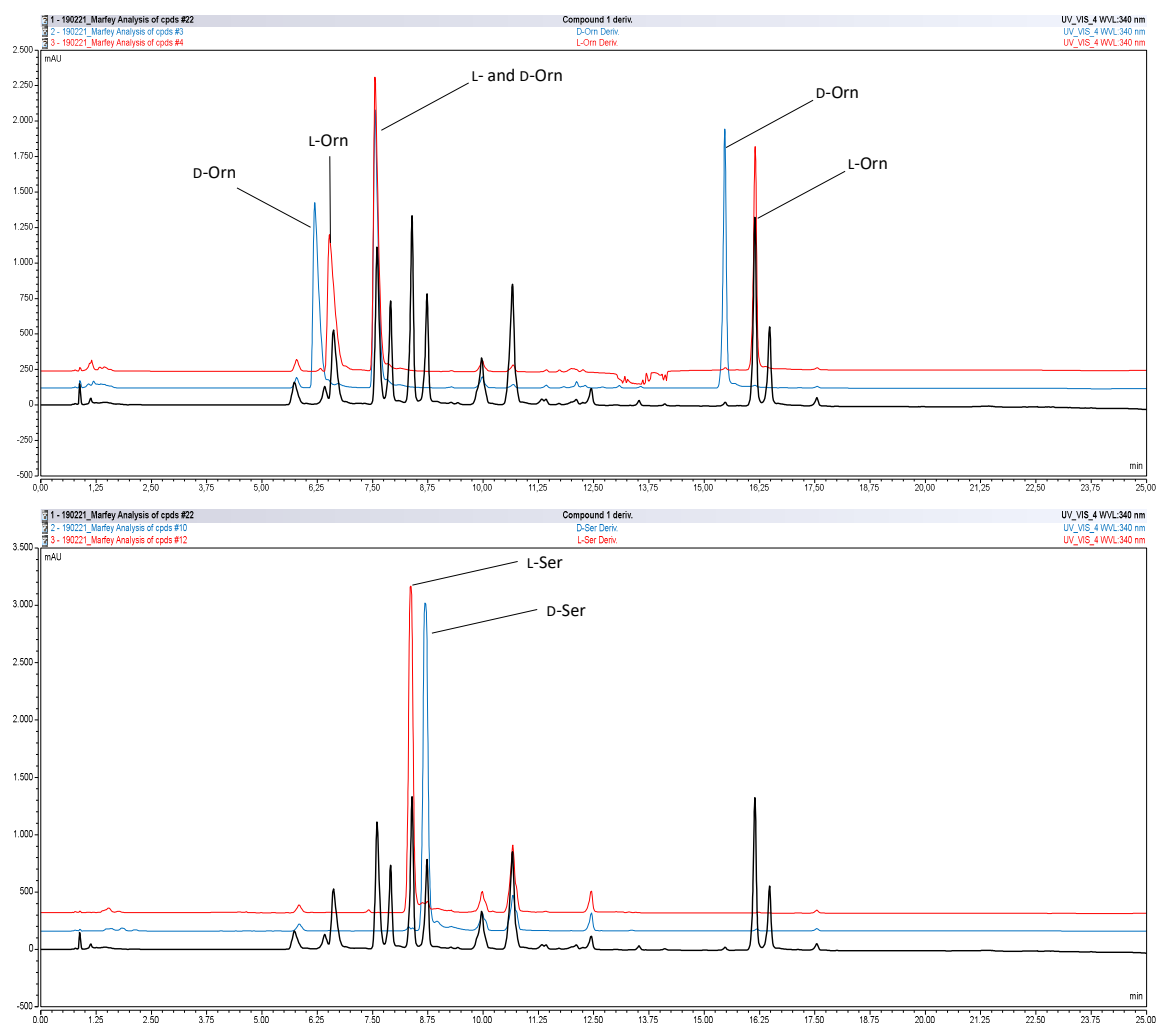
Compound 1 (23)

Figure 42: HPLC-UV chromatograms of Marfey's derivatives of the hydrolysate of compound **1** and the authentic D- and L-Orn and D- and L-Ser. Detection was done at 340 nm.

When the chromatograms of Marfey's derivatives of the hydrolysate of compound **1** and the authentic D- and L-Orn and D- and L-Ser are compared (Figure 42), it can be observed that the chromatogram of Marfey's derivative of the hydrolysate of compound **1** shares signals with the chromatograms of the derivatives of L-Orn as well as both D- and L-Ser. The signal at 7.50 min, which is assigned to the derivatives of D- and L-Orn, is present for the derivatized hydrolysate of compound **1**, D-Orn, and L-Orn. This signal is caused by Orn that was derivatized at the delta amino moiety. As the delta amino group does not contain any stereochemical information, these two Orn derivatives have the same retention time. Regarding the Ser moieties, the chromatogram of the derivative of

the hydrolysate of compound **1** shares signals with the derivatives of both stereoisomers of Ser indicating that compound **1** contains both D- and L-Ser.

Additionally, regarding the structure of compound **1**, integration of the peak areas indicated that it consists of two L-Ser and one D-Ser building blocks (relative peak area is 64.1 % for the L-Ser derivative and 35.9 % for the D-Ser derivative; Figure 43; Table 18).

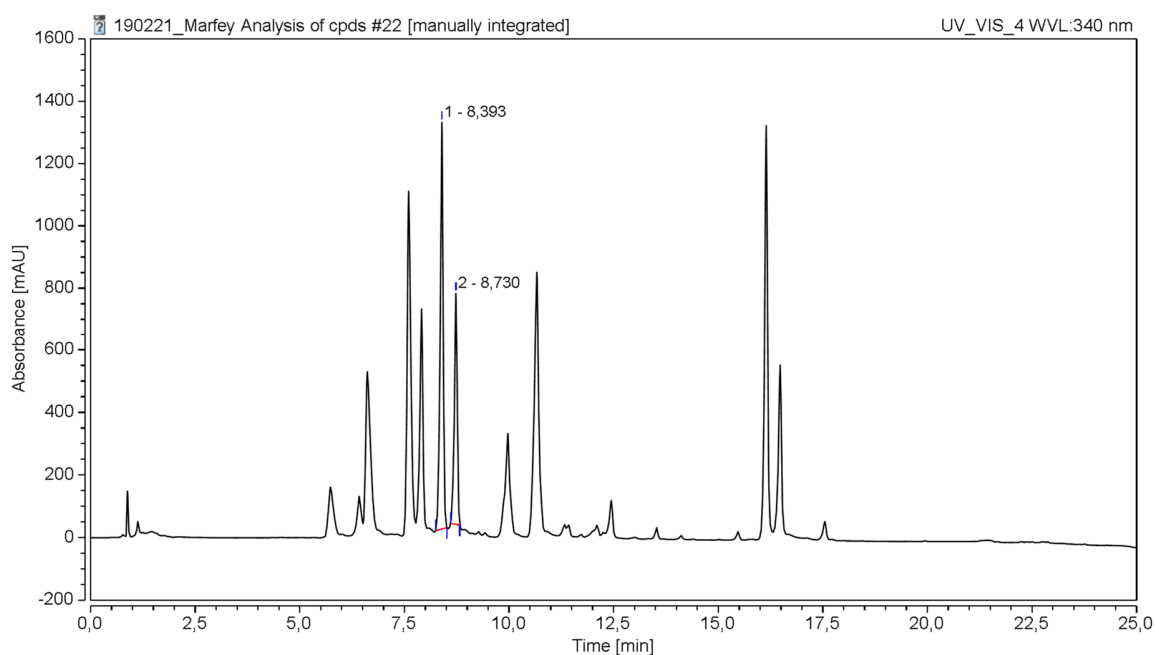


Figure 43: Integration report for Marfey's derivative of the hydrolysate of compound **1**.

Table 18: Integration report for Marfey's derivative of the hydrolysate of compound **1**.

No.	Peak Name	Retention Time [min]	Relative Area [%]
1		8,4	64,1
2		8,7	35,9
Total:			100

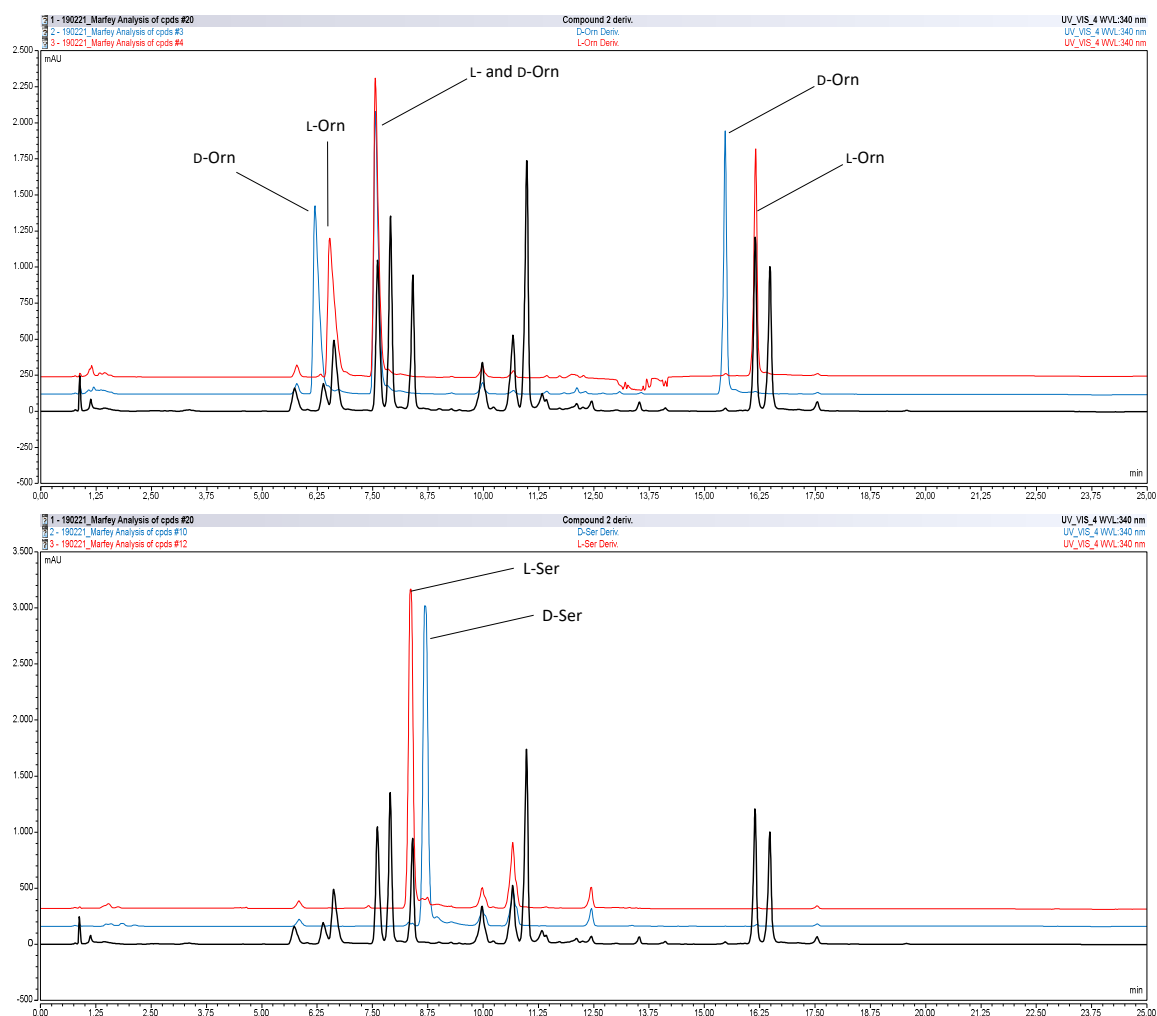
Compound 2 (24)

Figure 44: HPLC-UV chromatograms of Marfey's derivatives of the hydrolysate of compound **2** and the authentic D- and L-Orn and D- and L-Ser. Detection was done at 340 nm.

In the case of the derivatized hydrolysate of compound **2**, the chromatogram shares signals only with the derivatized L-stereoisomers of Orn and Ser (Figure 44), which means that compound **2** is composed of only the L-stereoisomers.

4. Conclusion and Outlook

In the course of this thesis, the combination of extraction techniques, analytical and semi-preparative HPLC, HRESIMS and NMR yielded the isolation and characterization of the novel leucine hydrazone, produced by the strain *S. fradiae* Tü 27. The determination of the FICI using the checkerboard assay revealed an additive cytotoxic effect of the compound in combination with the cytotoxic aminoglycoside antibiotic hygromycin B. Furthermore, synergistic cytotoxicity was observed for the combination of leucine hydrazone with another cytotoxic aminoglycoside antibiotic, G418, but not in combination with actinomycin D, which is produced by the strain Tü 27. Leucine hydrazone itself did not show relevant cytotoxic or antimicrobial activity.

Based on these results, future work could include testing for synergistic cytotoxicity of the compound in combination with further antibiotic classes. Moreover, structure elucidation of 4 additional isolated compounds followed by bioactivity assays can be performed.

For two previously isolated compounds (compound **1** and **2**), the absolute configuration was determined using Marfey's derivatization. It was shown that compound **1** contains D-Orn and both stereoisomers of Ser with a ratio of 1:2 (D-Ser:L-Ser). Compound **2**, on the other hand, is only composed of the L-stereoisomers of Orn and Ser.

As part of the project in cooperation with the Moroccan project partners, 10 endophytic bacteria were isolated from different macroalgae. Based on a bioactivity-guided workflow searching for compounds that inhibit the growth of 5 MDR pathogens, the production of globomycins was proven for these 10 strains by HPLC-UV and HPLC-MS.

As molecular biological analyses of the endophytes did not yield results, the application of 16S rRNA sequencing is an interesting topic for future work. Furthermore, the information for the in total 125 bacterial strains of Moroccan origin that was obtained by primary and secondary bioactivity screenings can serve as basis for future work with these strains.

5. References

1. Infectious Diseases Society of America. The 10 x '20 Initiative: pursuing a global commitment to develop 10 new antibacterial drugs by 2020. *Clinical infectious diseases*, 1081–1083 (2010).
2. David, M. Z. *et al.* Staphylococcus aureus bacteremia at 5 US academic medical centers, 2008–2011: significant geographic variation in community-onset infections. *Clinical infectious diseases*, 798–807 (2014).
3. Boucher, H., Miller, L. G. & Razonable, R. R. Serious infections caused by methicillin-resistant Staphylococcus aureus. *Clinical infectious diseases*, S183–97 (2010).
4. van Duin, D. & Paterson, D. L. Multidrug-Resistant Bacteria in the Community: Trends and Lessons Learned. *Infectious disease clinics of North America*, 377–390 (2016).
5. Gurusamy, K. S., Koti, R., Toon, C. D., Wilson, P. & Davidson, B. R. Antibiotic therapy for the treatment of methicillin-resistant Staphylococcus aureus (MRSA) infections in surgical wounds. *The Cochrane database of systematic reviews*, 1–24 (2013).
6. Magiorakos, A. P. *et al.* Multidrug-resistant, extensively drug-resistant and pandrug-resistant bacteria: an international expert proposal for interim standard definitions for acquired resistance. *Clinical Microbiology and Infection*, 268–281 (2012).
7. Montazeri, E. A., Khosravi, A. D., Jolodar, A., Ghaderpanah, M. & Azarpira, S. Identification of methicillin-resistant Staphylococcus aureus (MRSA) strains isolated from burn patients by multiplex PCR. *Burns*, 590–594 (2015).
8. DeLeo, F. R. & Chambers, H. F. Reemergence of antibiotic-resistant Staphylococcus aureus in the genomics era. *The Journal of clinical investigation*, 2464–2474 (2009).
9. DeLeo, F. R., Otto, M., Kreiswirth, B. N. & Chambers, H. F. Community-associated methicillin-resistant Staphylococcus aureus. *The Lancet*, 1557–1568 (2010).
10. Chen, X. *et al.* Molecular epidemiologic analysis of Staphylococcus aureus isolated from four burn centers. *Burns*, 738–742 (2012).
11. Saravolatz, L. D., Pohlod, D. J., Arking, L. M. Community-Acquired Methicillin-Resistant Staphylococcus aureus Infections: A New Source for Nosocomial Outbreaks /Community-acquired methicillin-resistant Staphylococcus aureus infections: a new source for nosocomial outbreaks. *Annals of Internal Medicine*, 325–329 (1982).
12. Guo, Y., Song, G., Sun, M., Wang, J. & Wang, Y. Prevalence and Therapies of Antibiotic-Resistance in Staphylococcus aureus. *Frontiers in cellular and infection microbiology*, 107 (2020).
13. Peacock, S. J. & Paterson, G. K. Mechanisms of Methicillin Resistance in Staphylococcus aureus. *Annual review of biochemistry*, 577–601 (2015).
14. Liu, Y. & Breukink, E. The Membrane Steps of Bacterial Cell Wall Synthesis as Antibiotic Targets. *Antibiotics* (2016).
15. Scheffers, D. J. & Pinho, M. G. Bacterial cell wall synthesis: new insights from localization studies. *Microbiology and molecular biology reviews*, 585–607 (2005).

16. Khan, S., Sallum, U. W., Zheng, X., Nau, G. J. & Hasan, T. Rapid optical determination of β -lactamase and. *BMC microbiology* (2014).
17. Gardete, S. & Tomasz, A. Mechanisms of vancomycin resistance in *Staphylococcus aureus*. *The Journal of clinical investigation*, 2836–2840 (2014).
18. Hasan, R., Acharjee, M. & Noor, R. Prevalence of vancomycin resistant *Staphylococcus aureus* (VRSA) in methicillin resistant *S. aureus* (MRSA) strains isolated from burn wound infections. *Tzu-chi medical journal*, 49–53 (2016).
19. van Hal, S. J. & Fowler, V. G. Is it time to replace vancomycin in the treatment of methicillin-resistant *Staphylococcus aureus* infections? *Clinical infectious diseases*, 1779–1788 (2013).
20. Boneca, I. G. & Chiosis, G. Vancomycin resistance: occurrence, mechanisms and strategies to combat it. *Expert opinion on therapeutic targets*, 311–328 (2003).
21. Faron, M. L., Ledebuer, N. A. & Buchan, B. W. Resistance Mechanisms, Epidemiology, and Approaches to Screening for Vancomycin-Resistant Enterococcus in the Health Care Setting. *Journal of clinical microbiology*, 2436–2447 (2016).
22. Bruinsma, N. *et al.* Influence of population density on antibiotic resistance. *The Journal of antimicrobial chemotherapy*, 385–390 (2003).
23. Bruinsma, N., Stobberingh, E., Smet, P. de & van den Bogaard, A. Antibiotic use and the prevalence of antibiotic resistance in bacteria from healthy volunteers in the dutch community. *Infection*, 9–14 (2003).
24. Cillóniz, C., Dominedò, C. & Torres, A. Multidrug Resistant Gram-Negative Bacteria in Community-Acquired Pneumonia. *Critical care*, (2019).
25. Rossolini, G. M., Arena, F., Pecile, P. & Pollini, S. Update on the antibiotic resistance crisis. *Current opinion in pharmacology*, 56–60 (2014).
26. Poole, K. Efflux-mediated multiresistance in Gram-negative bacteria. *Clinical Microbiology and Infection*, 12–26 (2004).
27. Rollauer, S. E., Soreshjani, M. A., Noinaj, N. & Buchanan, S. K. Outer membrane protein biogenesis in Gram-negative bacteria. *Philosophical transactions B* (2015).
28. Nakaido, H. Multidrug Efflux Pumps of Gram-Negative Bacteria. *Journal of Bacteriology* (1996).
29. Li, X.-Z., Plésiat, P. & Nikaido, H. The challenge of efflux-mediated antibiotic resistance in Gram-negative bacteria. *Clinical microbiology reviews*, 337–418 (2015).
30. Cowan, S. W. *et al.* Crystal structures explain functional properties of two *E. coli* porins. *Nature*, 727–733 (1992).
31. Mallea, M. *et al.* Porin alteration and active efflux: two in vivo drug resistance strategies used by *Enterobacter aerogenes*. *Microbiology*, 3003–3009 (1998).
32. Kojima, S. & Nikaido, H. Permeation rates of penicillins indicate that *Escherichia coli* porins function principally as nonspecific channels. *PNAS* (2013).
33. Chevalier, S. *et al.* Structure, function and regulation of *Pseudomonas aeruginosa* porins. *FEMS microbiology reviews*, 698–722 (2017).

34. Silhavy, T. J., Kahne, D. & Walker, S. The bacterial cell envelope. *Cold Spring Harbor perspectives in biology*, 1-16 (2010).
35. Sengstock, D. M. *et al.* Multidrug-resistant *Acinetobacter baumannii*: an emerging pathogen among older adults in community hospitals and nursing homes. *Clinical infectious diseases*, 1611–1616 (2010).
36. Falagas, M. E., Karveli, E. A., Kelesidis, I. & Kelesidis, T. Community-acquired *Acinetobacter* infections. *European journal of clinical microbiology & infectious diseases*, 857–868 (2007).
37. Munoz-Price, L. S. & Weinstein, R. A. *Acinetobacter* Infection. *The new England Journal of Medicine*, 1271–1281 (2008).
38. Young, L. S., Sabel, A. L. & Price, C. S. Epidemiologic, Clinical, and Economic Evaluation of an Outbreak of Clonal Multidrug-Resistant *Acinetobacter Baumannii* Infection in a Surgical Intensive Care Unit. *Infection Control & Hospital Epidemiology*, 1247–1254 (2007).
39. Abbott, I., Cerqueira, G. M., Bhuiyan, S. & Peleg, A. Y. Carbapenem resistance in *Acinetobacter baumannii*: laboratory challenges, mechanistic insights and therapeutic strategies. *Expert review of anti-infective therapy*, 395–409 (2013).
40. Lin, M.-F. & Lam, C.-Y. Antimicrobial resistance in *Acinetobacter baumannii*: From bench to bedside. *World journal of clinical cases*, 787–814 (2014).
41. Leclercq, R. *et al.* EUCAST expert rules in antimicrobial susceptibility testing. *Clinical Microbiology and Infection*, 141–160 (2013).
42. Dijkshoorn, L., Nemec, A. & Seifert, H. An increasing threat in hospitals: multidrug-resistant *Acinetobacter baumannii*. *Nature reviews. Microbiology*, 939–951 (2007).
43. Hassett, D. J. *et al.* *Pseudomonas aeruginosa* hypoxic or anaerobic biofilm infections within cystic fibrosis airways. *Trends in microbiology*, 130–138 (2009).
44. Rodríguez-Baño, J. *et al.* Epidemiology and clinical features of community-acquired, healthcare-associated and nosocomial bloodstream infections in tertiary-care and community hospitals. *Clinical Microbiology and Infection*, 1408–1413 (2010).
45. Singh, P. & Cole, S. T. *Mycobacterium leprae*: genes, pseudogenes and genetic diversity. *Future microbiology*, 57–71 (2011).
46. Bhat, R. M. & Prakash, C. Leprosy: an overview of pathophysiology. *Interdisciplinary perspectives on infectious diseases* (2012).
47. Smith, I. *Mycobacterium tuberculosis* pathogenesis and molecular determinants of virulence. *Clinical microbiology reviews*, 463–496 (2003).
48. Chai, Q., Zhang, Y. & Liu, C. H. *Mycobacterium tuberculosis*: An Adaptable Pathogen Associated With Multiple Human Diseases. *Frontiers in cellular and infection microbiology*, 158 (2018).
49. Houben, R. M. G. J. & Dodd, P. J. The Global Burden of Latent Tuberculosis Infection: A Re-estimation Using Mathematical Modelling. *PLoS medicine* (2016).
50. US Department of Health and Human Services/Centers for Disease Control and Prevention. Guidelines for the Treatment of Latent Tuberculosis Infection: Recommendations from the

- National Tuberculosis Controllers Association and CDC, 2020. *Morbidity and Mortality Weekly Report* (2020).
51. Rabahi, M. F., da Silva Júnior, J. L. R., Ferreira, A. C. G., Tannus-Silva, D. G. S. & Conde, M. B. Tuberculosis treatment. *Jornal brasileiro de pneumologia*, 472–486 (2017).
 52. Unissa, A. N., Subbian, S., Hanna, L. E. & Selvakumar, N. Overview on mechanisms of isoniazid action and resistance in Mycobacterium tuberculosis. *Infection, genetics and evolution*, 474–492 (2016).
 53. Schubert, K. *et al.* The Antituberculosis Drug Ethambutol Selectively Blocks Apical Growth in CMN Group Bacteria. *mBio* (2017).
 54. Zhang, Y., Shi, Shi, W., Zhang, W. & Mitchison, D. Mechanisms of Pyrazinamide Action and Resistance. *Microbiology Spectrum* (2014).
 55. Kim, J. H. *et al.* Mechanism Investigation of Rifampicin-Induced Liver Injury Using Comparative Toxicoproteomics in Mice. *International journal of molecular sciences* (2017).
 56. Metushi, I., Uetrecht, J. & Phillips, E. Mechanism of isoniazid-induced hepatotoxicity: then and now. *British journal of clinical pharmacology*, 1030–1036 (2016).
 57. Wang, P., Pradhan, K., Zhong, X.-B. & Ma, X. Isoniazid metabolism and hepatotoxicity. *Acta pharmaceutica Sinica. B*, 384–392 (2016).
 58. Ramappa, V. & Aithal, G. P. Hepatotoxicity Related to Anti-tuberculosis Drugs: Mechanisms and Management. *Journal of clinical and experimental hepatology*, 37–49 (2013).
 59. Seung, K. J., Keshavjee, S. & Rich, M. L. Multidrug-Resistant Tuberculosis and Extensively Drug-Resistant Tuberculosis. *Cold Spring Harbor perspectives in medicine* (2015).
 60. Parida, S. K. *et al.* Totally drug-resistant tuberculosis and adjunct therapies. *Journal of internal medicine*, 388–405 (2015).
 61. Sandy, J., Holton, S., Fullam, E., Sim, E. & Noble, M. Binding of the anti-tubercular drug isoniazid to the arylamine N-acetyltransferase protein from Mycobacterium smegmatis. *Protein science*, 775–782 (2005).
 62. Yendapally, R. & Lee, R. E. Design, synthesis, and evaluation of novel ethambutol analogues. *Bioorganic & medicinal chemistry letters*, 1607–1611 (2008).
 63. Chaitanya V, S., Das, M., Bhat, P. & Ebenezer, M. Computational Modelling of Dapsone Interaction With Dihydropteroate Synthase in Mycobacterium leprae; Insights Into Molecular Basis of Dapsone Resistance in Leprosy. *Journal of cellular biochemistry*, 2293–2303 (2015).
 64. Blok, D. J., Vias, S. J. de & Richardus, J. H. Global elimination of leprosy by 2020: are we on track? *Parasites & vectors*, 548 (2015).
 65. Fischer, M. Leprosy - an overview of clinical features, diagnosis, and treatment. *Journal der Deutschen Dermatologischen Gesellschaft*, 801–827 (2017).
 66. Kar, H. K. & Gupta, R. Treatment of leprosy. *Clinics in dermatology*, 55–65 (2015).
 67. Ramos-e-Silva, M. & Rebello, P. F. B. Leprosy Recognition and Treatment. *Therapy in Practice*, 203–211 (2001).

68. Worobec, S. M. Current approaches and future directions in the treatment of leprosy. *Research and reports in tropical medicine*, 79–91 (2012).
69. Shlaes, D. M., Sahm, D., Opiela, C. & Spellberg, B. The FDA reboot of antibiotic development. *Antimicrobial agents and chemotherapy*, 4605–4607 (2013).
70. Llor, C. & Bjerrum, L. Antimicrobial resistance: risk associated with antibiotic overuse and initiatives to reduce the problem. *Therapeutic Advances in Drug Safety* (2014).
71. Niederman, M. S. Principles of appropriate antibiotic use. *Antimicrobial agents*, 170–175 (2005).
72. Pechere, J.-C., Hughes, D., Kardas, P. & Cornaglia G. Non-compliance with antibiotic therapy for acute community infections: a global survey. *International journal of antimicrobial agents*, 245–253 (2007).
73. Falagas, M. E., Karagiannis, A. K. A., Nakouti, T. & Tansarli, G. S. Compliance with once-daily versus twice or thrice-daily administration of antibiotic regimens: a meta-analysis of randomized controlled trials. *PloS one* (2015).
74. Chang, Q., Wang, W., Regev-Yochay, G., Lipsitch, M. & Hanage, W. P. Antibiotics in agriculture and the risk to human health: how worried should we be? *Evolutionary applications*, 240–247 (2015).
75. Chattopadhyay, M. K. Use of antibiotics as feed additives: a burning question. *Frontiers in microbiology*, 334 (2014).
76. Manyi-Loh, C., Mamphweli, S., Meyer, E. & Okoh, A. Antibiotic Use in Agriculture and Its Consequential Resistance in Environmental Sources: Potential Public Health Implications. *Molecules* (2018).
77. Gyles, C. & Boerlin, P. Horizontally transferred genetic elements and their role in pathogenesis of bacterial disease. *Veterinary pathology*, 328–340 (2014).
78. Kay, E., Vogel, T. M., Bertolla, F., Nalin, R. & Simonet, P. In situ transfer of antibiotic resistance genes from transgenic (transplastomic) tobacco plants to bacteria. *Applied and environmental microbiology*, 3345–3351 (2002).
79. Frost, L. S., Lepiae, R., Summers, A. O. & Toussaint, A. Mobile genetic elements: the agents of open source evolution. *Nature reviews. Microbiology* **3**, 722–732 (2005).
80. Ochman, H., Lawrence, J. G. & Groisman, E. A. Lateral gene transfer and the nature of bacterial innovation. *Nature*, 299–304 (2000).
81. Sharma, A. K. *et al.* Bacterial Virulence Factors: Secreted for Survival. *Indian journal of microbiology*, 1–10 (2017).
82. Hogan, L. H., Klein, B. & Levitz, S. M. Virulence Factors of Medically Important Fungi. *Clinical microbiology reviews*, 469–488 (1996).
83. Schrauwen, E. J. A. *et al.* Determinants of virulence of influenza A virus. *European journal of clinical microbiology & infectious diseases*, 479–490 (2014).
84. Lopez-Rubio, J. L., Riviere, L. & Scherf, A. Shared epigenetic mechanisms control virulence factors in protozoan parasites. *Current opinion in microbiology*, 560–568 (2007).

85. Siegel, S. J. & Weiser, J. N. Mechanisms of Bacterial Colonization of the Respiratory Tract. *Annual review of microbiology*, 425–444 (2015).
86. Ho Sui, S. J., Fedynak, A., Hsiao, W. W. L., Langille, M. G. I. & Brinkman, F. S. L. The association of virulence factors with genomic islands. *PLoS one* (2009).
87. Rudkin, J. K., McLoughlin, R. M., Preston, A. & Massey, R. C. Bacterial toxins: Offensive, defensive, or something else altogether? *PLoS pathogens* (2017).
88. Vandenesch, F., Lina, G. & Henry, T. Staphylococcus aureus hemolysins, bi-component leukocidins, and cytolytic peptides: a redundant arsenal of membrane-damaging virulence factors? *Frontiers in cellular and infection microbiology*, 12 (2012).
89. Sheng, H., Lim, J. Y., Knecht, H. J., Li, J. & Hovde, C. J. Role of Escherichia coli O157:H7 virulence factors in colonization at the bovine terminal rectal mucosa. *Infection and immunity*, 4685–4693 (2006).
90. Davies, J. Antibiotic resistance and the golden age of microbiology. *Uppsala journal of medical sciences*, 65–67 (2014).
91. Bérdy, J. Thoughts and facts about antibiotics: where we are now and where we are heading. *The Journal of antibiotics*, 385–395 (2012).
92. Goodfellow, M. & Williams, S. T. Ecology of actinomycetes. *Annual review of microbiology*, 189–216 (1983).
93. Barka, E. A. *et al.* Taxonomy, Physiology, and Natural Products of Actinobacteria. *Microbiology and molecular biology reviews*, 1–43 (2016).
94. Chankhamhaengdecha, S., Hongvijit, S., Srichaisupakit, A., Charnchai, P. & Panbangred, W. Endophytic actinomycetes: a novel source of potential acyl homoserine lactone degrading enzymes. *BioMed research international*, 1–8 (2013).
95. Sessitsch, A., Reiter, B., Pfeifer, U. & Wilhelm, E. Cultivation-independent population analysis of bacterial endophytes in three potato varieties based on eubacterial and Actinomycetes-specific PCR of 16S rRNA genes. *FEMS microbiology ecology*, 23–32 (2002).
96. Khare, E., Mishra, J. & Arora, N. K. Multifaceted Interactions Between Endophytes and Plant: Developments and Prospects. *Frontiers in microbiology* (2018).
97. Gouda, S., Das, G., Sen, S. K., Shin, H.-S. & Patra, J. K. Endophytes: A Treasure House of Bioactive Compounds of Medicinal Importance. *Frontiers in microbiology* (2016).
98. Etminani, F. & Harighi, B. Isolation and Identification of Endophytic Bacteria with Plant Growth Promoting Activity and Biocontrol Potential from Wild Pistachio Trees. *The plant pathology journal*, 208–217 (2018).
99. Slonczewski, J. L. & Foster, J. W. *Mikrobiologie. Eine Wissenschaft mit Zukunft*. 2nd ed. (Springer Spektrum, 2011).
100. Rosenblueth, M. & Martínez-Romero, E. Bacterial Endophytes and Their Interactions with Hosts. *The American Phytopathological Society*, 827–837 (2006).

101. Strobel, G. The Emergence of Endophytic Microbes and Their Biological Promise. *Journal of fungi* (2018).
102. Yadav, A. Exploring the Potential of Endophytes in Agriculture: A Minireview. *Advances in Plants & Agriculture Research* (2017).
103. White, J. F. *et al.* Review: Endophytic microbes and their potential applications in crop management. *Pest management science*, 2558–2565 (2019).
104. Le Cocq, K., Gurr, S. J., Hirsch, P. R. & Mauchline, T. H. Exploitation of endophytes for sustainable agricultural intensification. *Molecular plant pathology*, 469–473 (2017).
105. Golinska, P. *et al.* Endophytic actinobacteria of medicinal plants: diversity and bioactivity. *Antonie van Leeuwenhoek*, 267–289 (2015).
106. Nalini, M. S. & Prakash, H. S. Diversity and bioprospecting of actinomycete endophytes from the medicinal plants. *Letters in applied microbiology*, 261–270 (2017).
107. Srinivasan, M. C., Laxman, R. S. & Deshpande, M. V. Physiology and nutritional aspects of actinomycetes: an overview. *Journal of microbiology and biotechnology*, 171–184 (1991).
108. Ventura, M. *et al.* Genomics of Actinobacteria: tracing the evolutionary history of an ancient phylum. *Microbiology and molecular biology reviews*, 495–548 (2007).
109. Zheng, H. & Wu, H. Gene-centric association analysis for the correlation between the guanine-cytosine content levels and temperature range conditions of prokaryotic species. *BMC bioinformatics* (2010).
110. Ahmed, M. & Kelley, S. O. Enhancing the Potency of Nalidixic Acid toward a Bacterial DNA Gyrase with Conjugated Peptides. *ACS chemical biology*, 2563–2569 (2017).
111. Schneider-Poetsch, T. *et al.* Inhibition of eukaryotic translation elongation by cycloheximide and lactimidomycin. *Nature chemical biology*, 209–217 (2010).
112. Gao, B. & Gupta, R. S. Phylogenetic framework and molecular signatures for the main clades of the phylum Actinobacteria. *Microbiology and molecular biology reviews*, 66–112 (2012).
113. Bérdy, J. Bioactive microbial metabolites. *The Journal of antibiotics*, 1–26 (2005).
114. Maiti, P. K., Das, S., Sahoo, P. & Mandal, S. Streptomyces sp SM01 isolated from Indian soil produces a novel antibiotic picolinamycin effective against multi drug resistant bacterial strains. *Scientific reports*, 10092 (2020).
115. Maghembe, R. *et al.* Omics for Bioprospecting and Drug Discovery from Bacteria and Microalgae. *Antibiotics* (2020).
116. Sekurova, O. N., Schneider, O. & Zotchev, S. B. Novel bioactive natural products from bacteria via bioprospecting, genome mining and metabolic engineering. *Microbial biotechnology*, 828–844 (2019).
117. Becker, B. & Cooper, M. A. Aminoglycoside antibiotics in the 21st century. *ACS chemical biology*, 105–115 (2013).
118. Gao, W., Wu, Z., Sun, J., Ni, X. & Xia, H. Modulation of kanamycin B and kanamycin A biosynthesis in *Streptomyces kanamyceticus* via metabolic engineering. *PloS one*, 1-19 (2017).

119. Sonousi, A., Shcherbakov, D., Vasella, A., Böttger, E. C. & Crich, D. Synthesis, ribosomal selectivity, and antibacterial activity of netilmicin 4'-derivatives. *Medicinal Chemistry Communications*, 946–950 (2019).
120. Raja, A., Prabakarana, P. Actinomycetes and Drug-An Overview. *American Journal of Drug Discovery and Development*, 75–84 (2011).
121. Oliynyk, M. *et al.* Complete genome sequence of the erythromycin-producing bacterium *Saccharopolyspora erythraea* NRRL23338. *Nature biotechnology*, 447–453 (2007).
122. Gupta, S., Lakshmanan, V., Kim, B. S., Fecik, R. & Reynolds, K. A. Generation of novel pikromycin antibiotic products through mutasynthesis. *ChemBioChem*, 1609–1616 (2008).
123. Fouces, R., Mellado, E., Diez, B. & Barredo, J. L. The tylosin biosynthetic cluster from *Streptomyces fradiae*: genetic organization of the left region. *Microbiology*, 855–868 (1999).
124. Zhong, J., Lu, Z., Dai, J. & He, W. Identification of two regulatory genes involved in carbomycin biosynthesis in *Streptomyces thermotolerans*. *Archives of microbiology*, 1023–1033 (2017).
125. Fernández-Martínez, L., Borsetto, C. Gomez-Escribano, J. P., Bipp, M. J. & Al-Bassam, M. M., Chandra, G., Bibb, M. J. New insights into chloramphenicol biosynthesis in *Streptomyces venezuelae* ATCC 10712. *Antimicrobial agents and chemotherapy*, 7441–7450 (2014).
126. Verma, M. *et al.* Whole genome sequence of the rifamycin B-producing strain *Amycolatopsis mediterranei* S699. *Journal of Bacteriology*, 5562–5563 (2011).
127. Li, C.-R. *et al.* In vitro antibacterial activity of vertilmicin and its susceptibility to modifications by the recombinant AAC6'-APH2" enzyme. *Antimicrobial agents and chemotherapy*, 3875–3882 (2008).
128. Tan, G.-Y., Deng, Z. & Liu, T. Recent advances in the elucidation of enzymatic function in natural product biosynthesis. *F1000Research* (2015).
129. Rangseekaew, P. & Pathom-Aree, W. Cave Actinobacteria as Producers of Bioactive Metabolites. *Frontiers in microbiology* (2019).
130. Jiang, L. *et al.* Huanglongmycin A-C, Cytotoxic Polyketides Biosynthesized by a Putative Type II Polyketide Synthase From *Streptomyces* sp. CB09001. *Frontiers in chemistry* (2018).
131. Jiang, Z. *et al.* Xiakemycin A, a novel pyranonaphthoquinone antibiotic, produced by the *Streptomyces* sp. CC8-201 from the soil of a karst cave. *The Journal of antibiotics*, 771–774 (2015).
132. Axenov-Gribanov, D. V. *et al.* Actinobacteria Isolated from an Underground Lake and Moonmilk Speleothem from the Biggest Conglomeratic Karstic Cave in Siberia as Sources of Novel Biologically Active Compounds. *PLoS one*, 1-12 (2016).
133. Zhang, X., Ye, X., Chai, W., Lian, X.-Y. & Zhang, Z. New Metabolites and Bioactive Actinomycins from Marine-Derived *Streptomyces* sp. ZZ338. *Marine drugs* (2016).
134. Wichner, D. *et al.* Isolation and anti-HIV-1 integrase activity of lentzeosides A-F from extremotolerant *lentzea* sp. H45, a strain isolated from a high-altitude Atacama Desert soil. *The Journal of antibiotics*, 448–453 (2017).

135. Dou, J.-L., Jiang, Yi-Wei, J., Xie, J.-Q. & Zhang, X.-G. New Is Old, and Old Is New: Recent Advances in Antibiotic-Based, Antibiotic-Free and Ethnomedical Treatments against Methicillin-Resistant *Staphylococcus aureus* Wound Infections. *International journal of molecular sciences* (2016).
136. Katz, M. I., Mueller, L. V., Polyakov, M. & Weinstock, S. F. Where have all the antibiotic patents gone? *Nature biotechnology*, 1529–1531 (2006).
137. Wenzel, R. P. The Antibiotic Pipeline—Challenges, Costs, and Values. *The New England Journal of Medicine*, 523–526 (2004).
138. Günthard, H. F. *et al.* Antiretroviral Drugs for Treatment and Prevention of HIV Infection in Adults: 2016 Recommendations of the International Antiviral Society-USA Panel. *Journal of the American Medical Association*, 191–210 (2016).
139. Eakle, R., Venter, F. & Rees, H. Pre-exposure prophylaxis (PrEP) in an era of stalled HIV prevention: Can it change the game? *Retrovirology*, 29 (2018).
140. Miller, T. W. *et al.* Quantitative high-throughput screening assays for the discovery and development of SIRP α -CD47 interaction inhibitors. *PloS one* (2019).
141. Churko, J. M., Mantalas, G. L., Snyder, M. P. & Wu, J. C. Overview of high throughput sequencing technologies to elucidate molecular pathways in cardiovascular diseases. *Circulation research*, 1613–1623 (2013).
142. Allard, P.-M. *et al.* Integration of Molecular Networking and In-Silico MS/MS Fragmentation for Natural Products Dereplication. *Analytical chemistry*, 3317–3323 (2016).
143. Yang, J. Y. *et al.* Molecular networking as a dereplication strategy. *Journal of natural products*, 1686–1699 (2013).
144. Wang, M. *et al.* Sharing and community curation of mass spectrometry data with Global Natural Products Social Molecular Networking. *Nature biotechnology*, 828–837 (2016).
145. van der Hooft, J. J. J., Padmanabhan, S., Burgess, K. E. V. & Barrett, M. P. Urinary antihypertensive drug metabolite screening using molecular networking coupled to high-resolution mass spectrometry fragmentation. *Metabolomics*, 125 (2016).
146. Watrous, J. *et al.* Mass spectral molecular networking of living microbial colonies. *Proceedings of the National Academy of Sciences of the United States of America* (2012).
147. Guo, Z. The modification of natural products for medical use. *Acta pharmaceutica Sinica. B*, 119–136 (2017).
148. Shugrue, C. R. & Miller, S. J. Applications of Nonenzymatic Catalysts to the Alteration of Natural Products. *Chemical reviews*, 11894–11951 (2017).
149. Robles, O. & Romo, D. Chemo- and site-selective derivatizations of natural products enabling biological studies. *Natural product reports*, 318–334 (2014).
150. Karimov, R. R. & Hartwig, J. F. Transition-Metal-Catalyzed Selective Functionalization of C(sp³)-H Bonds in Natural Products. *Angewandte Chemie*, 4234–4241 (2018).
151. WHO. 2019 Antibacterial agents in clinical development (2019).

152. Katz, L. & Baltz, R. H. Natural product discovery: Past, present, and future. *Journal of industrial microbiology & biotechnology*, 155–176 (2016).
153. Prabhavathi Fernandes. Antibacterial discovery and development— the failure of success? *Nature biotechnology*, 1497–1503 (2006).
154. Demay, J., Bernard, C., Reinhardt, A. & Marie, B. Natural Products from Cyanobacteria: Focus on Beneficial Activities. *Marine drugs* (2019).
155. Dittmann, E., Gugger, M., Sivonen, K. & Fewer, D. P. Natural Product Biosynthetic Diversity and Comparative Genomics of the Cyanobacteria. *Trends in microbiology*, 642–652 (2015).
156. Pan, R., Bai, X., Chen, J., Zhang, H. & Wang, H. Exploring Structural Diversity of Microbe Secondary Metabolites Using OSMAC Strategy: A Literature Review. *Frontiers in microbiology* (2019).
157. Abdelnasser, S. S. I., Ali, A. A. S., Ashraf, A. H., Mohammed, S. E. S. & Shebl, S. S. I. Tapping uncultured microorganisms through metagenomics for drug discovery. *African Journal of Biotechnology*, 15823–15834 (2012).
158. Hemaiswarya, S., Kruthiventi, A. K. & Doble, M. Synergism between natural products and antibiotics against infectious diseases. *Phytomedicine*, 639–652 (2008).
159. Mohs, R. C. & Greig, N. H. Drug discovery and development: Role of basic biological research. *Alzheimer's & dementia*, 651–657 (2017).
160. Zarkotou, O. *et al.* Predictors of mortality in patients with bloodstream infections caused by KPC-producing *Klebsiella pneumoniae* and impact of appropriate antimicrobial treatment. *Clinical Microbiology and Infection*, 1798–1803 (2011).
161. Ainoda, Y. *et al.* *Klebsiella pneumoniae* carbapenemase (KPC)-producing *Klebsiella pneumoniae* ST258 isolated from a Japanese patient without a history of foreign travel - a new public health concern in Japan: a case report. *BMC infectious diseases* (2019).
162. Batirel, A. *et al.* Comparison of colistin-carbapenem, colistin-sulbactam, and colistin plus other antibacterial agents for the treatment of extremely drug-resistant *Acinetobacter baumannii* bloodstream infections. *European journal of clinical microbiology & infectious diseases*, 1311–1322 (2014).
163. Tumbarello, M. *et al.* Predictors of mortality in bloodstream infections caused by *Klebsiella pneumoniae* carbapenemase-producing *K. pneumoniae*: importance of combination therapy. *Clinical infectious diseases*, 943–950 (2012).
164. Tzouvelekis, L. S., Markogiannakis, A., Piperaki, E., Souli, M. & Daikos, G. L. Treating infections caused by carbapenemase-producing Enterobacteriaceae. *Clinical Microbiology and Infection*, 862–872 (2014).
165. Tyers, M. & Wright, G. D. Drug combinations: a strategy to extend the life of antibiotics in the 21st century. *Nature reviews. Microbiology*, 141–155 (2019).
166. Lim, L. M. *et al.* Resurgence of colistin: a review of resistance, toxicity, pharmacodynamics, and dosing. *Pharmacotherapy*, 1279–1291 (2010).

167. Vicari, G., Bauer, S. R., Neuner, E. A. & Lam, S. W. Association between colistin dose and microbiologic outcomes in patients with multidrug-resistant gram-negative bacteremia. *Clinical infectious diseases*, 398–404 (2013).
168. Falagas, M. E., Grammatikos, A. P. & Michalopoulos, A. Potential of old-generation antibiotics to address current need for new antibiotics. *Expert review of anti-infective therapy*, 593–600 (2008).
169. González-Bello, C. Antibiotic adjuvants - A strategy to unlock bacterial resistance to antibiotics. *Bioorganic & medicinal chemistry letters*, 4221–4228 (2017).
170. Worthington, R. J. & Melander, C. Combination approaches to combat multidrug-resistant bacteria. *Trends in biotechnology*, 177–184 (2013).
171. Wright, G. D. Antibiotic Adjuvants: Rescuing Antibiotics from Resistance. *Trends in microbiology*, 862–871 (2016).
172. Gleice C. L. *et al.* Effect of Antibiotics Combination and Comparison of Methods for Detection of Synergism in Multiresistant Gram-Negative Bacteria. *Journal of Infectious Diseases and Therapy* (2015).
173. Piggot, P. J. Mapping of Asporogenous Mutations of Bacillus: a minimum estimate of the number of sporulation operons. *Journal of Bacteriology*, 1241–1253 (1973).
174. Helge Björn Bode, Barbara Bethe, Regina Höfs, and Axel Zeeck. Big Effects from Small Changes: Possible Ways to Explore Nature's Chemical Diversity. *ChemBioChem*, 619–627 (2002).
175. Shirling, E. B. & Gottlieb, D. Methods for characterization of Streptomyces species. *INTERNATIONAL JOURNAL OF SYSTEMATIC BACTERIOLOGY*, 313–340 (1966).
176. William M. Haynes (94 th ed.). *Handbook of Chemistry and Physics* (CRC Press, 2014).
177. Urban, A. *et al.* Novel whole-cell antibiotic biosensors for compound discovery. *Applied and environmental microbiology*, 6436–6443 (2007).
178. Kawaguchi, T., Chen, Y. P., Norman, R. S. & Decho, A. W. Rapid screening of quorum-sensing signal N-acyl homoserine lactones by an in vitro cell-free assay. *Applied and environmental microbiology*, 3667–3671 (2008).
179. Santiago, H. *et al.* Development of a recombination system for the generation of occlusion positive genetically modified Anticarsia gemmatalis multiple nucleopolyhedrovirus. *Viruses*, 1599–1612 (2015).
180. Vichai, V. & Kirtikara, K. Sulforhodamine B colorimetric assay for cytotoxicity screening. *Nature protocols*, 1112–1116 (2006).
181. Meletiadis, J., Pournaras, S., Roilides, E. & Walsh, T. J. Defining fractional inhibitory concentration index cutoffs for additive interactions based on self-drug additive combinations, Monte Carlo simulation analysis, and in vitro-in vivo correlation data for antifungal drug combinations against Aspergillus fumigatus. *Antimicrobial agents and chemotherapy*, 602–609 (2010).

182. Cook, A. E. & Meyers, P. R. Rapid identification of filamentous actinomycetes to the genus level using genus-specific 16S rRNA gene restriction fragment patterns. *International journal of systematic and evolutionary microbiology*, 1907–1915 (2003).
183. Thomas P. Curtis, William T. Sloan, and Jack W. Scannell. Estimating prokaryotic diversity and its limits. *PNAS*, 10494–10499 (2002).
184. Müllhardt, C. (7 th ed.). *Der Experimentator Molekularbiologie/Genomics* (Springer Spektrum, 2013).
185. Marfey, P. Determination of D-amino acids. II. Use of a bifunctional reagent, 1,5-difluoro-2,4-dinitrobenzene. *Carlsberg Research Communications*, 591–596 (1984).
186. Bhushan, R. & Brückner, H. Marfey's reagent for chiral amino acid analysis: a review. *Amino acids*, 231–247 (2004).
187. Eida, A. A. & Mahmud, T. The secondary metabolite pactamycin with potential for pharmaceutical applications: biosynthesis and regulation. *Applied microbiology and biotechnology*, 4337–4345 (2019).
188. Eida, A. A., Abugrain, M. E., Brumsted, C. J. & Mahmud, T. Glycosylation of acyl carrier protein-bound polyketides during pactamycin biosynthesis. *Nature chemical biology*, 795–802 (2019).
189. Bhuyan, B. K. Pactamycin, an antibiotic that inhibits protein synthesis. *Biochemical pharmacology*, 1411–1420 (1967).
190. Sharpe, R. J. *et al.* Preparation and biological evaluation of synthetic and polymer-encapsulated congeners of the antitumor agent pactamycin: insight into functional group effects and biological activity. *Bioorganic & medicinal chemistry*, 1849–1857 (2015).
191. Zhang, X., Ye, X., Chai, W., Lian, X.-Y. & Zhang, Z. New Metabolites and Bioactive Actinomycins from Marine-Derived *Streptomyces* sp. ZZ338. *Marine drugs* (2016).
192. Chopra, I. & Roberts, M. Tetracycline antibiotics: mode of action, applications, molecular biology, and epidemiology of bacterial resistance. *Microbiology and molecular biology reviews*, 232-260 (2001).
193. Tanaka, K. *et al.* Anti-inflammatory effects of green soybean extract irradiated with visible light. *Scientific reports*, 4732 (2014).
194. Barić, D. & Maksić, Z. B. On the origin of Baeyer strain in molecules – an ab initio and DFT analysis. *Theoretical Chemistry Accounts*, 222–228 (2005).
195. Stražić, D., Benković, T., Gembarovski, D., Kontrec, D. & Galić, N. Comprehensive ESI-MS and MS/MS analysis of aromatic hydrazones derived from nicotinic acid hydrazide. *International Journal of Mass Spectrometry*, 54–64 (2014).
196. Kovaríková, P. *et al.* HPLC-DAD and MS/MS analysis of novel drug candidates from the group of aromatic hydrazones revealing the presence of geometric isomers. *Journal of pharmaceutical and biomedical analysis*, 295–302 (2008).

197. Ivanov, I. P. *et al.* Synthesis, structural analysis and application of a series of solid-state fluorochromes—aryl hydrazones of 4-hydrazino-N-hexyl-1,8-naphthalimide. *Tetrahedron*, 712–721 (2013).
198. Nawrat, C. C. & Moody, C. J. Natural products containing a diazo group. *Natural product reports*, 1426–1444 (2011).
199. Le Goff, G. Ouazzani, J. Natural hydrazine-containing compounds: Biosynthesis, isolation, biological activities and synthesis. *Bioorganic & medicinal chemistry*, 6529–6544 (2014).
200. Abdelfattah, M. S., Toume, K., Arai, M. A., Masu, H. & Ishibashi, M. Katorazone, a new yellow pigment with a 2-azaquinone-phenylhydrazone structure produced by *Streptomyces* sp. IFM 11299. *Tetrahedron Letters*, 3346–3348 (2012).
201. Abdelfattah, M. S., Toume, K. & Ishibashi, M. Yoropyrazone, a new naphthopyridazone alkaloid isolated from *Streptomyces* sp. IFM 11307 and evaluation of its TRAIL resistance-overcoming activity. *The Journal of antibiotics*, 245–248 (2012).
202. Hamada, M. *et al.* A new antibiotic, negamycin. *The Journal of antibiotics*, 170–171 (1970).
203. Uehara, Y., Kondo, S., Umezawa, H., Suzukake, K. & Hori, M. Negamycin, a miscoding antibiotic with a unique structure. *The Journal of antibiotics*, 685–688 (1972).
204. Taguchi, A. *et al.* Negamycin analogue with readthrough-promoting activity as a potential drug candidate for duchenne muscular dystrophy. *ACS medicinal chemistry letters*, 118–122 (2012).
205. Kuroda, Y. *et al.* FR-900137, A new antibiotic. *The Journal of antibiotics*, 280–283 (1980).
206. Takasawa, S. *et al.* A new antibiotic XK-90. *The Journal of antibiotics*, 1015–1018 (1976).
207. Takai, H., Yoshida, M., Iida, T., Matsubara, I. A new antibiotic XK-90. II. The structure of XK-90. *The Journal of antibiotics*, 1253–1257 (1976).
208. Ogita, T., Gunji, S., Fukazawa, Y. & Terahara, A. The structure of fosfazinomycin A and B. *Tetrahedron Letters*, 2283–2286 (1983).
209. Rollas, S. & Küçükgül, S. G. Biological Activities of Hydrazone Derivatives. *Molecules*, 1910–1939 (2007).
210. Padmini, K. *et al.* A Review on Biological Importance of Hydrazones. *International Journal of Pharma Research & Review*, 43–58 (2013).
211. Le Goff, G. *et al.* Isolation and characterization of unusual hydrazides from *Streptomyces* sp. impact of the cultivation support and extraction procedure. *Journal of natural products*, 142–149 (2013).
212. Garg, R. P., Qian, X. L., Alemany, L. B., Moran, S. & Parry, R. J. Investigations of valanimycin biosynthesis: Elucidation of the role of seryl_tRNA. *PNAS* (2008).
213. Phelps, J. B., Hoffman, W. P., Lee, C., Murphy, G. P. & Garriott, M. L. Relative cytotoxicity values at the lowest effective concentration for 12 positive chemicals in the in vitro micronucleus test utilizing Chinese hamster ovary cells. *Mutation research*, 153–158 (2004).

214. Qi, Y.-I., Liao, F., Zhao, C., Lin, Y. & Zuo, M. Cytotoxicity, apoptosis induction, and mitotic arrest by a novel podophyllotoxin glucoside, 4DPG, in tumor cells. *Acta pharmacologica Sinica*, 1000–1008 (2005).
215. Yörük, E. & Albayrak, G. Geneticin (G418) resistance and electroporation-mediated transformation of *Fusarium graminearum* and *F. culmorum*. *Biotechnology, biotechnological equipment*, 268–273 (2015).
216. Oung, H.-M., Lin, K.-C., Wu, T.-M., Chandrika, N. N. P. & Hong, C.-Y. Hygromycin B-induced cell death is partly mediated by reactive oxygen species in rice (*Oryza sativa* L.). *Plant molecular biology*, 577–588 (2015).
217. Liu, M. *et al.* Identification of the Actinomycin D Biosynthetic Pathway from Marine-derived *Streptomyces costaricanus* SCSIO ZS0073. *Marine drugs* (2019).
218. Borovinskaya, M. A., Shoji, S., Fredrick, K. & Cate, J. H. D. Structural basis for hygromycin B inhibition of protein biosynthesis. *RNA*, 1590–1599 (2008).
219. Vicens, Q. & Westhof, E. Crystal Structure of Geneticin Bound to a Bacterial 16S Ribosomal RNA A Site Oligonucleotide. *Journal of Molecular Biology*, 1175–1188 (2003).
220. Geisslinger, Menzel, Gudermann, Hinz, Ruth (11 th ed.). *Mutschler Arzneimittelwirkung* (Wissenschaftliche Verlagsgesellschaft, 2020).
221. Moreno-Martinez, E., Vallières, C., Holland, S. L. & Avery, S. V. Novel, Synergistic Antifungal Combinations that Target Translation Fidelity. *Scientific reports* (2015).
222. Vallières, C., Raulo, R., Dickinson, M. & Avery, S. V. Novel Combinations of Agents Targeting Translation That Synergistically Inhibit Fungal Pathogens. *Frontiers in microbiology* (2018).
223. Markovich, D. Physiological Roles and Regulation of Mammalian Sulfate Transporters. *Physiological reviews*, 1499–1533 (2001).
224. Achan, J. *et al.* Quinine, an old anti-malarial drug in a modern world: role in the treatment of malaria. *Malaria journal* (2011).
225. Khozoie, C., Pleass, R. J. & Avery, S. V. The antimalarial drug quinine disrupts Tat2p-mediated tryptophan transport and causes tryptophan starvation. *The Journal of biological chemistry*, 17968–17974 (2009).
226. Matsui, Y. *et al.* Effect of a leucine-enriched essential amino acids mixture on muscle recovery. *the journal of Physical Therapy Science*, 95–101 (2019).
227. Ruddick, S. M. & Williams, S. T. Studies on the ecology of Actinomycetes in soil. *Soil biology and biochemistry*, 93–103 (1992).
228. Angert, E. R. Alternatives to binary fission in bacteria. *Nature reviews. Microbiology*, 214–224 (2005).
229. Romano, S., Jackson, S. A., Patry, S. & Dobson, A. D. W. Extending the "One Strain Many Compounds" (OSMAC) Principle to Marine Microorganisms. *Marine drugs* (2018).
230. Omoto, S., Suzuki, H. & Inouye, S. Isolation and structure elucidation of SF-1902 A5, a new globomycin analogue. *The Journal of antibiotics*, 83–86 (1979).

-
231. Inukai, M., Nakajima, M., Osawa, M., Haneishi, T. & Arai, M. Globomycin, a new peptide antibiotic with spheroblast-forming activity. *The Journal of antibiotics*, 421–425 (1978).
232. Sarabia, F., Chammaa, S. & García-Ruiz, C. Solid phase synthesis of globomycin and SF-1902 A5. *The Journal of organic chemistry*, 2132–2144 (2011).
233. Vogeley, L. *et al.* Structural basis of lipoprotein signal peptidase II action and inhibition by the antibiotic globomycin. *Science*, 876–880 (2016).
234. Inukai, M., Takeuchi, M. & Shimizu, K. Effects of Globomycin on the Morphology of Bacteria and the Isolation of Resistant Mutants. *Agricultural and Biological Chemistry*, 513–518 (1984).
235. Kitamura, S., Owensby, A., Wall, D. & Wolan, D. W. Lipoprotein Signal Peptidase Inhibitors with Antibiotic Properties Identified through Design of a Robust In Vitro HT Platform. *Cell chemical biology* (2018).
236. Omoto, S., Ogino, H. & Inouye, S. Studies on SF-1902 A2-A5. *The Journal of antibiotics*, 1416–1423 (1981).

6. Abbreviations

%	percentage
±	plus/minus
°C	Degree Celsius
µL	microliter
µL/mL	microliter per milliliter
µm	micrometer
¹³ C	carbon atom with an isotope mass of 13.003355 u
1-BuOH	1-butanol
1D	one dimensional
¹ H	hydrogen atom with an isotope mass of 1.0079 u
2D	two dimensional
(v/v)	volume ratio
ABRi	<i>Acinetobacter baumannii</i> resistant to imipenem
<i>A. baumannii</i>	<i>Acinetobacter baumannii</i>
ACD/Labs	Advanced Chemistry Development Labs
ACN	acetonitrile
ACN- <i>d</i> ₃	trideuteroacetonitrile
ATCC	American Type Culture Collection
<i>B. subtilis</i>	<i>Bacillus subtilis</i>
B3	Buffer 3
B5	Buffer 5
Bc	<i>Bacillus cereus</i>
BE	biomass extract
br s	broad singlet
BW	Washing buffer
C	Carbon
C-18	stationary phase modified with an 18 membered carbon chain
CoCl ₂ ·6H ₂ O	Cobalt(II) chloride hexahydrate
COSY	Correlation Spectroscopy
CuSO ₄ ·5H ₂ O	Copper(II)sulfate pentahydrate

d	days
d	doublet
D-	D-stereoisomer
DCM	dichloromethane
DMSO	dimethyl sulfoxide
DMSO- <i>d</i> ₆	hexadeuterodimethyl sulfoxide
DNA	Desoxyribonucleic acid
DNP	Dictionary of Natural Products
dNTP	desoxyribonucleotide triphosphate
D-Orn	D-stereoisomer of ornithine
D-Ser	D-stereoisomer of serine
<i>e.g.</i>	<i>exempli gratia</i>
Ec	<i>Escherichia coli</i>
<i>E. coli</i>	<i>Escherichia coli</i>
ECR	Escherichia coli resistant to extended-spectrum
EDTA	Ethylenediaminetetraacetic acid
ELSD	Evaporative Light Scattering Detection
ESI	Electrospray Ionization
<i>et al.</i>	<i>et alia</i>
EtOAc	ethyl acetate
FA	formic acid
fabH	fatty acid biosynthesis specific promoter
FDAA	1-fluoro-2-4-dinitrophenyl-5-alanine amide
Fe(III)citrate	Iron(III) citrate
G	guanine
g	gram
g/mol	gram per mole
GNPS	Global Natural Product Social Molecular Networking
h	hour
H	hydrogen
HCl	hydrochloric acid
HIV	human immunodeficiency virus

HMBC	Heteronuclear Multiple Bond Correlation
HPLC	High-Performance Liquid Chromatography
HPLC-HRMS	High-Performance Liquid Chromatography coupled High-Resolution Mass Spectrometry
HPLC-MS	High-Performance Liquid Chromatography coupled Mass Spectrometry
HPLC-UV	High-Performance Liquid Chromatography coupled Ultra Violet Detection
HRESIMS	High-Resolution Electrospray Ionization Mass Spectrometry
HSQC	Heteronuclear Single Quantum Coherence
HTS	High-throughput screening
Hz	Hertz
ID	Inner Diameter
ISP	International <i>Streptomyces</i> Project
J_{HH}	Scalar coupling between two hydrogen atoms
K_2HPO_4	Dipotassium hydrogen phosphate
Kp	<i>Klebsiella pneumoniae</i>
<i>K. pneumoniae</i>	<i>Klebsiella pneumoniae</i>
KPR	<i>Klebsiella pneumoniae</i> resistant to extended-spectrum
L	Liter
L-	L-stereoisomer
L10	<i>Candida krusei</i>
L18	<i>Candida parapsilopsis</i>
L4	<i>Candida albicans</i>
L7	<i>Candida glabrata</i>
<i>LacZ</i>	lac operon that encodes β -galactosidase
LB	Lysogeny Broth
<i>Lial</i>	cell wall biosynthesis specific promoter
L-Orn	L-stereoisomer of ornithine
L-Ser	L-stereoisomer of serine
LT-ELSD	Low temperature Light Scattering Detection
M	Molar (mol per liter)
m/z	mass-to-charge ration
MRSA	methicillin-resistant <i>Staphylococcus aureus</i>

mAu	milli-Absorption-Unit
MDR	Multidrug-resistant
ME(1-BuOH)	1-butanol medium extract
ME(DCM)	dichloromethane medium extract
ME(EtOAc)	ethyl acetate medium extract
MeOH	methanol
mg	milligram
mg/mL	milligram per milliliter
MH	Mueller-Hinton
MHz	mega Hertz
MiMo_ALe	Microorganisms from Moroccan ecosystems in Anti-infective Lead discovery
min	minute
mL	milliliter
MI	<i>Micrococcus luteus</i>
<i>M. leprae</i>	<i>Mycobacterium leprae</i>
mm	millimeter
mM	millimolar (millimole per liter)
[M+H] ⁺	positively charged hydrogen adduct
[M-H] ⁻	negatively charged hydrogen adduct
MnSO ₄ xH ₂ O	Manganese(II) sulfate mono hydrate
MOA	Mode Of Action
MS/MS	Tandem mass spectrometry
MS ²	Tandem mass spectrometry
<i>M. tuberculosis</i>	<i>Mycobacterium tuberculosis</i>
N	nitrogen
N2NP	nitrogen-nitrogen bond containing natural product
Na ₂ B ₄ O ₇ x10H ₂ O	Sodium tetraborate decahydrate
Na ₂ CO ₃	Sodium carbonate
Na ₂ MoO ₄ x2H ₂ O	Sodium molybdate dehydrate
NaHCO ₃	Sodium bicarbonate
NaOH	Sodium hydroxide

NCBI	National Center for Biotechnology Information
NH ₂	amino
nm	nanometer
NMR	Nuclear Magnetic Resonance
NP	natural product
N-Z Amine	a casein enzymatic hydrolysate
O	oxygen
OD ₅₄₆	optical density at 546 nm
OH	hydroxy
OSMAC	One Strain Many Compounds
Pa	<i>Pseudomonas aeruginosa</i>
<i>P. aeruginosa</i>	<i>Pseudomonas aeruginosa</i>
PARc	<i>Pseudomonas aeruginosa</i> resistant to ceftazidime
PCR	Polymerase Chain Reaction
PFP	pentafluorophenyl
PH	phenylhexyl
ppm	parts per million
<i>ppS</i>	RNA biosynthesis specific promoter
proteinase K	broad-spectrum proteinase
r.t.	room temperature
RNA	Ribonucleic acid
RP	reversed phase
rpm	rounds per minute
Sa	<i>Staphylococcus aureus</i>
<i>S. aureus</i>	<i>Staphylococcus aureus</i>
<i>S. fradiae</i>	<i>Streptomyces fradiae</i>
sp.	species
sp ²	sp ² hybridized
sp ³	sp ³ hybridized
TAE	Tris-acetate-EDTA
TOCSY	Total Correlation Spectroscopy
Tü	Tübingen

X-Gal	5-bromo-4-chloro-3-indolyl- β -D-galactopyranoside
YECD	Yeast extract casein hydrolysate
<i>yheI</i>	protein biosynthesis specific promoter
<i>yorB</i>	DNA biosynthesis specific promoter
<i>ypuA</i>	cell wall biosynthesis specific promoter
<i>yvgS</i>	RNA biosynthesis specific promoter
ZnCl ₂	Zinc chloride
δ_c	¹³ C chemical shift
δ_H	¹ H chemical shift

7. Curriculum Vitae

 +49 176 832 993 60
 dominik.wichner@web.de
 Jacobstraße 47,
06110 Halle (Saale)
 24.11.1990, Traunstein
 ledig



BERUFSERFAHRUNG

Sachverständiger

Seit 04/2021

DEKRA Automobil GmbH, Labor für Umwelt- und
Produktanalytik, Standort Halle (Saale)

Wissenschaftlicher Mitarbeiter

(Promotion)

Titel der Dissertation

„Isolation and characterization of novel anti-infective
specialized metabolites from Actinobacteria“

05/2017 – 10/2020

Martin-Luther-Universität Halle-Wittenberg

Institut für Pharmazie

03/2017 – 05/2017

Eberhard Karls Universität Tübingen

Interfakultäres Institut für Mikrobiologie und

Infektionsmedizin

AUSBILDUNG

STUDIUM

12/2016	Universität Regensburg, Abschluss M.Sc. Chemie Fakultät für Chemie und Pharmazie Gesamtnote: 1.2
10/2015 – 12/2016	Universität Regensburg, M.Sc. Chemie Fakultät für Chemie und Pharmazie Grundmodule: <ul style="list-style-type: none">- Bioanalytik- Biochemie- Organische Chemie Aufbaumodule: <ul style="list-style-type: none">- Bioanalytik: Sensors, Arrays, Screening- Organische Chemie
07/2015	Universität Regensburg, Abschluss B.Sc. Fakultät für Chemie und Pharmazie
09/2014 – 06/2015	University of Aberdeen, Schottland, Großbritannien Marine Biodiscovery Centre, Department of Chemistry Forschungsarbeit Titel: „ <i>New microbial secondary metabolites from underexplored habitats</i> “ (anerkannt als Masterarbeit an der Universität Regensburg, Note: 1.0)
10/2011 – 07/2014	Universität Regensburg, B.Sc. Chemie Fakultät für Chemie und Pharmazie

SCHULAUSBILDUNG

09/2002 – 05/2011	Chiemgau-Gymnasium Traunstein Abiturnote: 2.2
-------------------	---

QUALIFIKATIONEN

FUNDIERTE KENNTNISSE IN DER INSTRUMENTELLEN ANALYTIK

HPLC-UV/VIS

HPLC-MS

NMR

FUNDIERTE EDV KENNTNISSE

MS Office

FreeStyle™ 1.5

Chromeleon™ 7

ACD/Structure Elucidator

SPRACHKENNTNISSE

Deutsch

Muttersprache

Englisch

Verhandlungssicher

Französisch

Grundkenntnisse

ZERTIFIKATE

07/2020

Good Manufacturing Practice

Humboldt-Universität zu Berlin

02/2019

Q Exactive Operations

8. Appendix

Table of contents

1.	Leucine hydrazone.....	126
1.1.	HPLC chromatograms after the additional extraction.....	126
1.2.	HPLC method development	129
1.3.	NMR data of leucine hydrazone.....	132
1.4.	Mass spectrometric data of leucine hydrazone	137
1.5.	Cytotoxicity assay	138
2.	MiMo_ALe project.....	145
2.1.	Antibiograms of the applied MDR strains.....	145
2.2.	Results of the secondary screening of the MiMo_ALe strains.....	146
2.3.	Representative HPLC-UV chromatograms for the medium extracts of the MiMo_ALe strains.....	155
3.	Devices.....	157
4.	Chemicals	158

List of Tables

Table A 1: Normalized data of a simple cytotoxicity assay of leucine hydrazone.	138
Table A 2: Normalized data of the cytotoxicity assay testing for synergistic effects of leucine hydrazone and G418.	139
Table A 3: Normalized data of the cytotoxicity assay testing for synergistic effects of leucine hydrazone and hygromycin B.	140
Table A 4: Normalized data of the cytotoxicity assay testing for synergistic effects of leucine hydrazone and actinomycin D (Act D).	141
Table A 5: Normalized data of the checkerboard assay.	142
Table A 6: Results of the secondary screening against PARc. The tested samples were the supernatants of strain MiMo_ALe#2 obtained by the OSMAC approach. (+) stands for inhibitory activity and (-) for no inhibitory activity. (±) represents inhibitory activity that was only observed for one replicate but not for the other. The assay was performed in duplicates.	146
Table A 7: Results of the secondary screening against PARc. The tested samples were the supernatants of strain MiMo_ALe#3 obtained by the OSMAC approach. (+) stands for inhibitory activity and (-) for no inhibitory activity. ± represents inhibitory activity that was only observed for one replicate but not for the other. The assay was performed in duplicates.	147
Table A 8: Results of the secondary screening against PARc. The tested samples were the supernatants of strain MiMo_ALe#4 obtained by the OSMAC approach. (+) stands for inhibitory activity and (-) for no inhibitory activity. ± represents inhibitory activity that was only observed for one replicate but not for the other. The assay was performed in duplicates.	148
Table A 9: Results of the secondary screening against PARc. The tested samples were the supernatants of strain MiMo_ALe#5 obtained by the OSMAC approach. (+) stands for inhibitory activity and (-) for no inhibitory activity. ± represents inhibitory activity that was only observed for one replicate but not for the other. The assay was performed in duplicates.	149
Table A 10: Results of the secondary screening against PARc. The tested samples were the supernatants of strain MiMo_ALe#6 obtained by the OSMAC approach. (+) stands for inhibitory activity and (-) for no inhibitory activity. ± represents inhibitory activity that was only observed for one replicate but not for the other. The assay was performed in duplicates.	150
Table A 11: Results of the secondary screening against PARc. The tested samples were the supernatants of strain MiMo_ALe#7 obtained by the OSMAC approach. (+) stands for inhibitory	

activity and (-) for no inhibitory activity. ± represents inhibitory activity that was only observed for one replicate but not for the other. The assay was performed in duplicates.....	151
Table A 12: Results of the secondary screening against PARc. The tested samples were the supernatants of strain MiMo_ALe#8 obtained by the OSMAC approach. (+) stands for inhibitory activity and (-) for no inhibitory activity. ± represents inhibitory activity that was only observed for one replicate but not for the other. The assay was performed in duplicates.....	152
Table A 13: Results of the secondary screening against PARc. The tested samples were the supernatants of strain MiMo_ALe#9 obtained by the OSMAC approach. (+) stands for inhibitory activity and (-) for no inhibitory activity. ± represents inhibitory activity that was only observed for one replicate but not for the other. The assay was performed in duplicates.....	153
Table A 14: Results of the secondary screening against PARc. The tested samples were the supernatants of strain MiMo_ALe#10 obtained by the OSMAC approach. (+) stands for inhibitory activity and (-) for no inhibitory activity. ± represents inhibitory activity that was only observed for one replicate but not for the other. The assay was performed in duplicates.....	154

List of Figures

Figure A 1: HPLC-UV chromatogram of fraction 1 of the additional extraction. Detection was done at 210 nm (blue), 254 nm (magenta), 280 nm (brown), 430 nm (green) and with the ELSD (black).	126
Figure A 2: HPLC-UV chromatogram of fraction 2 of the additional extraction. Detection was done at 210 nm (blue), 254 nm (magenta), 280 nm (brown), 430 nm (green) and with the ELSD (black).	126
Figure A 3: HPLC-UV chromatogram of fraction 3 of the additional extraction. Detection was done at 210 nm (blue), 254 nm (magenta), 280 nm (brown), 430 nm (green) and with the ELSD (black).	127
Figure A 4: HPLC-UV chromatogram of fraction 4 of the additional extraction. Detection was done at 210 nm (blue), 254 nm (magenta), 280 nm (brown), 430 nm (green) and with the ELSD (black).	127
Figure A 5: HPLC-UV chromatogram of fraction 5 of the additional extraction. Detection was done at 210 nm (blue), 254 nm (magenta), 280 nm (brown), 430 nm (green) and with the ELSD (black).	128
Figure A 6: HPLC-UV chromatograms of fraction 3 using a Phenomenex® Luna (5 µm) C-18, 250x4.6 mm column with (A) acetonitrile and water (+ 0.1 % (v/v) FA each) and (B) methanol and water (+ 0.1 % (v/v) FA each) as mobile phase. Detection was done at 210 nm (blue), 254 nm (magenta), 280 nm (brown), 430 nm (green) and with the ELSD (black).	129
Figure A 7: HPLC-UV chromatograms of fraction 3 using a Phenomenex® Luna (5 µm) PFP, 250x4.6 mm column with (A) acetonitrile and water (+ 0.1 % (v/v) FA each), (B) methanol and water (+ 0.1 % (v/v) FA each) and (C) with methanol and water without FA as mobile phase. Detection was done at 210 nm (blue), 254 nm (magenta), 280 nm (brown), 430 nm (green) and with the ELSD (black). .	130
Figure A 8: HPLC-UV chromatogram of fraction 3 using a Phenomenex® Luna (5 µm) PH, 250x4.6 mm column with (A) acetonitrile and water (+ 0.1 % (v/v) FA each) and (B) methanol and water (+ 0.1 % (v/v) FA each) as mobile phase. Detection was done at 210 nm (blue), 254 nm (magenta), 280 nm (brown), 430 nm (green) and with the ELSD (black).	131
Figure A 9: ¹ H-NMR spectrum (600 MHz) of leucine hydrazone in DMSO-d ₆	132
Figure A 10: ¹ H-NMR spectrum (600 MHz) of leucine hydrazone in DMSO-d ₆ . (A) From 0.65 ppm to 2.4 ppm and (B) from 7.00 ppm to 11.75 ppm.	133
Figure A 11: ¹³ C-NMR spectrum (150 MHz) of leucine hydrazone in DMSO-d ₆	134

Figure A 12: HSQC spectrum (600 MHz) of leucine hydrazone in DMSO-d ₆	135
Figure A 13: HMBC spectrum (600 MHz) of leucine hydrazone in DMSO-d ₆	135
Figure A 14: TOCSY spectrum (600 MHz) of leucine hydrazone in DMSO-d ₆	136
Figure A 15: COSY spectrum (600 MHz) of leucine hydrazone in DMSO-d ₆	136
Figure A 16: Base peak chromatogram of leucine hydrazone	137
Figure A 17: Mass spectrum of leucine hydrazone	137
Figure A 18: MS ² spectrum of leucine hydrazone	137
Figure A 19: HPLC-UV chromatograms of the ethyl acetate (upper) and 1-butanol (bottom) medium extracts of MiMo_ALe#3 after cultivation in medium NL300 for 3 days. For analysis, a Phenomenex® Kinetex (2.6 µm) C-18, 100x3.0 mm ID column at 50 °C was used. Detection was done at 210 nm (blue), 254 nm (magenta), 280 nm (brown), 360 nm (green) and with the ELSD (black)	155
Figure A 20: HPLC-UV chromatograms of the ethyl acetate (upper) and 1-butanol (bottom) medium extracts of MiMo_ALe#3 after cultivation in medium NL300 for 7 days. For analysis, a Phenomenex® Kinetex (2.6 µm) C-18, 100x3.0 mm ID column at 50 °C was used. Detection was done at 210 nm (blue), 254 nm (magenta), 280 nm (brown), 360 nm (green) and with the ELSD (black)	156
Figure A 21: HPLC-UV chromatogram of the ethyl acetate medium extract of MiMo_ALe#7 after cultivation in NL333 for 4 days. The vertical dashed lines indicate the separate micro-fractions. For micro-fractionation, a Phenomenex® Luna (5 µm) C-18, 250x4.6 mm ID column at 25 °C was used. Detection was done at 210 nm (black), 254 nm (blue), 280 nm (magenta), and 360 nm (brown).	156

1. Leucine hydrazone

1.1. HPLC chromatograms after the additional extraction

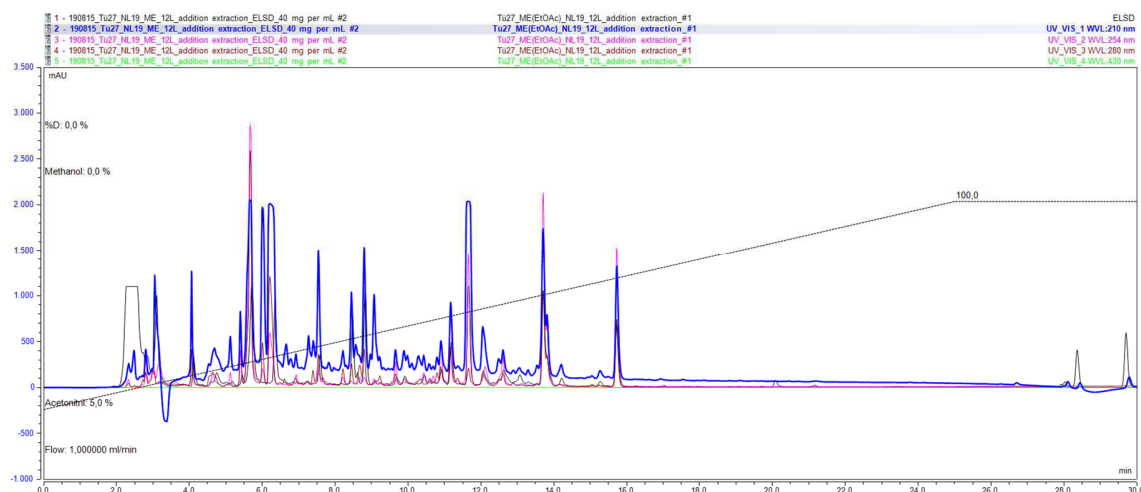


Figure A 1: HPLC-UV chromatogram of fraction 1 of the additional extraction. Detection was done at 210 nm (blue), 254 nm (magenta), 280 nm (brown), 430 nm (green) and with the ELSD (black).

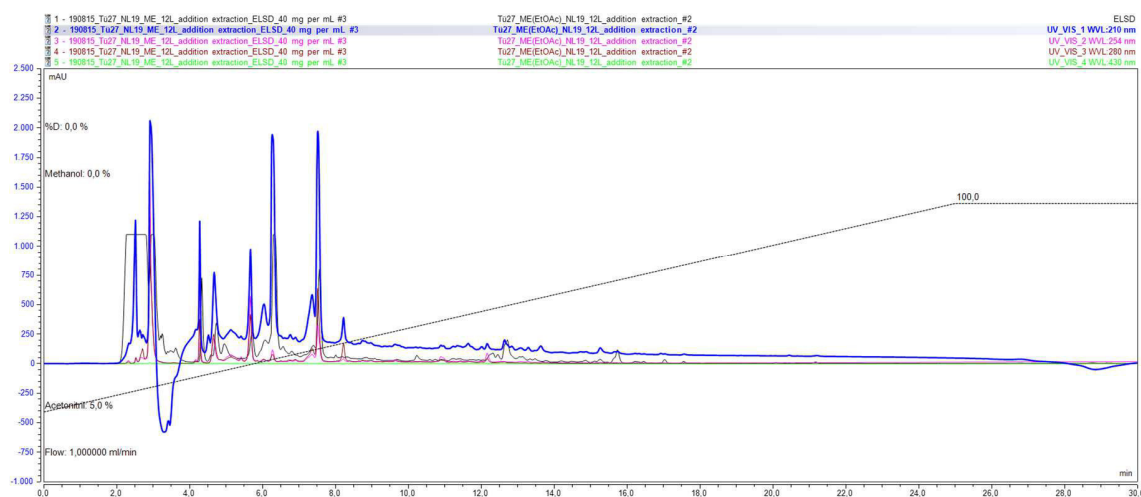


Figure A 2: HPLC-UV chromatogram of fraction 2 of the additional extraction. Detection was done at 210 nm (blue), 254 nm (magenta), 280 nm (brown), 430 nm (green) and with the ELSD (black).

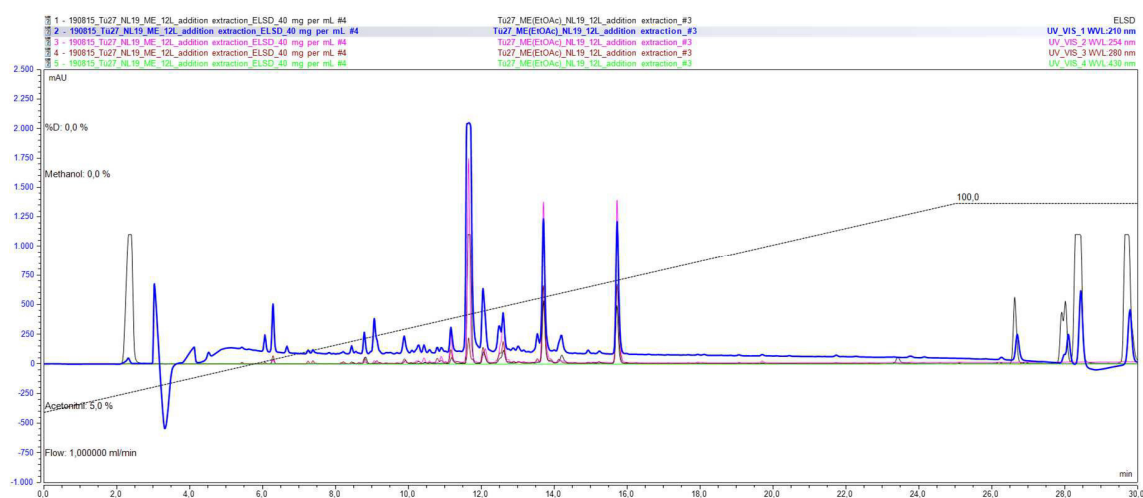


Figure A 3: HPLC-UV chromatogram of fraction 3 of the additional extraction. Detection was done at 210 nm (blue), 254 nm (magenta), 280 nm (brown), 430 nm (green) and with the ELSD (black).

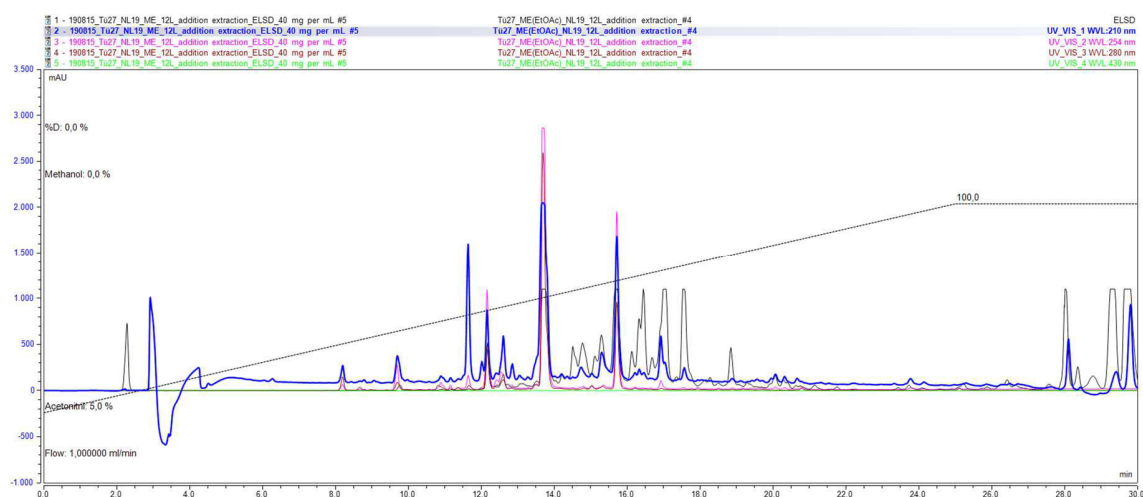


Figure A 4: HPLC-UV chromatogram of fraction 4 of the additional extraction. Detection was done at 210 nm (blue), 254 nm (magenta), 280 nm (brown), 430 nm (green) and with the ELSD (black).

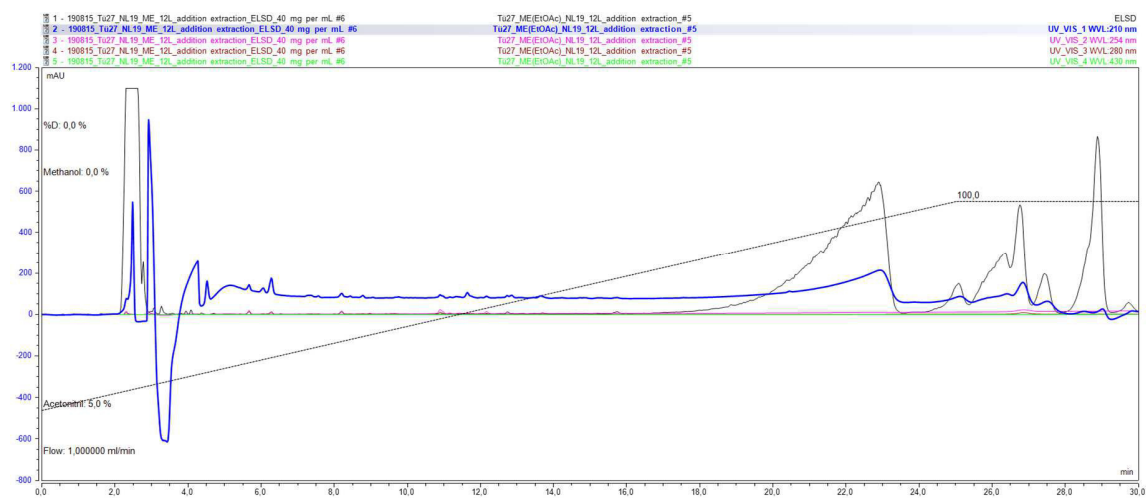


Figure A 5: HPLC-UV chromatogram of fraction 5 of the additional extraction. Detection was done at 210 nm (blue), 254 nm (magenta), 280 nm (brown), 430 nm (green) and with the ELS40 (black).

1.2. HPLC method development

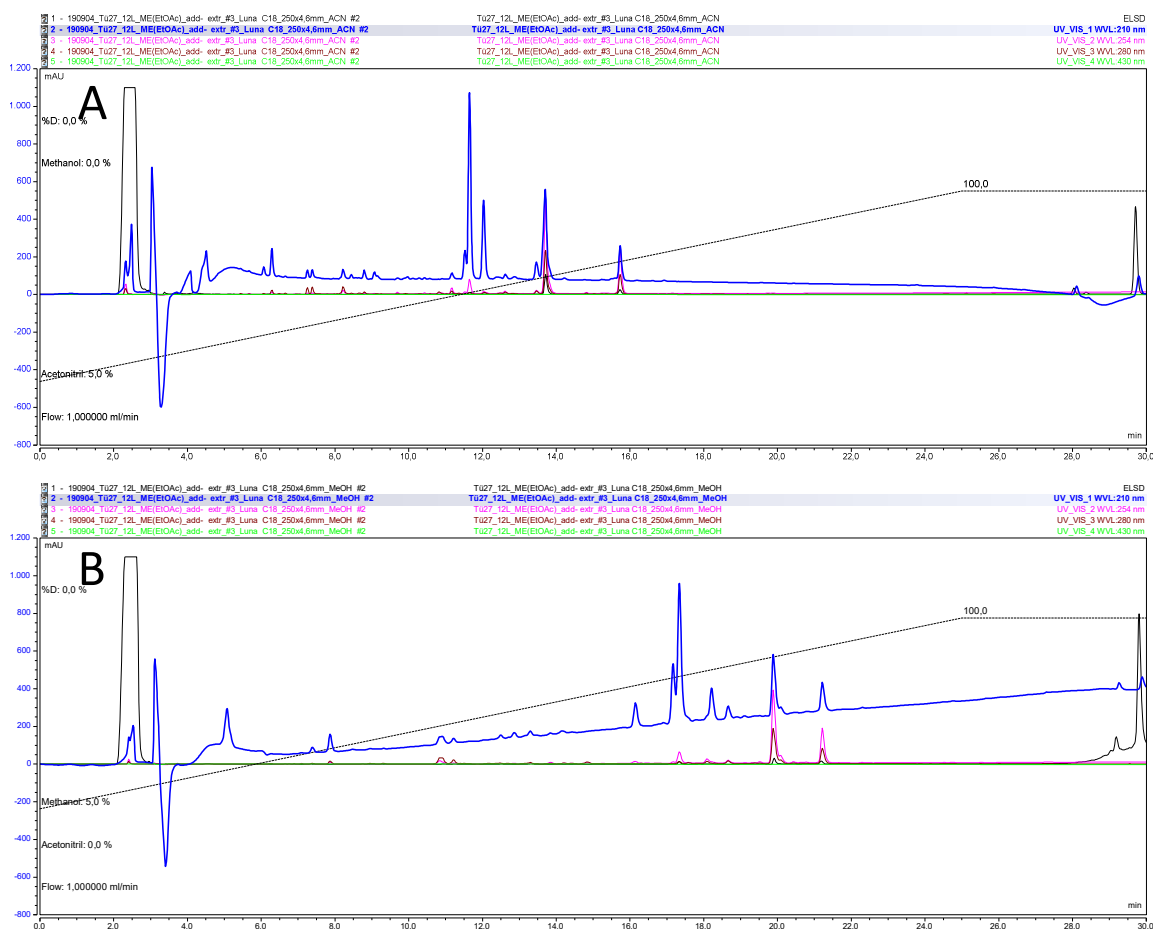
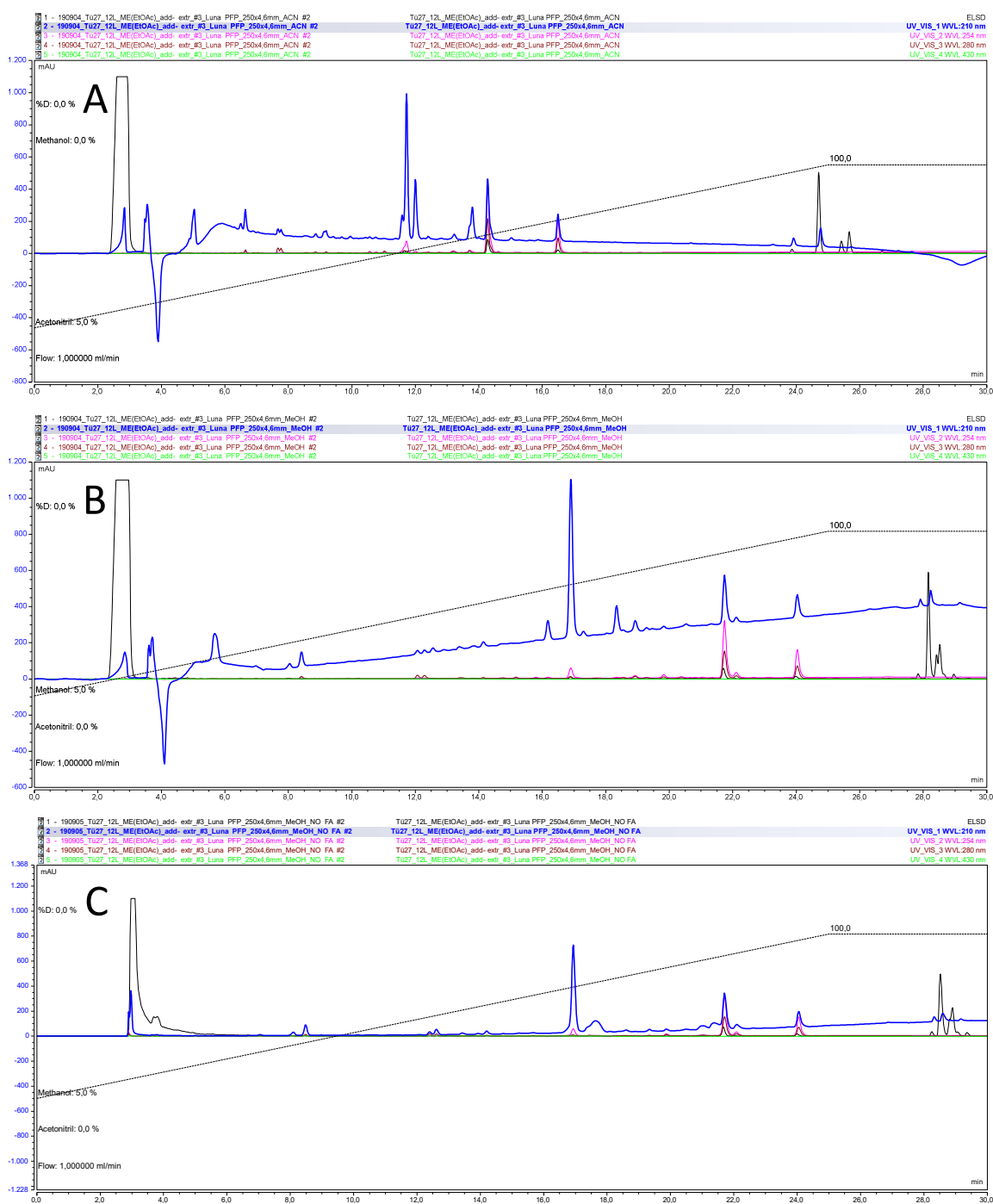


Figure A 6: HPLC-UV chromatograms of fraction 3 using a Phenomenex® Luna (5 µm) C-18, 250x4.6 mm column with (A) acetonitrile and water (+ 0.1 % (v/v) FA each) and (B) methanol and water (+ 0.1 % (v/v) FA each) as mobile phase. Detection was done at 210 nm (blue), 254 nm (magenta), 280 nm (brown), 430 nm (green) and with the ELSD (black).



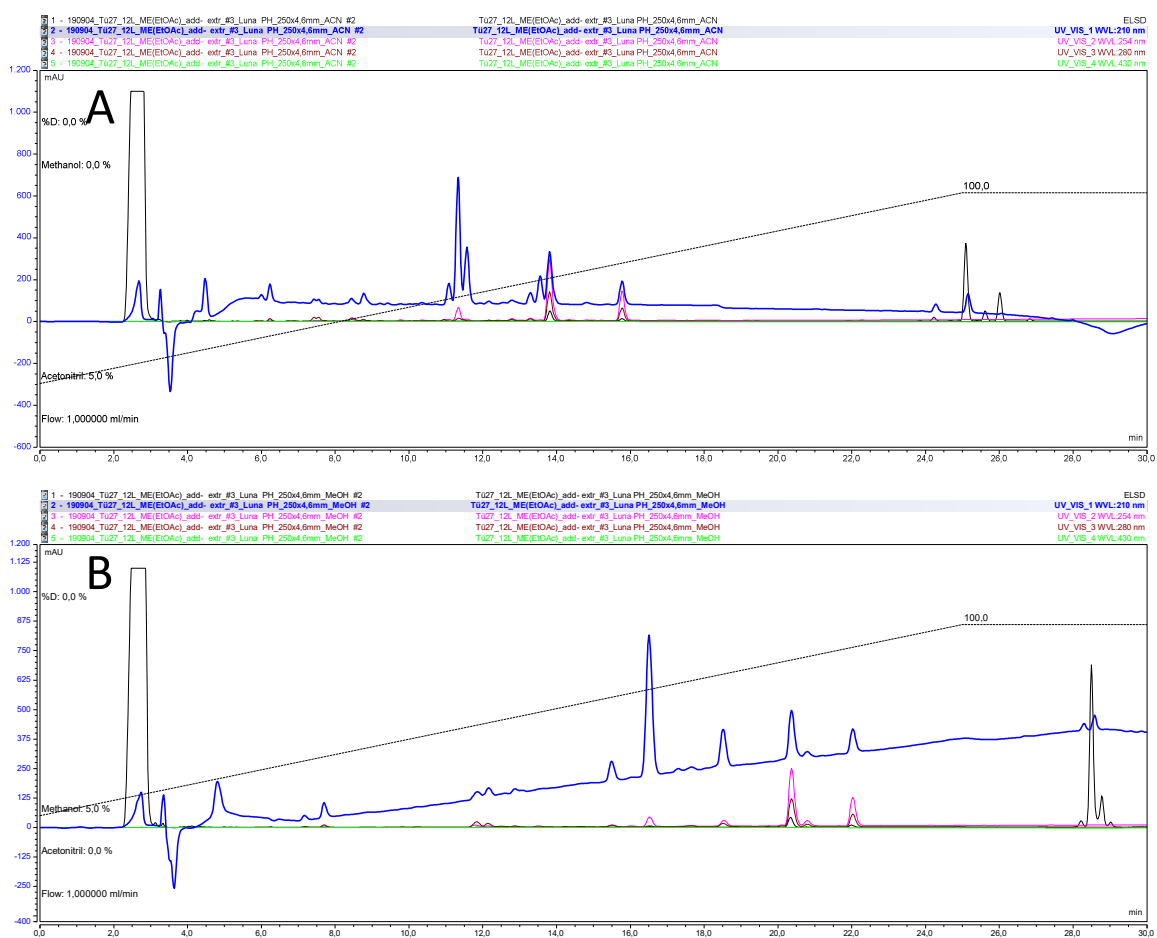
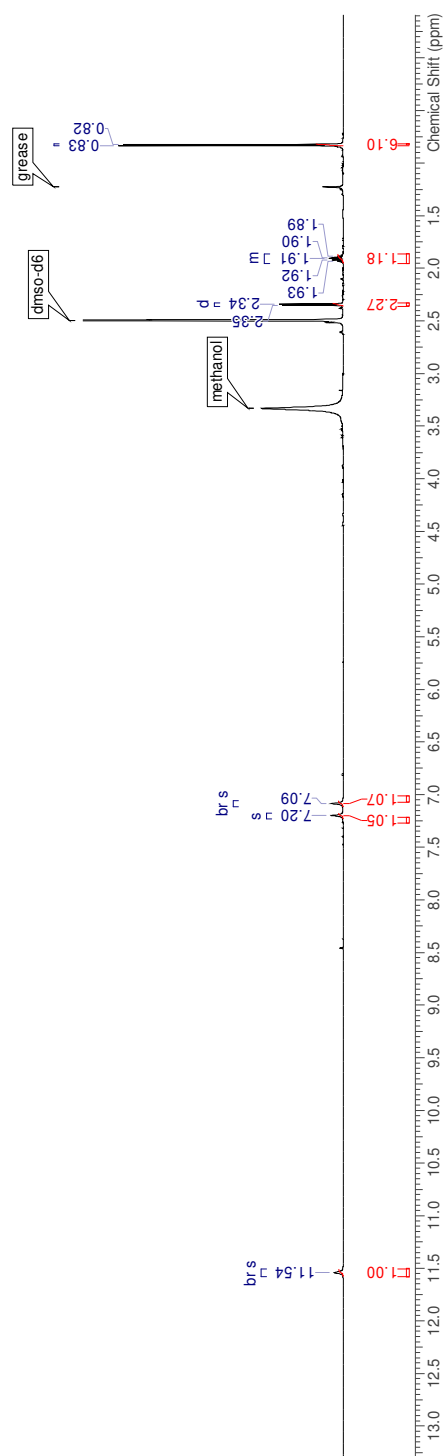


Figure A 8: HPLC-UV chromatogram of fraction 3 using a Phenomenex® Luna (5 µm) PH, 250x4.6 mm column with (A) acetonitrile and water (+ 0.1 % (v/v) FA each) and (B) methanol and water (+ 0.1 % (v/v) FA each) as mobile phase. Detection was done at 210 nm (blue), 254 nm (magenta), 280 nm (brown), 430 nm (green) and with the ELSD (black).

1.3. NMR data of leucine hydrazone

Figure A 9: $^1\text{H-NMR}$ spectrum (600 MHz) of leucine hydrazone in $\text{DMSO-}d_6$.

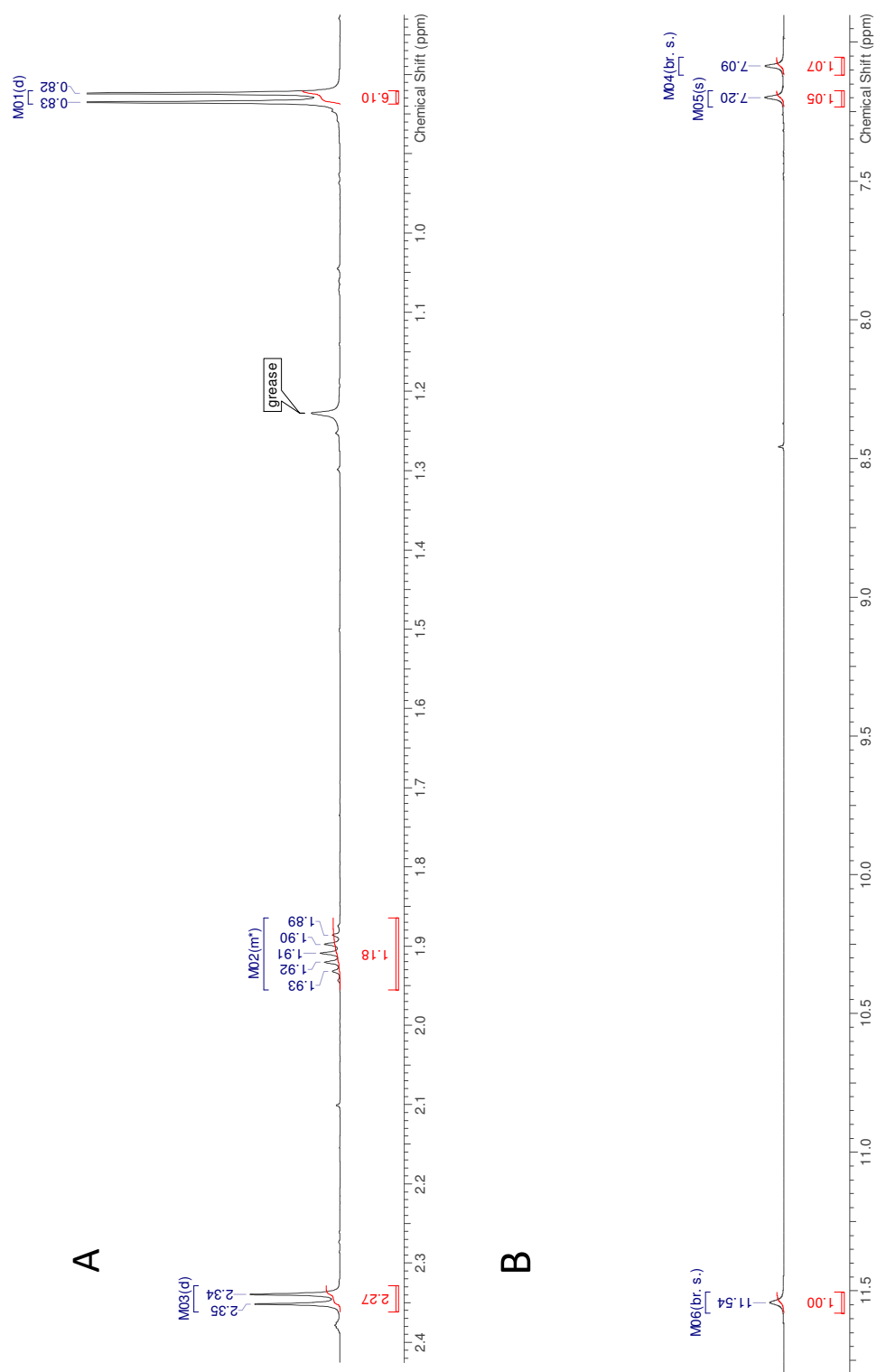
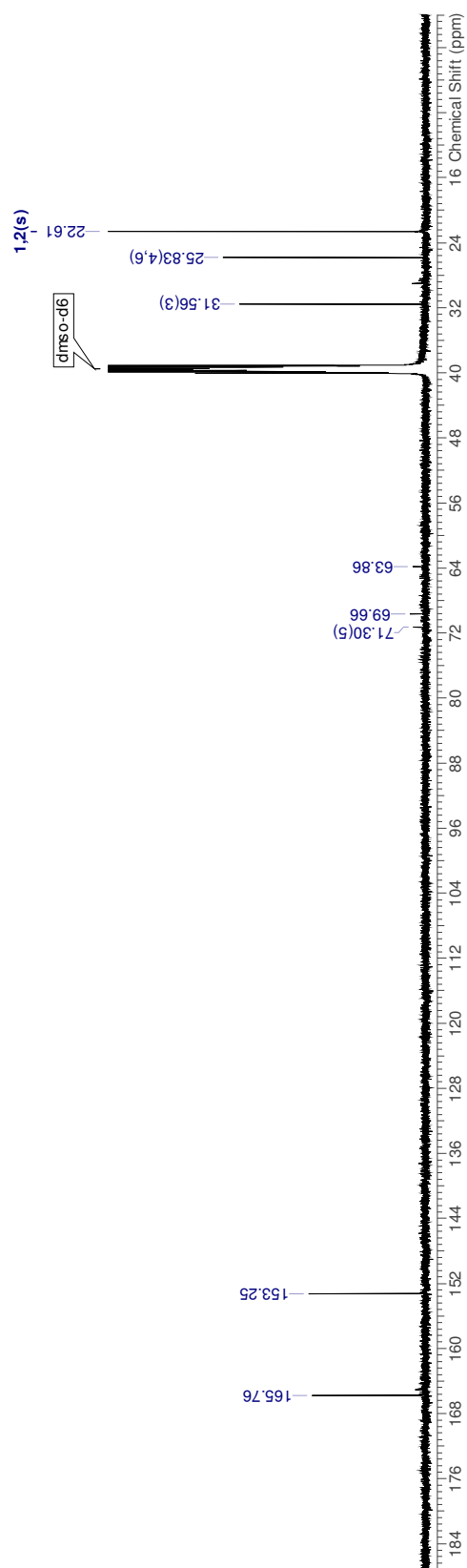
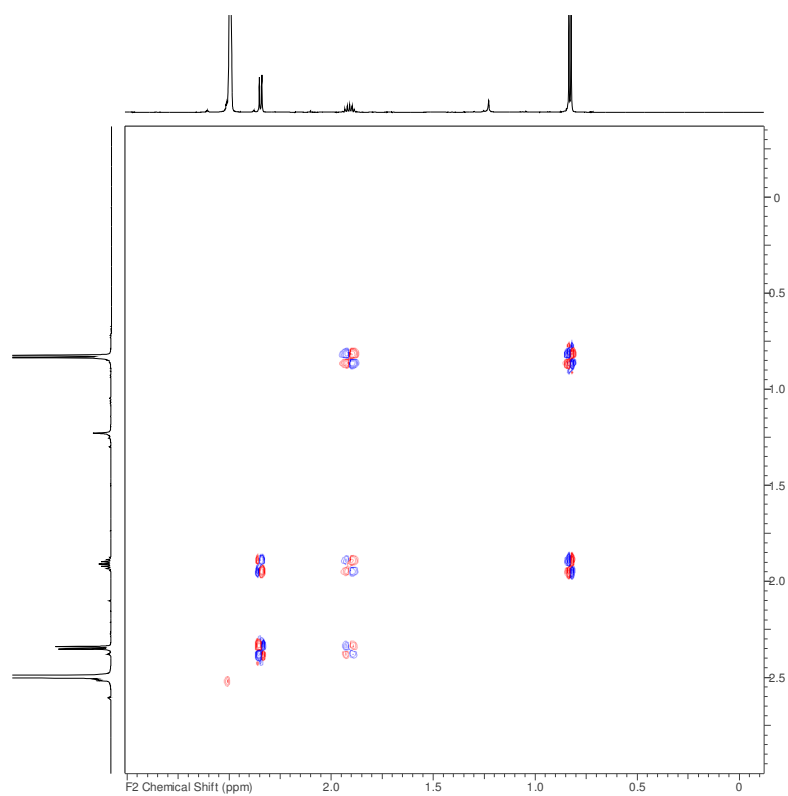
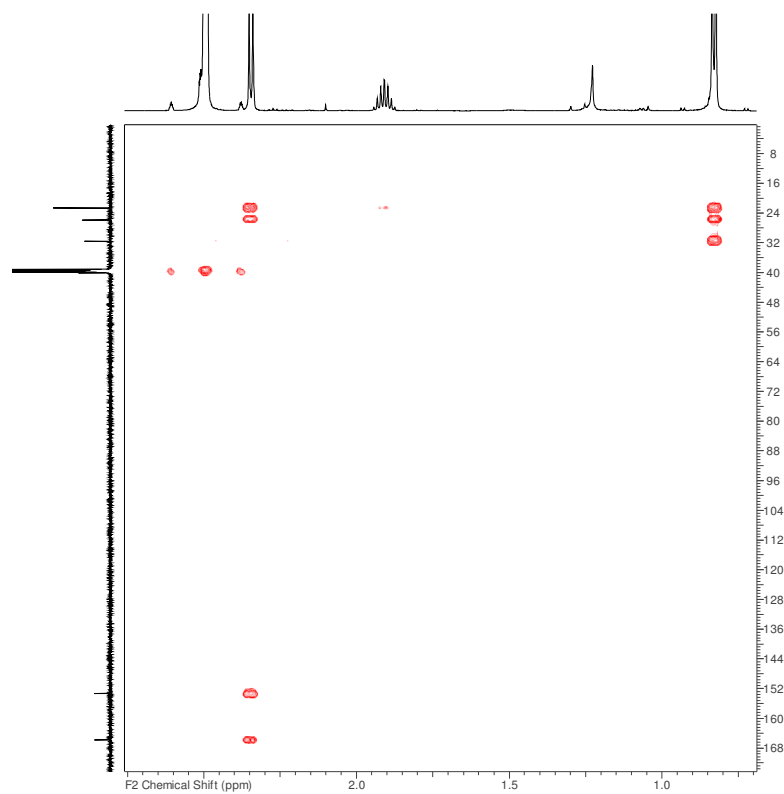
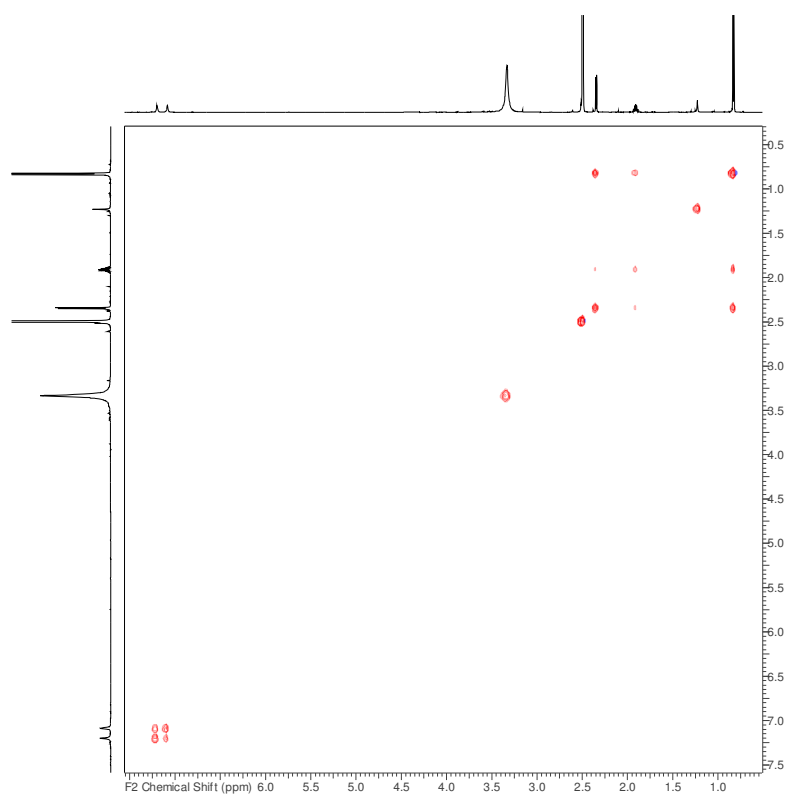
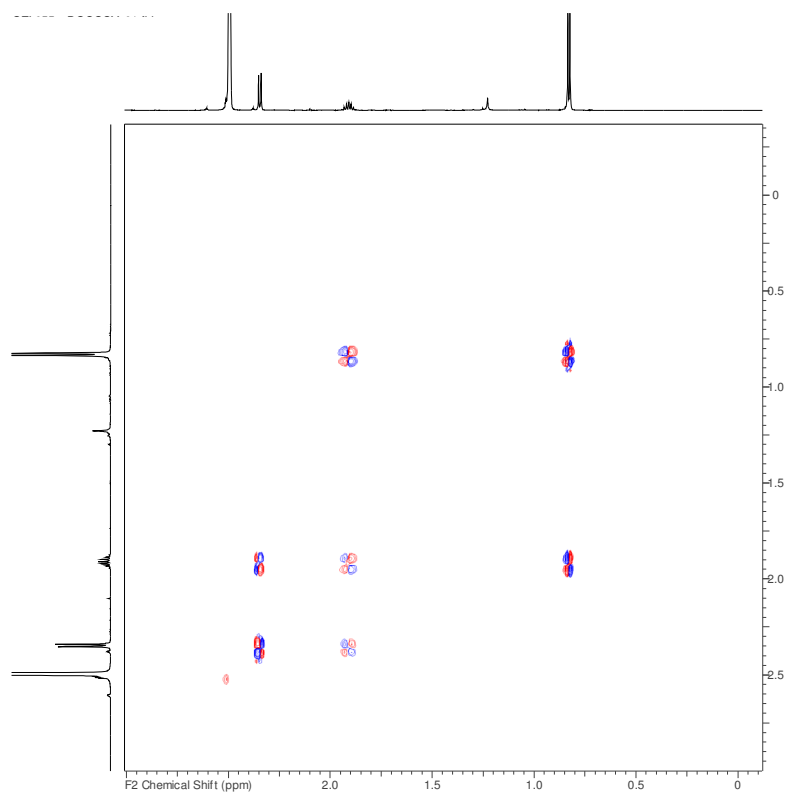


Figure A 10: ^1H -NMR spectrum (600 MHz) of leucine hydrazone in DMSO-d_6 . **(A)** From 0.65 ppm to 2.4 ppm and **(B)** from 7.00 ppm to 11.75 ppm.

Figure A 11: ^{13}C -NMR spectrum (150 MHz) of leucine hydrazone in $\text{DMSO-}d_6$.

Figure A 12: HSQC spectrum (600 MHz) of leucine hydrazone in DMSO-*d*₆.Figure A 13: HMBC spectrum (600 MHz) of leucine hydrazone in DMSO-*d*₆.

Figure A 14: TOCSY spectrum (600 MHz) of leucine hydrazone in DMSO-*d*₆.Figure A 15: COSY spectrum (600 MHz) of leucine hydrazone in DMSO-*d*₆.

1.4. Mass spectrometric data of leucine hydrazone

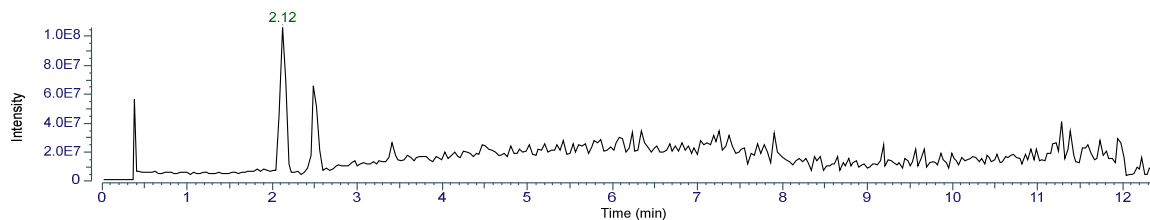


Figure A 16: Base peak chromatogram of leucine hydrazone.

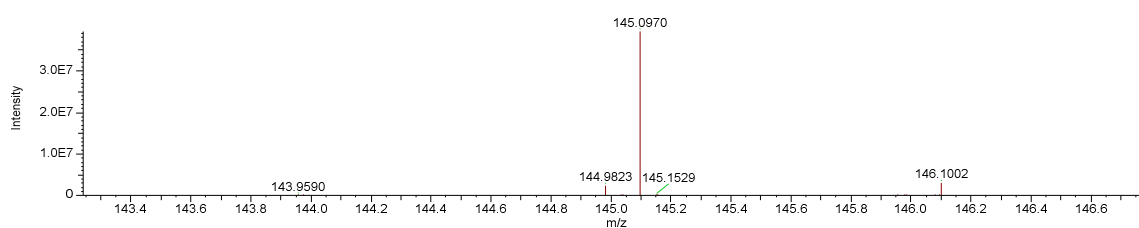
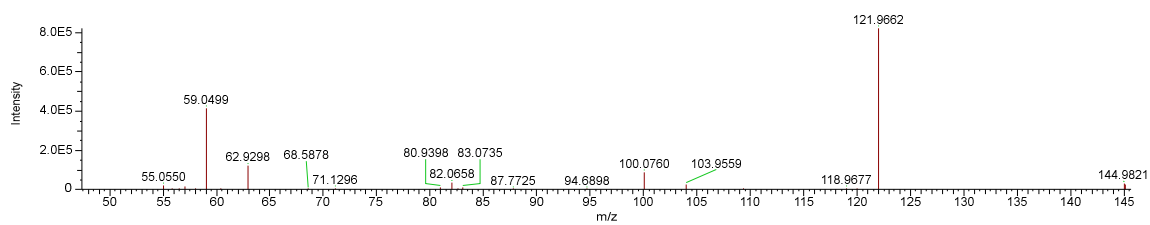


Figure A 17: Mass spectrum of leucine hydrazone.

Figure A 18: MS² spectrum of leucine hydrazone.

1.5. Cytotoxicity assay

Normalized simple cytotoxicity data of leucine hydrazone

Table A 1: Normalized data of a simple cytotoxicity assay of leucine hydrazone.

Sample	Absorbance replicate 1	Absorbance replicate 2	Absorbance replicate 3
694 μM	8.030856	-4.627947	-3.402901
347 μM	22.45917	17.72535	18.78403
174 μM	54.32548	60.17847	65.39626
87 μM	80.42953	80.92862	82.39565
43 μM	94.20751	81.59408	87.67393
22 μM	88.32426	86.78162	83.3031
11 μM	88.24864	82.16879	82.8645
5.4 μM	94.31338	100.7865	94.96371
2.7 μM	91.81792	89.38295	81.94194
negative control	108.3787	98.01877	93.60255

Normalized data of synergistic cytotoxicity of leucine hydrazone with G418

Table A 2: Normalized data of the cytotoxicity assay testing for synergistic effects of leucine hydrazone and G418.

Sample	Absorbance replicate 1	Absorbance replicate 2	Absorbance replicate 3	Absorbance replicate 4
Leucine hydrazone 347 μ M	32.72676	22.459170	17.72535	18.78403
Leucine hydrazone 174 μ M	77.34518	54.325480	60.17847	65.39626
Leucine hydrazone 87 μ M	94.06122	80.429530	80.92862	82.39565
Leucine hydrazone 43 μ M	95.66935	94.207510	81.59408	87.67393
Leucine hydrazone 22 μ M	96.89660	88.324260	86.78162	83.30310
Leucine hydrazone 11 μ M	99.18183	88.248640	82.16879	82.86450
Leucine hydrazone 5 μ M	100.00000	94.313380	100.78650	94.96371
G418 29 μ M	57.07434	55.931720	57.68091	-
G418 14 μ M	69.50204	55.959930	88.10834	-
G418 7 μ M	73.31077	59.909720	96.50163	-
G418 3.6 μ M	74.97531	59.684020	91.19763	-
G418 1.8 μ M	76.10383	66.878270	99.73199	-
G418 0.9 μ M	79.27776	57.412900	94.08944	-
G418 0.5 μ M	71.85781	60.995910	93.94837	-
G418 0.25 μ M	76.08971	62.392440	91.56440	-
347 μ M + G418 14.4 μ M	28.57949	-2.242914	-	-
174 μ M + G418 7.2 μ M	54.78912	29.961910	-	-
87 μ M + G418 3.6 μ M	91.76189	68.655660	-	-
43 μ M μ g/ml+ G418 1.7 μ M	95.27438	88.051910	-	-
22 μ M + G418 0.9 μ M	94.72422	88.870090	-	-
11 μ M + G418 0.4 μ M	94.00480	97.489070	-	-
5.4 μ M + G418 0.4 μ M	90.70391	96.910710	-	-
2.7 μ M + G418 0.14 μ M	100.66300	94.103550	-	-
Negative control	97.71477	90.294820	97.37622	-

Normalized data of synergistic cytotoxicity of leucine hydrazone with hygromycin B

Table A 3: Normalized data of the cytotoxicity assay testing for synergistic effects of leucine hydrazone and hygromycin B.

Sample	Absorbance replicate 1	Absorbance replicate 2	Absorbance replicate 3
Leucine hydrazone 694 μ M	8.030856	-4.627947	-3.402901
Leucine hydrazone 347 μ M	22.459170	17.725350	18.784030
Leucine hydrazone 174 μ M	54.325480	60.178470	65.396260
Leucine hydrazone 87 μ M	80.429530	80.928620	82.395650
Leucine hydrazone 43 μ M	94.207510	81.594080	87.673930
Leucine hydrazone 22 μ M	88.324260	86.781620	83.303100
Leucine hydrazone 11 μ M	88.248640	82.168790	82.864500
Leucine hydrazone 5 μ M	94.313380	100.786500	94.963710
Leucine hydrazone 3 μ M	91.817920	89.382950	81.941940
Hygro 3 mM	13.164180	7.893201	10.021760
Hygro 1.5 mM	17.240830	4.559690	3.869633
Hygro 0.75 mM	38.483990	26.885720	22.596740
Hygro 0.38 mM	64.642490	44.195550	52.762890
Hygro 0.19 mM	83.194440	69.664000	73.236370
174 μ M + Hygro 3 mM	1.260585	0.6959472	-
87 μ M + Hygro 1.5 mM	-0.695951	1.956534	-
43 μ M + Hygro 0.75 mM	14.142210	16.689650	-
22 μ M + Hygro 0.4 mM	49.084110	50.187110	-
11 μ M + Hygro 0.2 mM	77.460440	81.124020	-
5 μ M + Hygro 0.1 mM	98.785380	87.033030	-
3 μ M + Hygro 0.05 mM	92.745060	97.012670	-
Negative control	98.941330	96.052640	88.657000

Normalized data of synergistic cytotoxicity of leucine hydrazone with actinomycin D

Table A 4: Normalized data of the cytotoxicity assay testing for synergistic effects of leucine hydrazone and actinomycin D (Act D).

Sample	Absorbance replicate 1	Absorbance replicate 2	Absorbance replicate 3
Act D 0.1 μ M	8.352597	0.000	5.486208
Leucine hydrazone 120 μ M + Act D 0.1 μ M	13.91586	12.683	17.56049
Leucine hydrazone 120 μ M	78.9798	81.75373	73.60918
Control	98.22006	100.000	97.13361

Normalized data for the determination of the FICI

Table A 5: Normalized data of the checkerboard assay.

Well #	Absorbance	Absorbance	Absorbance
	replicate 1	replicate 2	replicate 3
1	14.55491	11.67259	14.78847
2	19.36408	14.7407	12.63868
3	14.06126	14.97425	14.608
4	16.84803	12.74484	15.09103
5	13.3075	5.393068	15.25028
6	20.98307	5.653167	16.03588
7	13.24911	3.184883	14.46998
8	19.62419	7.590636	8.275387
9	13.16418	7.893201	10.02176
10	97.40433	85.35485	89.12363
11	26.05765	19.08275	18.44578
12	18.6528	12.70768	14.83094
13	15.64839	17.39476	15.00611
14	14.34259	10.95069	13.20665
15	13.38181	6.199904	10.85514
16	16.08366	7.882585	15.53692
17	10.44641	8.047137	8.094911
18	22.894	8.286002	6.475927
19	17.24083	4.55969	3.869633
20	98.50842	84.52678	83.21567
21	37.70901	27.61293	21.7899
22	41.10091	26.16912	24.19449
23	27.60231	36.78009	23.76453
24	45.45358	41.12745	29.2213
25	42.57126	36.0104	29.25845

Continued.

26	41.63173	39.92781	32.6185
27	42.31116	33.06439	27.43245
28	55.55497	36.57837	26.40798
29	38.48399	26.88572	22.59674
30	98.30671	85.3867	92.76501
31	39.48724	27.63416	22.00223
32	48.81363	24.35374	33.22894
33	57.10494	40.78242	31.36579
34	62.15298	52.63549	44.6202
35	64.43018	57.59329	56.73868
36	71.76071	63.37385	62.9492
37	70.23727	52.93274	60.90026
38	74.97744	54.44026	57.52959
39	64.64249	44.19555	52.76289
40	100.000	88.93253	89.18201
41	42.78358	24.30065	26.6787
42	56.47327	38.22921	32.34248
43	62.4874	52.29577	41.52025
44	82.35044	73.29476	58.43198
45	79.48936	78.96916	69.11726
46	85.55125	82.33983	73.84681
47	85.81135	76.9733	77.39265
48	91.04517	75.7365	80.31212
49	83.19444	69.664	73.23637
50	96.25246	90.11625	83.18913
51	40.55417	26.85387	22.79845
52	87.9346	56.7546	36.36074
53	81.45337	69.31366	66.48973
54	98.02538	88.58219	80.97564
55	95.87027	92.14927	86.60757

Continued.

56	99.46388	89.15017	86.53326
57	95.88088	89.59074	86.39525
58	98.97023	88.05138	90.20118
59	96.07198	84.85588	85.53532
60	98.13685	88.60874	84.03844

2. MiMo_ALe project

2.1. Antibiograms of the applied MDR strains

Methicillin-resistant *Staphylococcus aureus* (MRSA)

Resistant to imipenem, kanamycin, cefotaxime, sulfamethoxazole, penicillin, erythromycin, ceftazidime, norfloxacin, nitrofurantoin, ticarcillin, penicillin G

Sensitive to lincomycin, vancomycin, pristinamycin

Imipenem-resistant *Acinetobacter baumannii* (ABRI)

Resistant to amoxicillin + clavulanic acid, ticarcillin, piperacillin + tazobactam, cefotaxime, fosfomicin, amikacin, ceftazidime, aztreonam

Sensitive to imipenem, sulfamethoxazole

Ceftazidime-resistant *Pseudomonas aeruginosa* (PARc)

Resistant to amoxicillin + clavulanic acid, ticarcillin, piperacillin + tazobactam, cefotaxime, fosfomicin, amikacin, ceftazidime, aztreonam

Sensitive to colistin

Klebsiella pneumoniae resistant to extended spectrum (KPR)

Resistant to amoxicillin, amoxicillin + clavulanic acid, ticarcillin, ceftazidime, aztreonam, cefalotin, pefloxacin, netilmicin, sulfamethoxazole, norfloxacin

Sensitive to ceftazidime, amikacin, imipenem, colistin

Escherichia coli resistant to extended spectrum (ECR)

Resistant to amoxicillin, amoxicillin + clavulanic acid, ticarcillin, ceftazidime, aztreonam, cefalotin, pefloxacin, netilmicin, sulfamethoxazole, norfloxacin

Sensitive to ceftazidime, amikacin, imipenem, colistin

The term “extended spectrum” was chosen by the Moroccan project partners to describe the antibiotic resistance profile of KPR and ECR.

2.2. Results of the secondary screening of the MiMo_ALe strains

MiMo_ALe#2

Table A 6: Results of the secondary screening against PARc. The tested samples were the supernatants of strain MiMo_ALe#2 obtained by the OSMAC approach. (+) stands for inhibitory activity and (-) for no inhibitory activity. (±) represents inhibitory activity that was only observed for one replicate but not for the other. The assay was performed in duplicates.

Medium	Bennett	ISP3	NL19	NL200	NL300	NL333	NL400	NL410	NL500
Day									
3	-	-	-	+	+	+	+	+	-
4	-	-	-	+	+	+	+	+	-
5	-	-	+	+	+	+	+	+	-
6	±	-	+	+	+	+	+	+	-
7	-	-	±	±	±	±	±	±	-
10	+	-	+	+	+	+	+	+	-
11	±	-	-	+	±	+	+	+	-
12	+	-	+	+	+	+	+	+	-
13	+	-	+	+	+	+	+	+	-
14	±	-	+	+	+	+	+	+	-

MiMo_ALe#3

Table A 7: Results of the secondary screening against PARc. The tested samples were the supernatants of strain MiMo_ALe#3 obtained by the OSMAC approach. (+) stands for inhibitory activity and (-) for no inhibitory activity. \pm represents inhibitory activity that was only observed for one replicate but not for the other. The assay was performed in duplicates.

Medium	Bennett	ISP3	NL19	NL200	NL300	NL333	NL400	NL410	NL500
Day									
3	-	-	-	-	-	-	-	-	-
4	-	-	-	-	\pm	\pm	\pm	-	-
5	\pm	\pm	+	+	+	+	\pm	\pm	
6	+	+	+	+	+	+	+	+	\pm
7	+	+	+	+	+	+	+	+	\pm
10	+	+	+	+	+	+	+	+	\pm
11	\pm	+	+	+	+	+	+	+	\pm
12	+	+	+	+	+	+	+	+	\pm
13	+	+	+	+	+	+	+	+	+
14	+	+	+	+	+	+	+	+	+

MiMo_ALe#4

Table A 8: Results of the secondary screening against PARc. The tested samples were the supernatants of strain MiMo_ALe#4 obtained by the OSMAC approach. (+) stands for inhibitory activity and (-) for no inhibitory activity. \pm represents inhibitory activity that was only observed for one replicate but not for the other. The assay was performed in duplicates.

Medium	Bennett	ISP3	NL19	NL200	NL300	NL333	NL400	NL410	NL500
Day									
3	-	-	-	\pm	\pm	-	\pm	\pm	-
4	-	-	-	\pm	\pm	-	\pm	\pm	-
5	-	-	\pm	\pm	\pm	-	\pm	\pm	-
6	-	-	\pm	\pm	\pm	-	\pm	\pm	-
7	-	-	\pm	\pm	\pm	-	\pm	\pm	-
10	\pm	-	+	+	\pm	\pm	+	+	-
11	+	-	+	+	+	\pm	+	+	\pm
12	\pm	-	+	+	+	\pm	+	+	-
13	+	-	+	+	+	\pm	+	+	-
14	-	-	\pm	\pm	\pm	\pm	\pm	\pm	-

MiMo_ALe#5

Table A 9: Results of the secondary screening against PARc. The tested samples were the supernatants of strain MiMo_ALe#5 obtained by the OSMAC approach. (+) stands for inhibitory activity and (-) for no inhibitory activity. ± represents inhibitory activity that was only observed for one replicate but not for the other. The assay was performed in duplicates.

Medium	Bennett	ISP3	NL19	NL200	NL300	NL333	NL400	NL410	NL500
Day									
3	-	-	-	-	-	+	-	+	+
4	-	-	+	+	+	+	+	+	+
5	-	-	+	+	+	+	+	+	+
6	-	+	+	+	+	+	+	+	+
7	-	+	+	+	-	+	+	+	-
10	+	-	+	+	-	-	+	+	-
11	+	-	+	+	-	+	+	-	-
12	+	-	+	+	+	-	+	+	-
13	-	-	+	+	-	-	-	-	-
14	+	-	+	+	-	-	-	-	-

MiMo_ALe#6

Table A 10: Results of the secondary screening against PARc. The tested samples were the supernatants of strain MiMo_ALe#6 obtained by the OSMAC approach. (+) stands for inhibitory activity and (-) for no inhibitory activity. \pm represents inhibitory activity that was only observed for one replicate but not for the other. The assay was performed in duplicates.

Medium	Bennett	ISP3	NL19	NL200	NL300	NL333	NL400	NL410	NL500
Day									
3	-	-	-	\pm	\pm	\pm	\pm	-	-
4	-	-	-	-	-	-	-	-	-
5	-	-	+	+	+	+	+	-	-
6	-	-	+	+	+	+	+	-	-
7	-	\pm	+	+	+	+	+	-	-
10	-	-	+	+	+	+	+	\pm	-
11	-	-	+	+	+	+	+	\pm	-
12	-	-	+	+	+	+	+	\pm	-
13	-	\pm	+	+	+	+	+	\pm	-
14	-	\pm	+	+	+	+	+	\pm	-

MiMo_ALe#7

Table A 11: Results of the secondary screening against PARc. The tested samples were the supernatants of strain MiMo_ALe#7 obtained by the OSMAC approach. (+) stands for inhibitory activity and (-) for no inhibitory activity. \pm represents inhibitory activity that was only observed for one replicate but not for the other. The assay was performed in duplicates.

Medium	Bennett	ISP3	NL19	NL200	NL300	NL333	NL400	NL410	NL500
Day									
3	-	-	\pm	+	-	+	+	+	-
4	-	-	+	+	+	+	+	+	-
5	-	-	\pm	+	+	+	\pm	+	-
6	-	-	+	+	+	+	+	+	-
7	-	-	+	+	+	+	+	+	-
10	-	-	+	+	+	+	+	+	-
11	-	-	+	+	+	+	+	+	-
12	-	-	+	+	+	+	+	+	-
13	-	-	+	+	+	+	+	+	-
14	-	-	+	+	+	+	+	+	-

MiMo_ALe#8

Table A 12: Results of the secondary screening against PARc. The tested samples were the supernatants of strain MiMo_ALe#8 obtained by the OSMAC approach. (+) stands for inhibitory activity and (-) for no inhibitory activity. \pm represents inhibitory activity that was only observed for one replicate but not for the other. The assay was performed in duplicates.

Medium	Bennett	ISP3	NL19	NL200	NL300	NL333	NL400	NL410	NL500
Day									
3	-	-	-	-	-	\pm	\pm	-	-
4	-	-	-	-	-	-	-	-	-
5	-	-	+	+	+	+	+	+	-
6	-	-	\pm	\pm	\pm	\pm	+	+	-
7	-	-	+	+	+	+	+	+	-
10	-	-	\pm	\pm	\pm	\pm	\pm	\pm	-
11	-	-	\pm	\pm	\pm	\pm	\pm	\pm	-
12	-	-	\pm	\pm	\pm	\pm	\pm	\pm	-
13	-	-	+	+	+	+	+	+	-
14	-	-	\pm	+	+	+	+	+	-

MiMo_ALe#9

Table A 13: Results of the secondary screening against PARc. The tested samples were the supernatants of strain MiMo_ALe#9 obtained by the OSMAC approach. (+) stands for inhibitory activity and (-) for no inhibitory activity. \pm represents inhibitory activity that was only observed for one replicate but not for the other. The assay was performed in duplicates.

Medium	Bennett	ISP3	NL19	NL200	NL300	NL333	NL400	NL410	NL500
Day									
3	-	-	-	-	-	+	+	-	-
4	-	-	\pm	+	+	+	+	-	-
5	-	-	+	+	+	+	+	+	-
6	-	-	+	\pm	+	+	+	+	-
7	-	-	+	+	+	+	+	+	-
10	-	-	+	+	+	+	+	+	-
11	-	-	+	+	+	+	+	+	-
12	-	-	+	+	+	+	+	+	\pm
13	-	-	+	+	+	+	+	+	-
14	-	-	+	+	+	+	+	+	-

MiMo_ALe#10

Table A 14: Results of the secondary screening against PARc. The tested samples were the supernatants of strain MiMo_ALe#10 obtained by the OSMAC approach. (+) stands for inhibitory activity and (-) for no inhibitory activity. \pm represents inhibitory activity that was only observed for one replicate but not for the other. The assay was performed in duplicates.

Medium	Bennett	ISP3	NL19	NL200	NL300	NL333	NL400	NL410	NL500
Day									
3	-	-	-	-	-	-	-	-	-
4	-	-	-	-	-	-	-	-	-
5	-	\pm	+	+	+	+	+	+	-
6	-	-	+	+	+	+	+	\pm	-
7	-	-	\pm	+	+	+	+	+	-
10	-	-	-	+	+	+	+	+	-
11	\pm	\pm	+	+	+	+	+	+	-
12	-	\pm	+	+	+	+	+	+	-
13	-	-	+	+	+	+	+	+	-
14	-	-	+	+	+	+	+	+	-

2.3. Representative HPLC-UV chromatograms for the medium extracts of the MiMo_Ale strains

The HPLC-UV chromatograms shown in the Figures A 19 and A 20 serve as representatives for the HPLC-UV chromatograms that were obtained from the ethyl acetate and 1-butanol medium extracts of the strains MiMo_Ale#1-10. All chromatograms share the signals at 7.0-8.5 min regarding retention time and peak shape whereas the signal intensity is higher in the ethyl acetate medium extracts compared to the 1-butanol medium extracts. The signal at 4.25 min can be found in the chromatograms of the medium extracts generated after 7 days.

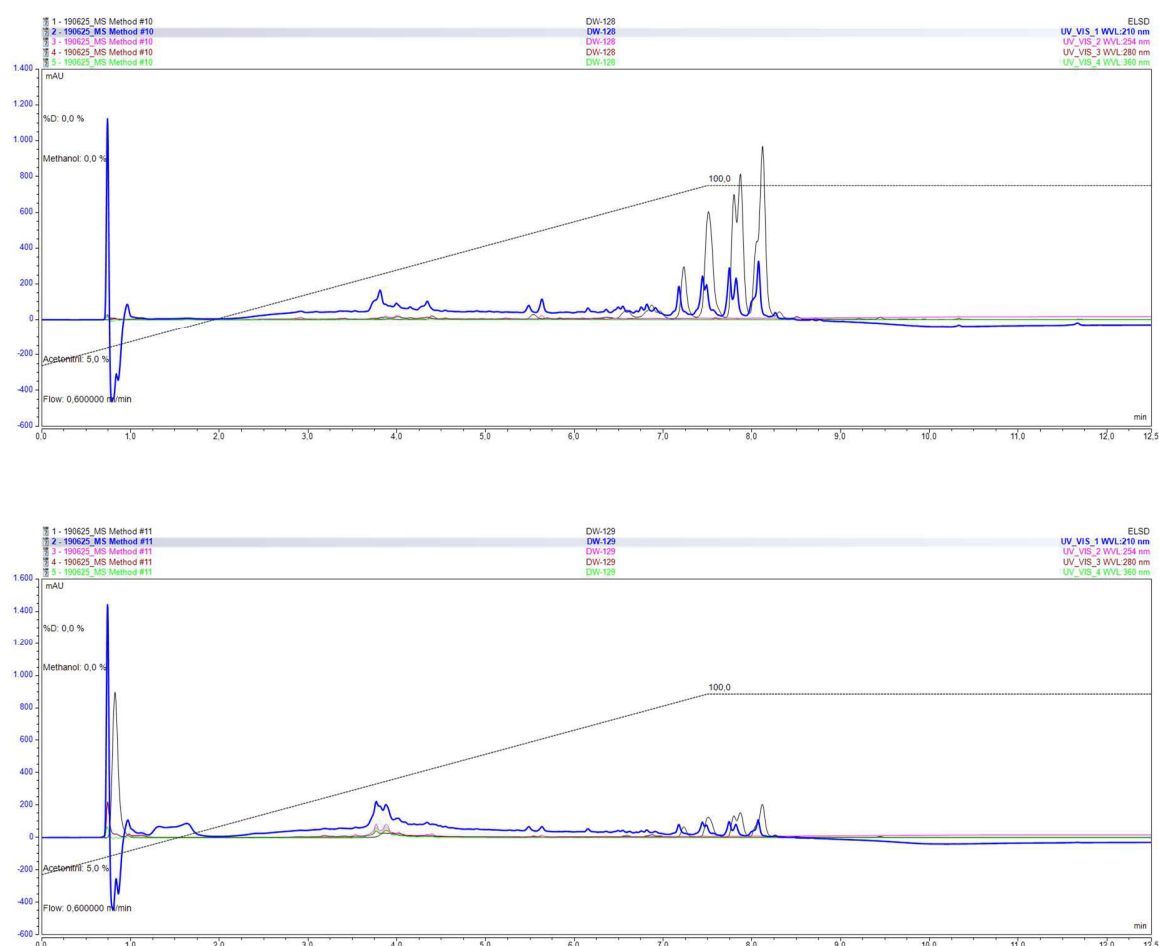


Figure A 19: HPLC-UV chromatograms of the ethyl acetate (upper) and 1-butanol (bottom) medium extracts of MiMo_Ale#3 after cultivation in medium NL300 for 3 days. For analysis, a Phenomenex® Kinetex (2.6 μ m) C-18, 100x3.0 mm ID column at 50 °C was used. Detection was done at 210 nm (blue), 254 nm (magenta), 280 nm (brown), 360 nm (green) and with the ELSD (black).

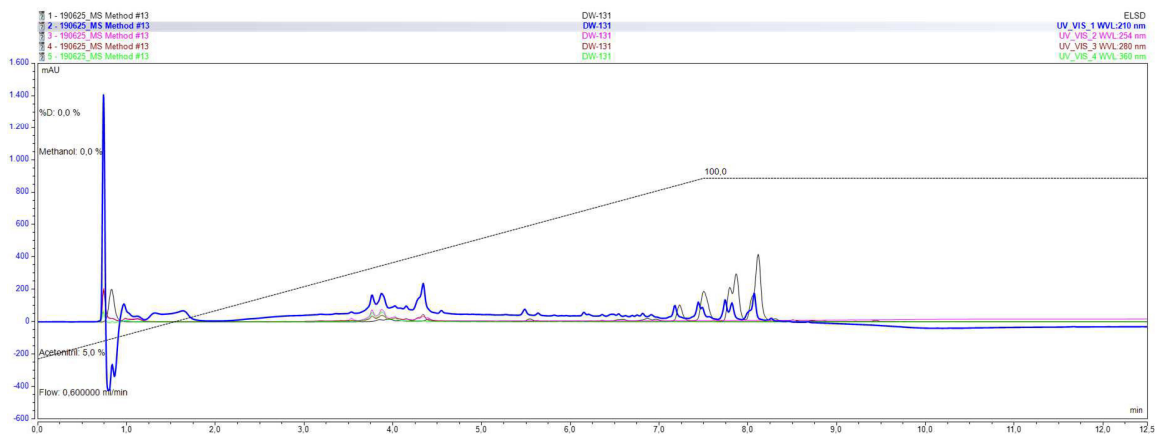
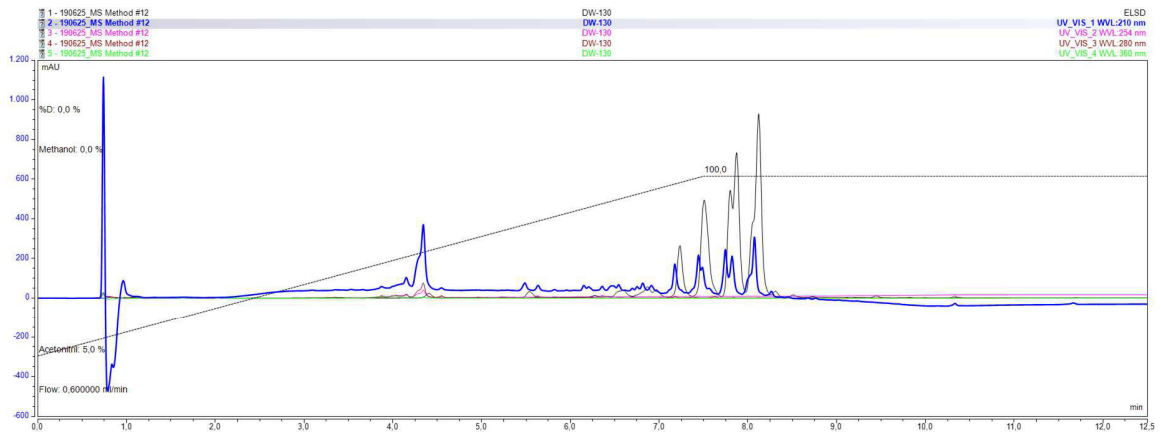


Figure A 20: HPLC-UV chromatograms of the ethyl acetate (upper) and 1-butanol (bottom) medium extracts of MiMo_ALe#3 after cultivation in medium NL300 for 7 days. For analysis, a Phenomenex® Kinetex (2.6 µm) C-18, 100x3.0 mm ID column at 50 °C was used. Detection was done at 210 nm (blue), 254 nm (magenta), 280 nm (brown), 360 nm (green) and with the ELSD (black).

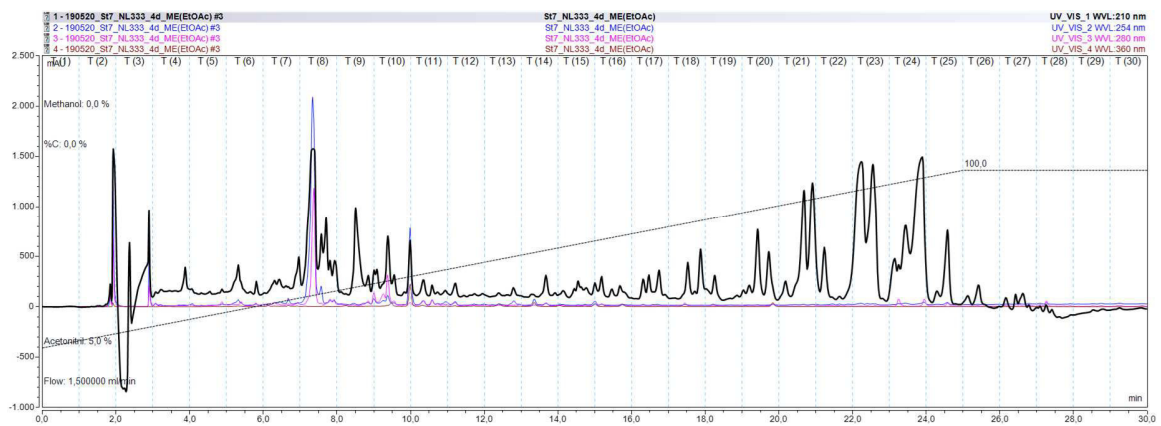


Figure A 21: HPLC-UV chromatogram of the ethyl acetate medium extract of MiMo_ALe#7 after cultivation in NL333 for 4 days. The vertical dashed lines indicate the separate micro-fractions. For micro-fractionation, a Phenomenex® Luna (5 µm) C-18, 250x4.6 mm ID column at 25 °C was used. Detection was done at 210 nm (black), 254 nm (blue), 280 nm (magenta), and 360 nm (brown).

3. Devices

Device	Manufacturer
96 universal thermocycler	PEQLAB Biotechnology GmbH
Alpha 1-2LD plus (Freeze dryer)	Christ
Avance-II spectrometer	Bruker
Biofuge fresco	Heraeus Instruments
Branson 2510	Brandson
Centrifuge 5415C	Eppendorf
Cleanbenches SAFE 2020	Thermo Scientific
EZ-2.3 Elite	Genevac
GENEQUANT® 1300 Spectrophotometer	biochrom
Heraeus Multifuge 1S-R Centrifuge	Thermo Electron Corporation
HLC	Ditabis
Incubator	Binder
Incubator	Heraeus Instruments
Infinite MPlax	TECAN
Labor rota S300	Resona Technics
LT-ELSD	Sedere
Mupid®-One electrophoresis system	Advance
NanoQuant infinite M200	TECAN
Overhead shaker	Heidolph
Q Exactive Plus mass spectrometer	Thermo Scientific
Rotary evaporators	Heidolph
Sonorex Digiplus	Bandelin
TJ-25 Centrifuge	Beckman Coulter
Tower shaker VKS75	Edmund Bühler
UltiMate 3000 HPLC system	Thermo Scientific
Vacuum pump	Welch by Gardner Denver

4. Chemicals

Chemical	Provider
1-Butanol	VWR
5 x buffer	Thermo Fisher Scientific
Acetic acid	AppliChem
Acetone (HPLC grade)	Promochem®
Acetonitrile (HPLC grade)	Promochem®
Acetonitrile (LCMS grade)	Honeywell Riedel-de Haën™
Acetonitrile- d_3	Roth
Actinomycin D	AppliChem
Agar Agar	Sigma-Aldrich/Roth
Agarose	Roth
Ammonium nitrate	Appli Chem
Ampicillin	Sigma-Aldrich
Apramycin	Sigma-Aldrich
B3 buffer	Machery-Nagel
B5 buffer	Machery-Nagel
Bacto casamino acids	DB Bacto
Bacto peptone	DB bacto
BE buffer	Machery-Nagel
Beef extract	BD difco
Binding buffer	Machery-Nagel
BW buffer	Machery-Nagel
CaCl ₂ x2H ₂ O	Merck
CaCO ₃	Sigma-Aldrich
Calcium carbonate (Morocco)	Sigma-Aldrich
Celite® 545	Roth
Chloramphenicol	SERVA
CoCl ₂ x6H ₂ O	Alpha Aesar
Corn steep solids	Sigma-Aldrich
Cotton seeds	Sigma-Aldrich

CuSO ₄ x5H ₂ O	Roth
Cycloheximide (Morocco)	Sigma-Aldrich
D-(+)-Glucose	Sigma-Aldrich
D-(+)-Mannitol	AppliChem
Deep well 96 well MTP	VWR
Dichloromethane	VWR
DMSO (for PCR)	Thermo Fisher Scientific
DMSO (reporter-based bioassay)	Thermo Fisher Scientific
DMSO- <i>d</i> ₆	VWR Chemicals
dNTPs	Thermo Fisher Scientific
D-Orn	Sigma-Aldrich
D-Ser	Sigma-Aldrich
Dulbecco's modified Essential Medium	Roth
Elution buffer	Machery-Nagel
Ethanol (96 %)	Roth/BrüggemannAlcohol Heilbronn GmbH
Ethanol (Morocco)	Riedel-de Haën TM
Ethyl acetate	Honeywell Riedel-de Haën TM
Ethylenediamintetraacetic acid (ETDA)	Roth
FDAA	Thermo Scientific
Fe-(III)-citrat	Roth
Fetal bovine serum	Sigma-Aldrich
Fish flour (anchovy)	CommonBaits
Formic acid (LCMS grade)	VWR Chemicals
Fosfomycin	Sigma-Aldrich
Full fat soy flour	Hensel
G418	Sigma-Aldrich
GeneRuler DNA ladder	Thermo Fisher Scientific
Glycerol	Roth
HCl	AppliChem
Hydrogen iodide	Sigma-Aldrich
Hygromycin B	Invitrogen
Isopropanol (HPLC grade)	Honeywell Riedel-de Haën TM

Kanamycin	Roth
KCl	Roth
KH ₂ PO ₄	Roth
LB medium	Roth
LB medium (reporter-based bioassy)	BD Difco
L-Orn	Sigma-Aldrich
L-Ser	Sigma-Aldrich
Malt extract	Oxoid
Methanol (HPLC grade)	Honeywell Riedel-de Haën™
MH agar (Morocco)	Biogar Dignostics
MH medium	Sigma-Aldrich
MnSO ₄ xH ₂ O	Sigma-Aldrich
Na ₂ B ₄ O ₇ x10H ₂ O	Roth
Na ₂ CO ₃	VWR
Na ₂ HPO ₄ xH ₂ O	Roth
Na ₂ MoO ₄ x2H ₂ O	Riedel de Haen AG
NaCl (Morocco)	Sigma-Aldrich
NaHCO ₃	Diagonal
Nalidixic acid (Morocco)	Sigma-Aldrich
NaOH	Chemapol
N-Z amine A	Sigma-Aldrich
Oat meal	Holo Bio Hafergold
Primer	Eurofins genomics
Proteinase K	Machery-Nagel
Rifampicin	Roth
Roticell-glutamine-solution	Roth
Rotistain®	Roth
Sea salts	Instant ocean, Aquarium systems
Sodium dodecyl sulfate (Morocco)	Sigma-Aldrich
Sodium hypochlorite (Morocco)	Sigma-Aldrich
Soluble starch	AppliChem
Sulforhodamine B	Sigma-Aldrich

T1 buffer	Machery-Nagel
Taq polymerase	Thermo Fisher Scientific
Tetracycline	SERVA
Trichloroacetic acid	Roth
Tris base	Roth
Tryptan Blue	Sigma-Aldrich
Water (LCMS grade)	AppliChem
Yeast extract	Oxoid
ZnCl ₂	Roth
